2022

Analysis of the light signalling pathway for the degradation of the circadian clock protein ROC15 in the green alga *Chlamydomonas reinhardtii*

緑藻クラミドモナスの時計タンパク質 ROC15 の分解を誘導する光シグナル伝達経路の解析

GURURAJ Malavika

Laboratory of Multicellular Coordination
Department of Biological Science
Graduate School of Science
Nagoya University

CONTENTS

1. ABSTRACT

Circadian rhythms are the rhythms with a period of ~24 hours observed in phenomenon such as leaf movement of plants, the human sleep/wake cycle and phototaxis in protists like *Chlamydomonas reinhardtii.* These rhythms persist in constant environmental conditions and are generated by a molecular circadian clock. The clock comprises of an input, oscillator and output. Signals such as light and temperature reach the oscillator component via the input, the oscillator is a gene-protein system that generates and maintains the rhythm and the output involves genes that are part of metabolic pathways that play a role in the afore-mentioned phenomenon. The input to the clock ensures that the rhythm generated is synchronized to the external environment i.e. it resets the clock. Light plays a major role in resetting the circadian clock, allowing the organism to synchronize with the environmental day and night cycle. In *C. reinhardtii* the light-induced degradation of the circadian clock protein, RHYTHM OF CHLOROPLAST 15 (ROC15), is considered one of the key events in resetting the circadian clock. Red/violet and blue light signals have been shown to reach the clock via different molecular pathways; however, many of the participating components of these pathways are yet to be elucidated. In my research, I followed a forward genetics approach and a reverse genetics approach using a reporter strain that expresses a ROC15-luciferase fusion protein. As result of the forward genetics approach, I isolated a mutant that showed impaired ROC15 degradation in response to a wide range of visible wavelengths and impaired light-induced phosphorylation of ROC15. These results suggest that the effects of different wavelengths converge before acting on ROC15 or at ROC15 phosphorylation. Furthermore, the mutant showed a weakened phase resetting in response to light, but its circadian rhythmicity remained largely unaffected under constant light and constant dark conditions. Surprisingly, the gene disrupted in this mutant was found to encode a protein that possessed a very weak similarity to the *Arabidopsis thaliana* EARLY FLOWERING 3 (ELF3). The results suggest that this protein is involved in the many different light signaling pathways to the *C. reinhardtii* circadian clock. However, it may not influence the transcriptional oscillator of *C. reinhardtii* to a great extent. As a result of the reverse genetics approach, I demonstrated that the mutant of the photoreceptor plant cryptochrome (pCRY), also has an impaired ROC15 degradation in response to a wide range of wavelengths, and an impaired ROC15 phosphorylation in response to both blue and red light. These results suggest the possibility that the red/violet and blue light signaling pathways are integrated by pCRY before acting on ROC15. This study provides an opportunity to further understand the mechanisms underlying light-induced clock resetting and explore the evolution of the circadian clock architecture in Viridiplantae.

2. GENERAL INTRODUCTION

2.1. Circadian rhythms

One of the first observations of the existence of ~24-hour rhythm was in 1729 by the scientist Jean-Jacques d`Ortous de Marian. He observed that the *Mimosa* plant opened its leaves once approximately every 24 hours i.e. during the day and the leaves drooped once approximately every 24 hours i.e. at night (**De Marian 1729**). Since then a large number of organisms from mammals to cyanobacteria have been observed to have processes which occur once in ~24 hours. In case of humans this can be seen for the sleep-wake cycle and body temperature, in case of cyanobacteria it can be observed in nitrogen fixation and in the green alga *C. reinhardtii,* it can be observed in processes such as phototaxis and chemotaxis.

Another important characteristic of these processes is that they continue to occur at approximately the same intervals even in constant environments. An example is again an observation made by de Marian. He noticed that the leaf opening and closing phenomenon in the *Mimosa* plant was independent of the day/night alternation of the environment i.e. it occurred once in ~24 hours even in constant darkness at times corresponding to external day and night respectively (**De Marian 1729**). The rhythm is therefore, generated endogenously and not stimulated by the alternating environmental cycles. This endogenous rhythm with a period of ~24-hours is otherwise known as a circadian rhythm.

Observations similar to the ones made by de Marian were also made in animals. The Human isolation studies by M Siffre (1963), JN Mills (1964) and J Aschoff (1965) are some examples. The experiment involved being isolated in either a cave or bunker respectively. The subjects were therefore not exposed to the natural day and night alternation and were allowed to use very dim artificial light only during the times they were awake. It was observed that processes such a sleep-wake continued even in such isolation with a period of approximately 24 hours. It was however also observed that the time of sleep and wake occurred at a later hour as the days progressed. While the generation/existence of the rhythm is not dependent on the environmental conditions, without the influence of the environmental conditions the rhythm continues to exist in its own time. In other words, it free runs or is de-synchronized from the environment.

However, constant conditions are not the only time the rhythm becomes de-synchronized from the environment. In humans, the effects of being de-synchronized with the external day and night can also be observed on a more relatable level when we travel to a new time zone. In other words, when we experience a Jet lag. The ability of the internal rhythm to adapt to the new environment, that is become entrained to a new cycle is the feature that allows us to overcome Jet-lag. In other words, the organism's internal time is reset. At this point another crucial feature of the circadian rhythm comes into focus. That is entrainment. The ability of the rhythm to latch on to an external cycle and therefore synchronize with the environment. The significance of synchronization between the internal temporal organization and external environmental cycles was demonstrated in tomato plants by observing their growth in various constant and cyclic light and temperature conditions. It was demonstrated that cyclic light and cyclic temperature

conditions close to the internal temporal organization of 24 hours were preferred (**Aurthr et al., 1930, Highkin & Hanson 1954**, and **Hillman 1956**). A later study by Pittendrigh and Minis resulted in similar observations in animals (**Pittendrigh and Minis 1972**). They observed the mortality of fruit flies (*Drosophila melanogaster*) in periodic environments of varying day lengths (10.5h light/10.5hdark, 12h light/12h dark and 13.5h light/13.5h dark days; 1 day = 1 light and 1 dark cycle) and in an aperiodic environment (constant light). The survival rate was highest when the flies synchronized to an oscillating environment which had a period of 24 hours.

In addition to the above mentioned characteristics, the circadian rhythm is characterized by yet another important feature i.e. temperature compensation. The period of the rhythm does not change significantly with change in ambient temperature.

2.2. Circadian clock

While a rhythm is observed in sleep-wake, leaf movement and photo-taxis, rhythms are also observed at the cellular level as rhythms of gene and protein expression, post translational modifications, protein-protein interactions etc. (**Reppert and Weaver 2002**, **Mohawk et al., 2012**). The rhythms of the physiological processes are thought to be the result of the rhythm at the cellular level (**Mohawk et al., 2012**). Cells/organisms are said to possess a system at the molecular level called the circadian clock that generates and maintains the circadian rhythm. The clock is divided into three components: the input, oscillator and output. The input comprises of photoreceptors, thermally responsive proteins and signal proteins; components that interact with the external environment and convey signals such as light and temperature to the oscillator component. The output component of the clock is mainly constituted of genes involved in various metabolic and physiological processes. The expression of these genes is affected by the regulation of the oscillator genes.

The oscillator component is responsible for generating and maintaining the rhythm. There are two models to explain the nature of the oscillator. One of them is the TTFL model or the transcriptional – translational feedback loop model (**Hardin et al., 1990**). This model essentially states that the rhythm is a result of a negative feedback loop. The loop consists of negative and positive elements. The proteins that form the positive element, drive the expression of the proteins forming the negative element. The negative element then inhibits its own expression. The positive and negative elements are however involved in the expression of genes that are part of other metabolic and physiological processes. The rhythm in the expression and degradation of these elements therefore result in the rhythmic expression of the genes they affect. This system has been observed in various organisms ranging from cyanobacteria to mammals (**Dunlap, 1999**). For example, in case of mammals (humans and mice): Proteins BMAL1 and CLOCK form a heterodimer and drive the expression of *PERIOD (Per)* and *CRYPTOCHROME (CRY)* genes. PER and CRY proteins along with the action of Casein Kinase 1 (CK1) form a complex and repress the action of BMAL1 and CLOCK (**Partch et al., 2014**). In case of fungi: It is essentially the same mechanism. There is a positive element heterodimer made from the proteins White Collar-1 and White Collar-2 and a negative element complex made up of a protein called FREQUENCY (FRQ) and two enzymes: FRQ interacting RNA Helicase (FRH) and CK1 (**Fuller et al., 2014, Hurley et al., 2015**). However, it has also been observed that the circadian rhythms of physiological phenomena persist in cells without transcription e.g. in human red blood cells (**O'**

Neill et al., 2011), enucleated cells of the giant single cell *Acetabularia* (**Sweeney and Haxo, 1961**) and in the prokaryote *Cyanobacteria* (**Nakajima et al., 2005**). Therefore, there is a second model to explain the nature of the oscillator and it is called the post-translational model. It has been explored in *Cyanobacteria*. The system in *Cyanobacteria* comprises of three proteins KaiA, Kai B and KaiC. KaiC can phosphorylate and de-phosphorylate itself. KaiA promotes phosphorylation of KaiC and Kai B promotes the de-phosphorylation of KaiC (**Nishiwaki et al., 2004, Nakajima et al., 2005, Kageyama et al., 2006**). The system was also re-constituted in *in vitro* (**Nakajima et al., 2005**).

2.3. Light resetting of the circadian clock

While many factors such as light, temperature, time of food intake and social cues (in case of humans) are capable of synchronizing the individual with the environment, the role of light has been of particular interest to many scientists. There are two models that attempt to explain this phenomenon. One of them is the parametric model according to which the pace of the circadian clock gradually increases or decreases to eventually catch up to the external cycle (**Swade 1969, Daan 1977**). The other is the non-parametric model according to which light pulses (or light-dark transitions in nature) cause either a delay or advance in the time at which an event happens, resulting in the entrainment of the organism. (**Aschoff 1960, Bruce 1960, Pittendrigh 1966, Daan 2000, Johnson et.al., 2003**).

The action spectrum for non-parametric light resetting has been elucidated in a number of organisms such as *Neurospora* (**Sargent and Briggs 1967**)*, Gonyaulax* (**Hastings and Sweeny 1960**)*, D. melanogaster* (**Klemm and Ninneman 1976**) and even in mammals (**Takahashi et.al., 1984**). Light resetting has also been explored at a molecular level in many organisms. This includes identifying photoreceptors involved in receiving light for resetting as well as the molecular events downstream of light reception. In the fungus *Neurospora*, resetting is majorly associated with the light induction of the clock gene *frq* (through WC-1 and WCC) and the subsequent translation of the FRQ protein encoded by it (**Dunlap and Loros 2004, Loros 2020**). In mice, the genes *mPer1* and *mPer2* were shown to be necessary for normal photic resetting (**Zheng et.al., 2001**). The expression of both the genes happen to be induced by light. Although this event has been considered as one of the highly possible mechanisms for light resetting in mice (**Hirota and Fukada 2004**), other pathways have also been suggested (**Jakubcakova et.al., 2007**). In case of *D. melanogaster*, multiple photoreceptors appear to play a role in resetting. CRY is one of them. The light induced degradation of the clock protein TIMELESS (TIM) by interaction with CRY and the F-BOX protein JETLAG, as well as the JETLAG dependent degradation of CRY has been implicated in light resetting (**Myers et al., 1996, Ceriani et al., 1999, Koh et al., 2006**). However, it was revealed that CRY might not be the only photoreceptor participating in resetting (**Stanewsky et al., 1998**). Light resetting at the molecular level has also been investigated in the prasinophyte green alga, *Ostreococcus tauri*. This alga possesses a histidine kinase with a light, oxygen, and voltage sensing domain photoreceptor (LOV-HK), which is involved in circadian clock functions (**Djouani-Tahri et al., 2011**). Studies using experimental and mathematical modeling approaches have suggested that this LOV-HK photoreceptor—along with the other histidine kinase, Rhodopsin-HK—participates in a two-component signaling system to reset the *O. tauri* circadian clock using blue and green light (**Thommen et al., 2015**).

In my research I used the model organism *C. reinhardtii* to explore the resetting of the circadian clock at the molecular level. Due to its haploid nature and due to the fact that its entire genome

sequence is accessible, it is an extremely convenient model organism for a forward genetics approach. Furthermore, it has the ability to grow in the dark given an alternate carbon source making it a good model for circadian studies especially light induced-resetting of dark adapted cells (**Bruce 1970, Kondo et al., 1991**). Additionally, because it possesses homologs of both plant and animal proteins (**Merchant et al., 2007**), it is a great model organism for evolutionary studies on light resetting.

C. reinhardtii is a unicellular green algae belonging to the phyla Chlorophyta under the super-group Archaeplastida (**Leliaert et al, 2011, F Burki 2014**). It was shown to possess a circadian rhythm in phenomenon such as phototaxis (**Bruce, 1970**), stickiness to glass (**Straley and Bruce**, **1979**) and even chemotaxis (**Byrne et al., 1992**). Since then many components of the *C. reinhardtii* circadian clock have been identified such as the RNA binding protein CHLAMY 1 (**Mittag et al., 1996**) and the *RHYTHM OF CHLOROPLAST* genes; *ROC15, ROC40, ROC75, ROC55*, *ROC66* and *ROC114* (**Matsuo et al., 2008**). Apart from the proteins encoded by *ROC55* and *ROC114,* homologs of ROC15, ROC40, ROC75 and ROC66 have been identified in the land plant *Arabidopsis thaliana* (**Matsuo et al., 2008**).

2.4. Light resetting of the *C. reinhardtii* circadian clock

The action spectrum for the resetting of the circadian clock has been investigated in *C. reinhardtii* (**Kondo et al., 1991, Johnson et al., 1991**). A series of phase shift experiments over a broad range of wavelengths revealed that for dark-adapted *C. reinhardtii*, the phase resetting was sensitive to many wavelengths*,* especially to green and red wavelengths (i.e., 520 nm and 660 nm, respectively) (**Kondo et al., 1991**). It was later demonstrated that blue light (440 nm) could also reset the clock with high efficacy in another strain of *C. reinhardtii* (**Forbes-Stovall et al., 2014**). Therefore, many photoreceptors have been considered as candidates for those in resetting the circadian clock. Some of the candidates for responses to blue and/or green light include phototropin, rhodopsins, and cryptochromes (**Schulze et al., 2010**). Of these, the plant-like cryptochrome which plays a role in the oscillator is also involved in the input pathway of the *C. reinhardtii* circadian clock (**Forbes-Stovall et al., 2014, Müller et al., 2017**). Candidates for responses to red light include the animal-like cryptochrome, which has been shown to absorb red light in its dark form (the neutral radical state of flavin chromophore) in addition to absorbing blue light (oxidized state of flavin chromophore), and to regulate the blue and red light responses of some clock genes (**Beel et al., 2012**). Interestingly, no known homolog of the phytochrome photoreceptor family, which is known to be involved in the red light response of the circadian clock in *A. thaliana* (**Somers et al., 1998, Devlin and Kay 2000, Jones et al., 2015**), has been found in *C. reinhardtii* (**Merchant et al., 2007**, **Li et al., 2015**).

The identification of the clock gene, *ROC15* (**Matsuo et al., 2008**), has shed light on the molecular mechanisms of light resetting in *C. reinhardtii.* The encoded protein, ROC15, possesses a GARP DNA-binding motif similar to that of LUX ARRYTHMO (LUX) and BROTHER OF LUX ARRYTHMO (BOA) (**Matsuo et al., 2008**). Not only does ROC15 undergo circadian-phase-independent light-induced degradation, an insertional mutant of this gene also shows abnormal light resetting, as it fails to show a phase shift in response to a light pulse (**Niwa et al., 2013**). In addition, ROC15 degradation—similar to clock resetting—is sensitive to wavelengths across the entire visible spectrum (**Niwa et al., 2013, Kinoshita et al., 2017**). Therefore, the light-induced degradation of ROC15 has been suggested to be associated with light resetting in *C. reinhardtii* (**Niwa et al., 2013, Kinoshita et al., 2017**). The isolation of a mutant of *C. reinhardtii SHOC2/SUR8-like leucine-*

rich repeat (*CSL*) revealed the existence of at least two pathways (i.e., red/violet and blue light pathways) by which light information was communicated to the clock. This was because the mutant showed an impaired response of ROC15 to red and violet light, but not to blue light (**Kinoshita et al., 2017**).

However, while these findings have started to reveal the molecular pathways underlying light resetting in *C. reinhardtii*, there are still many questions that need to be answered. To this end, I used two approaches: a forward genetics and a reverse genetics approach in order to further elucidate the light signaling pathway for ROC15 degradation.

3. CHAPTER 1

A potential ELF3 homolog in *C. reinhardtii* is involved in the red/violet and blue light signalling pathways for the degradation of ROC15

3.1. INTRODUCTION

The circadian clock protein ROC15 possess a GARP domain that is similar to the *A. thaliana* transcription factors: LUX or BOA (**Matsuo et al., 2008**). In *Arabidopsis thaliana,* LUX and BOA form a complex with two other proteins EARLY FLOWERING 3 (ELF3) and EARLY FLOWERING 4 (ELF4). This complex known as the Evening Complex (EC) is considered to be part of the *A. thaliana* circadian oscillator (**Hsu and Harmer 2014, Nohales and Kay 2016, Huang and Nusinow 2016**). The component ELF3 is also involved in integrating light signals and the molecular clock (**Sanchez et al., 2020**). Interestingly, the *elf3* mutant shows an abnormal light resetting of the clock and a loss of circadian gating in the light induction of a clock-controlled *CHLOROPHYLL A/B-BINDING PROTEIN 2* gene, therefore, ELF3 is suggested to play a significant role in the light input pathway to the circadian clock (**McWatters et al., 2000, Covington et al., 2001**). In addition, ELF3 is known to interact with the phytochrome photoreceptors, Phy A-E (**Liu et al., 2001, Huang et al., 2016**). The direct interaction between ELF3 and CONSTITUTIVE PHOTOMORPHOGENIC 1 (COP1) is also thought to connect the clock to many light-signaling cascades, as COP1 is a common factor in these pathways (**Yu et al., 2008, Huang et al., 2016, Sanchez et al., 2020**).

In this study, to further elucidate the molecular mechanisms of light resetting in *C. reinhardtii,* I used the ROC15-LUC reporter strain (**Niwa et al., 2013**), which expresses a fusion protein of ROC15 and firefly luciferase. I then followed a forward genetics approach in order to isolate a mutant defective in light resetting. As a result, I isolated a mutant that showed an impaired ROC15 light response over a wide range of wavelengths. I then characterized this mutant to understand the significance of the gene disrupted in this mutant in the light resetting mechanism and the circadian oscillator.

3.2. RESULTS

Screening for mutants of ROC15 light response

Mutants were generated by random insertional mutagenesis of the ROC15-LUC reporter strain using the hygromycin resistance gene, *aph7"* (**Berthold et al., 2002**). Approximately 4700 transformants were subjected to two cycles of a 6 h dark/18 h light schedule (one red and one blue light cycle). Under these conditions, the wild type (WT) ROC15 bioluminescence levels increased in the dark period, decreased acutely at the start of light-on conditions, and remained low until the end of the light period (**Fig 1A**, WT). These patterns reflected the expression levels of ROC15 (**Niwa et al., 2013**). Two mutants (tentatively named M1 and M2) were isolated. The first mutant (M1) showed a gradual decrease instead of an acute one in ROC15 bioluminescence levels after the transition to the light phase (**Fig 1A**). In addition, M1 bioluminescence levels failed to remain low until the start of the dark phase (**Fig 1A**). These altered patterns of ROC15-

LUC bioluminescence were observed in both the red and blue cycles of screening (**Fig 1A**). The ROC15 light response in the mutant was further examined by exposing M1 to 5-min pulses of red and blue light. Unlike the WT, M1 failed to show an acute decrease in ROC15 bioluminescence levels in response to both light pulses (**Figs 1B and 1C**). Taken together, these results suggested that the light-dependent degradation of ROC15 was affected in the mutant. The second mutant (M2) also showed an altered ROC15 bioluminescence response to both red and blue lights, similar to the M1 phenotype (**Fig 2**). In conclusion, I was able to isolate two light response mutants that showed impaired ROC15 bioluminescence responses to both red and blue light.

Gene disrupted in the M1 mutant

To identify the disrupted genes in the mutants, I performed a genetic linkage analysis to confirm that the mutant phenotype was linked to hygromycin resistance. This was verified by backcrossing the mutants with the parental WT strain (ROC15-LUC reporter strain). In mutant M1, all hygromycin-resistant progeny failed to show an acute decrease in ROC15 bioluminescence after light-on, whereas all the hygromycin-sensitive progeny showed an acute decrease (**Figs 3A and 3B**). These results confirmed the genetic linkage of hygromycin resistance to the mutant phenotype. However, this pattern was not observed in the second mutant (M2) (**Figs 3C and 3D**)**.** Therefore, I continued my investigations only in the M1 mutant. In M1, the DNA flanking the hygromycin resistance marker was amplified by thermal asymmetric interlaced–polymerase chain reaction (TAIL-PCR) (**Liu et al., 1995**). This sequence was compared to the *C. reinhardtii* reference genome (*C. reinhardtii* v5.6, Joint Genome Institute), and the Cre07.g357500 gene on chromosome 7 was found to be disrupted (Corresponds to the ID Cre07.g800875 in the latest version (v6.1)). This gene appeared to have eight exons, and the insertion of the hygromycin marker was found to be in the third intron (**Fig 4A**). The insertion was confirmed by PCR using a gene-specific primer pair (**Figs 5A and 5B**). I further performed a reverse transcription-PCR (RT-PCR) on the transcript (**Fig 5A**). No band with a WT band size was detected in the mutant. The two bands detected could possibly correspond to mutant transcripts resulting from unexpected alternative splicing due to the insertion of the marker (**Fig 5C**). I also performed a sequencing analysis of the RT-PCR product of the entire coding sequence (CDS) of this gene from our laboratory WT strain. The results revealed that compared to the database sequence (v5.6), our laboratory strain had an in-frame 264 nucleotide insertion in the fifth exon (**Fig 4A,** purple box). Mutants with similar phenotypes (i.e., impaired ROC15 light response to both red and blue wavelengths) had been isolated previously (*b19* and *b20* mutants) (**Kinoshita et al., 2017**). TAIL-PCR analysis of *b19* revealed that the same gene (Cre07.g357500) was disrupted (**Fig 4A**). The insertion locus of the hygromycin marker was in the fifth intron in the *b19* mutant (**Figs 4A, 5A, and 5B**).

To confirm that the disruption of the Cre07.g357500 gene caused the altered response to light in mutants, the M1 mutant was transformed with the WT gene (**Fig 6A**) to determine whether the ROC15 light response would be restored to WT levels. A total of 654 transformants (414 transformed with the WT gene and 240 transformed with only the antibiotic resistance cassette as a control group) were subjected to two cycles of a 6 h dark/18 h light schedule, with the first and second light phases consisting of red and blue light, respectively (**Fig 6B**). The ROC15 light response to both blue and red wavelengths was restored to WT levels in 6 of 414 transformants that had been transformed with the WT Cre07.g357500 gene (i.e., ROC15 bioluminescence levels declined steeply in response to light) (**Figs 6B and 6C**). The complementation rate was

comparable to the rates observed in other mutants in previous studies (**Matsuo et al., 2008**). In contrast, 0 of the 240 control transformants showed a WT ROC15 light response (**Fig 6D**). The ROC15 light responses of the six complements were further confirmed via 5-min pulses of red and blue light. The ROC15 bioluminescence levels decreased acutely in response to red and blue light pulses in all six complements (**Figs 6E and 6F**). These results confirmed that the disruption of the Cre07.g357500 caused the altered response to light in the mutant.

Protein sequence alignment

The longest open reading frame of the Cre07.g357500 gene of our laboratory strain encodes a protein with an expected length of 2392 amino acids. This protein has not been well characterized in *Chlamydomonas*. Therefore, I performed a BLAST search of this protein sequence against Archaeplastida proteins via the algal multi-omics portal, PhycoCosm (**Grigoriev et al., 2021**). Using the default BLAST settings (e-value threshold = 1×10^{-5}), homologs were detected only in members of Chlorophyceae. Some of the organisms that showed homologs included other species of *Chlamydomonas* (such as *C. incerta* and *C. schloesseri*), other members of the order Chlamydomonadales (such as *Volvox carteri, Gonium pectorale,* and *Edaphochlamys debaryana*), and organisms belonging to the order Sphaeropleales (such as *Scenedesmus obliquus*). BLAST was performed once again with a lower E-value threshold (= 1). This resulted in hits in many more chlorophytes, including members of Trebouxiophyceae (such as *Chlorella sorokiniana*), Mamiellophyceae (such as *Micromonas commoda*), and members of another phylum—Streptophyta, such as *Selaginella moellendorfii* and *Populus trichocarpa.* Surprisingly, the streptophyte proteins included homologs of the *A. thaliana* ELF3. Additionally, a BLAST analysis of *A. thaliana* ELF3 against the *C. reinhardtii* proteome (v5.6_281) revealed the protein encoded by Cre07.g357500 as the best hit with an E-value of 0.016. Similarly, a BLAST analysis of the protein encoded by the gene Cre07.g357500 against the *A. thaliana* Araport11 protein sequences database, revealed ELF3 as the best hit with an E-value of 0.11. I then aligned 33 sequences (**Table 2**) obtained from the BLAST searches and the ELF3 homologs of the major species in Streptophyta. The results revealed two regions of similarity (Region 1 and Region 2) (**Figs 4B, 4C, and 7**). Region 2 was found only in chlorophyte proteins (**Fig 7**), whereas Region 1 was found in the proteins of both chlorophytes and streptophytes (**Figs 4B and 4C**). Region 1 happened to be part of a region in *A. thaliana* ELF3 referred to as Block II, which is one of the four highly conserved regions (the other three being Block I, Block III and Block IV) in angiosperm ELF3 (**Liu et al., 2001**). To further observe the conservation at all the Blocks, the protein encoded by Cre07. g357500 was aligned with *A. thaliana* ELF3 and its homologs from only other angiosperms using MAFFT and MUSCLE multiple sequence alignment algorithms. It was observed that while Block II aligned to the same sequence of the Cre07. g357500 protein in both algorithms, Blocks I, III, and IV aligned to slightly different sequences depending on the algorithm used (**Fig 8**). This data only weakly suggests the possibility of Cre07.g357500 being a homolog of ELF3. However, it is important to note that the Glycine residue (Gly-326) in Region 1, which when mutated is known to affect the circadian function of ELF3 (**Kolmos et al., 2011**), was fully conserved in the proteins analyzed (**Fig 4C**). In addition, Region 1 was immediately adjacent to the region that has been shown to interact with ELF4 in *A. thaliana* (**Jung et al., 2020**) (**Fig 4B,** patterned red box). Therefore, this gene is hereafter referred to as *Chlamydomonas-ELF3-like* (*CETL*), and the M1 and *b19* mutants are referred to as *cetl-1* and *cetl-2*, respectively.

CETL expression analyses

I analyzed whether *CETL* transcript level was rhythmic under constant light conditions (LL). The results of a reverse transcription-quantitative PCR (RT-qPCR) analysis revealed that the transcript-level was rhythmic, with a peak at approximately subjective dusk or early subjective night (**Fig 9**). This result indicated that *CETL* gene expression was evening-phased due to circadian control.

To assess the CETL protein expression, the mutant (*cetl-1*) was transformed with a gene fragment encoding hemagglutinin (HA) tagged CETL (**Fig 10A and 10B**). A total of 462 transformants were screened for restoration of ROC15 response to 6 h dark/18 h red light cycles (**Fig 10C**). ROC15 response was restored to WT levels in six of the 462 transformants (**Fig 10D**). HA-CETL expression was then analyzed in these six transformants by western blot analysis. A band of size 237kDa corresponding to HA-CETL was detected in five of the six complements (**Fig 10E**). The ROC15 light response of these five complements was further confirmed by exposure to 5-min pulses of red and blue light. The ROC15 bioluminescence levels decreased acutely in response to red and blue light in all five complements (**Fig 10F and 10G**), indicating that the HA tagged CETL was functional with respect to ROC15 light induced degradation. CETL protein expression was then examined in one of these five complements by a western blot analysis. Bands corresponding to HA-CETL were detected in the light phase in a LD cycle and even 30 minutes after exposure to red and blue light pulses in the dark phase (**Fig 11A**). These results suggest that CETL does not show ROC15-like responses to either red or blue light. Immunocytochemical staining was also performed in one of the five complements by using anti-HA antibody. The HA-CETL signals were detected just inside the Nuclear Pore complex (NPC) signal, similar to where the ROC15-HA signals were detected (**Fig 11C**). These results suggest that CETL localizes in close proximity to ROC15.

ROC15-LUC light response in the *cetl-1* mutant

The *cetl-1* mutant showed an impaired response to red and blue light (**Fig 1**). To understand the wavelength specificity of this mutant, its ROC15 light response was further characterized by testing other wavelengths (i.e., violet and yellow). The mutant and WT were exposed to a light pulse of four different wavelengths at two different intensities. At an intensity of 2 µmol m^{-2} s^{-1}, the WT showed an acute decrease in ROC15 bioluminescence levels at all wavelengths. In contrast, the mutant failed to show this acute decrease (**Fig 12A**). At a lower intensity of 0.2 µmol m^{-2} s^{-1}, the WT cells showed an acute decrease in ROC15 bioluminescence levels in response to red and violet wavelengths, and a slight decrease in ROC15 bioluminescence levels in response to yellow and blue wavelengths (**Fig 12B**). This result was consistent with those of previous studies (**Niwa et al., 2013, Kinoshita et al., 2017**). However, the mutant failed to show these decreases (**Fig 12B**). These results demonstrate that the mutant showed defective responses to violet and yellow wavelengths in addition to defective responses to blue and red wavelengths. Therefore, the ROC15 light response in the mutant was impaired across the visible range.

The effect of the *cetl-1* mutation on light-induced degradation of ROC15 was further observed in a *csl* mutant genetic background. The *cetl-1/csl* double mutant strain was obtained via a genetic cross. The double mutant was exposed to three different wavelengths (red, blue, and violet) at two different intensities. At both 2 µmol m^{-2} s^{-1} and 0.2 µmol m^{-2} s^{-1}, the *cetl-1/csl*

double mutant failed to show the ROC15-LUC bioluminescence decreases observed in the WT in response to all the wavelengths tested (**Figs 13A and 13B**). These results indicate that the blue light response in *csl* was lost due to the *cetl-1* mutation (**Kinoshita et al., 2017**).

Intracellular localization and light-induced phosphorylation of ROC15 in the *cetl-1* mutant

Previous studies have suggested that ROC15 localizes to the nucleus and undergoes light-induced phosphorylation (**Niwa et al., 2013**). To investigate these characteristics of ROC15 in the *cetl-1* mutant, the *ROC15-HA* genetic construct was introduced into the mutant genetic background via a genetic cross. To investigate ROC15 localization, I performed immunocytochemical staining with an anti-HA antibody. The results showed that ROC15-HA signals were detected immediately inside the NPC signals in both the WT and mutant cells (**Figs 14A and 14B**). This suggests that the *cetl-1* mutation did not affect the localization of the ROC15 protein. However, it was observed that the ROC15 expression between mutant cells was not as uniform as between WT cells (**Fig 14B**). This is probably due to the weak ability of this mutant to respond to synchronizing light/dark conditions (See below). This was followed by an analysis of ROC15 light-induced phosphorylation in response to red and blue lights. ROC15 phosphorylation has been reported to be visible as an electrophoretic mobility shift of ROC15-HA, as the shift was not observed when cell-extracts were subjected to phosphatase treatment (**Niwa et al., 2013**). This electrophoretic mobility shift was not observed in the mutant in response to red and blue light pulses (**Fig 15A**). The mobility shift was restored in the complement strains in both cases (**Figs 15B and 15C**), indicating that CETL was required for ROC15 to undergo light-induced phosphorylation.

Circadian rhythm and resetting in the *cetl-1* mutant

To characterize the mutant, I observed its circadian rhythm in constant darkness (DD) and LL conditions. I introduced the chloroplast luciferase reporter gene (*tufA promoter-lucCP*; *lucCP* is a firefly luciferase gene that is codon-optimized for the *C. reinhardtii* chloroplast) (**Matsuo et al., 2006**) of the CBR strain (**Matsuo et al., 2008**) into a mutant genetic background via a genetic cross. A stable rhythm was detected in the *cetl-1* mutant under both DD and LL conditions (**Fig 16A**), with a slight tendency toward longer period lengths and lower amplitudes (**Fig 16B**). Similar results were observed in the *cetl-2* mutant under DD and LL conditions (**Figs 17A and 17B**). This result suggested that *CETL* did not play a major role in the oscillator of the *C. reinhardtii* circadian clock. However, the peak phase of *cetl-1* showed a wider distribution with a tendency to advance the phase, especially under LL conditions (**Fig 16C**). This is again close to what was observed in the *cetl-2* mutant under LL conditions **Fig 17C**). As observed in the *cetl-1* mutant, the variation in phase was pronounced between independent trials of a single progeny, and also between progenies within a single trial, rather than between biological replicates of a single progeny within a single trial (**Figs 18 and 19**). These unstable phase phenotypes might be indications of insufficient phase resetting in the mutants. Therefore, I investigated phase resetting using light pulses. The *cetl-1* mutant and WT were maintained in DD conditions and exposed to light pulses of four different wavelengths at late subjective night. The WT showed an advance in the phase in response to all four wavelengths, consistent with previous reports (**Kinoshita et al., 2017**). Although the *cetl-1* mutant also showed a slight phase advance, the advance was significantly reduced compared to that of the WT (**Fig 20**). These results indicated that phase resetting was impaired in the *cetl-1* mutant.

Phase distribution in the single colony protocol in the *cetl-1* mutant

To further examine the phase resetting in the mutant, I also analyzed the chloroplast bioluminescence rhythm of cultures that had been prepared in a manner different to that of our standard protocol. The biological replicates for the current experiment originated from independent colonies (single colony protocol), as opposed to our standard protocol, where the biological replicates were obtained from a single patch on storage plates (**Fig 21**). The quadruplicate spots from an independent culture of the single colony protocol were exposed to either the same light schedule as in **Fig 16A** (**Fig 22Ai**) or to additional progressive LD cycles (**Fig 22Aii, 22Aiii and 22Aiv**) before monitoring in LL conditions. Surprisingly, after light schedule i, the peak phases appeared to vary largely between the biological replicates of *cetl-1* (**Fig 22B**). When visualized as a phase diagram, the wide distribution of peak phases was evident (**Fig 22C**). I also noted that the distribution of peak phases of *cetl-1* varied with trials, and sometimes appeared more synchronized (**Figs 23A and 23B**). However, I again observed that the period and amplitude of the rhythm of the mutant were close to those of the WT in this protocol (**Figs 22D and 23C**)**.** After each additional light/dark cycle (**Fig 22Aii, 22Aiii, and 22Aiv**), the peak phases of the rhythms in the mutant cultures were detected much closer to those of the WT (**Fig 22E**). Collectively, these results suggested that the mutant was severely affected in its ability to reset the clock, but that the ability is not completely lost.

Light responses of clock gene mRNAs in the *cetl-1* mutant

Previous studies have demonstrated that the mRNA of some clock genes, such as those of *ROC15* and *ROC40,* are downregulated in response to light (**Beel et al., 2012, Niwa et al., 2013, Kinoshita et al., 2017, Matsuo et al., 2020**). Here, I investigated this phenomenon in the *cetl-1* mutant. RT-qPCR was performed on samples from WT and *cetl-1* cultures exposed to light for 1 h in the late night. In WT, the mRNA levels of *ROC15* and *ROC40* were much lower in the light-exposed samples than in the dark controls (**Figs 24A and 24B**). The mRNA levels of the *ROC15* and *ROC40* genes also appeared to be downregulated in the light-exposed sample of *cetl-1* (**Figs 24A and 24B**). However, the decline in mRNA levels was much lesser in the *cetl-1* mutant than in the WT (**Figs 24C**). The weak responses of both the mRNAs were restored to WT levels in the complement strain (**Fig 24D and 24E**). These results suggested that *CETL* played a role in the light responses of *ROC15* and *ROC40* mRNAs.

Circadian rhythm of clock genes in the *cetl-1* mutant

The mRNAs of certain clock genes have been shown to be rhythmic under LL conditions (**Matsuo et al., 2008**). I examined whether the *cetl-1* mutation had any effect on the expression rhythm of clock genes (*ROC15, ROC40, ROC66,* and *ROC75)* under LL conditions. The RT-qPCR analysis (**Fig 25**) revealed that all four clock genes tested in the mutant had rhythmic gene expression patterns. However, some differences were observed in certain cases. The level of *ROC15* mRNA appeared to be slightly lower in *cetl-1* mutants, whereas the *ROC40* mRNA levels appeared to be slightly higher, especially during the subjective day (**Figs 25A and 25B**). The phase of expression of *ROC40* and *ROC66* appeared to be slightly delayed in *cetl-1* mutants (**Figs 25B and 25D**). These results suggested that *CETL* might not have a great influence on the transcriptional oscillator.

3.3. DISCUSSION

Light signaling pathway for ROC15 degradation

Three possible models for light induced ROC15 degradation are depicted in **Fig 26**. A previous study indicated that a wide range of wavelengths were capable of causing ROC15 degradation (**Niwa et al., 2013**). The CSL protein, which mainly localizes in the cytoplasm, was indicated to be specific to the red/violet light signalling pathway upstream of ROC15 phosphorylation (**Kinoshita et al., 2017**) (**Fig 26**). In contrast, the clock protein ROC114, which localizes in the nucleus, was shown to be common to the different light signalling pathways downstream of ROC15 phosphorylation (**Niwa et al., 2013**) (**Fig 26**). In this study, I revealed that CETL, another protein which appears to localize in the nucleus (**Fig 11B**), is also common to the different light signalling pathways (**Fig 12**). In addition, impairment of the light induced phosphorylation in the *cetl-1* mutant (**Fig 15**) indicates that unlike ROC114, CETL plays a role upstream of ROC15 phosphorylation (**Fig 26**). Furthermore, since the blue light response that remained in the *csl* mutant was completely lost in the *csl*/*cetl* double mutant (**Fig 13**), it seems likely that these light signals are integrated downstream of CSL. The possibilities are that i) the different light signalling pathways are integrated by CETL (**Fig 26A**) or ii) at another unidentified component X upstream of CETL (**Fig 26B**). In addition, there also exists a possibility where CETL is essential for the expression of other unknown components (X and Y) that are upstream of ROC15 phosphorylation (**Fig 26C**).

Mechanisms contributing to light resetting in *C. reinhardtii*

The light resetting ability of the circadian clock was not completely lost in the *cetl-1* mutant (**Figs 20, 22 and 23**) despite a defect in the light-induced degradation of ROC15 in response to a wide range of wavelengths (**Fig 12**). This pattern points to the possibility of other mechanisms regulating the light-induced resetting of the *C. reinhardtii* circadian clock. One such mechanism is the light response of the mRNAs of clock genes, such as *C3, ROC15, ROC40,* and *ROC75* (**Beel et al., 2012, Niwa et al., 2013, Kinoshita et al., 2017, Matsuo et al., 2020**). The light-induced downregulation of *ROC15* and *ROC40* mRNAs was diminished in the *cetl-1* mutant (**Fig 24**), which is in contrast to the trend observed in the *csl* mutant (**Kinoshita et al., 2017**). In the *csl* mutant, the red light-induced degradation of the ROC15 protein was impaired, whereas the light responses of the *ROC15* and *ROC40* mRNAs were similar to those of the WT under strong red light conditions (200 µmol m^{-2} s^{-1}) (**Kinoshita et al., 2017**). The possibility that the *csl* mutant may show a defect in the mRNA response at the weaker light intensities used in the current study (30 µmol m^{-2} s^{-1}) cannot be excluded. However, the *cetl-1* mutant is the first mutant in which a defect in both light-induced ROC15 degradation and the light responses of clock gene mRNAs was confirmed. It is intriguing that the *cetl-1* mutant did not completely lose its resetting ability (**Figs 20, 22 and 23**) even with both the potential resetting mechanisms affected. This suggests the existence of yet another contributing factor which is currently unknown.

Wide distribution of phases in the *cetl-1* mutant

Interestingly, mutants obtained using the single colony protocol exhibited a wide distribution of phases in some cases (**Fig 22**). A recent study has demonstrated that a liquid culture of *C.*

reinhardtii comprises cells in various circadian phases (**Ma et al., 2021**). Another study that analyzed co-expression networks in *C. reinhardtii* further estimated that 21-96% of cells from a culture grown in LL conditions were synchronized (**Salomé and Merchant 2021**). It has also been shown that in mammalian cells, the circadian rhythm of mother cells is resumed in daughter cells after cell division (**Nagoshi et al., 2004**). In the single colony protocol, the colonies are therefore assumed to have a distribution of phases, with each colony possessing the phase of one of the cells in the liquid culture. This phase distribution should be reset by either the 12-hour dark period or the light/dark cycles (for the WT cells). I speculate that the wide distribution of phases observed in the mutant (**Figs 22C and 23B**) is a reflection of the phase distribution of the liquid culture, possibly due to the reduced ability of the mutant to be reset by the light/dark regime before release into LL conditions. This is contrary to the narrower distribution of phases observed within a single trial of the standard protocol (**Fig 16**). This difference may also suggest that cells in patch cultures had a more uniform phase than those in liquid culture. Furthermore, the variation in the distribution of phases between trials in the mutant (**Figs 22C and 23B**) may be attributed to the variation in the synchronization of cells in the liquid culture (**Salomé and Merchant 2021**).

Comparison of CETL and ELF3

i) Similarities between CETL and ELF3

The notion that CETL is a potential homolog of ELF3 (**Figs 4B, 4C, and 7**) is extremely curious, as no obvious homolog of ELF3 has been found in *C. reinhardtii* to date (**Mittag et al., 2005, Linde et al., 2017**). Comparison of the characteristics of the two reveals three main points of similarity. The first involves their expression patterns: similar to the *ELF3* expression pattern (**Hicks et al., 2001**), *CETL* gene expression was also shown to be under circadian control, with an expression peak during subjective dusk (**Fig 9**). The second similarity is with respect to their involvement in the input pathway of the circadian clock. Our results suggest that *CETL* integrates red and blue light inputs (in addition to violet and yellow lights) into the circadian clock (**Figs 1 and 12**), which is similar to one of the roles of *ELF3* i.e., integrating red and blue light into the *A. thaliana* circadian clock (**Covington et al., 2001**). The third similarity is their close involvement with circadian-clock-related GARP proteins that are expressed at night (i.e., LUX/BOA in *A. thaliana* and ROC15 in *C. reinhardtii*). ELF3 has been shown to be directly associated with LUX and BOA in *A. thaliana* EC (**Nusinow et al., 2011**). Although there is no evidence for a direct association between CETL and ROC15, the similar localization patterns of CETL and ROC15 (**Fig 11B**) and the involvement of CETL in the ROC15 light response (**Figs 12 and 15**) suggests a close relationship between the two. Importantly, CETL was found by random screening using the GARP protein, ROC15, as an indicator. Based on these similarities, I suggest the possibility of functional conservation of the CETL and ELF3 proteins during evolution.

ii) Differences between CETL and ELF3

CETL appears to differ from *ELF3* in some aspects, with respect to its role in the clock. The first difference is regarding their effect on the input to the clock. Since the ROC15 light response was impaired in the *cetl-1* mutant (**Figs 12 and 15A**)—which is likely a loss-of-function mutant— *CETL* appears to facilitate the light input to the clock. However, it has been suggested that *ELF3* antagonizes the light input to the clock (**McWatters et al., 2000, Covington et al., 2001**). The second difference is the rhythmicity under LL and DD conditions. The *cetl-1* and the *cetl-2* mutants were found to be rhythmic under both LL (**Figs 16A, 17A, 19, 22B, and 23A**) and DD

conditions (**Figs 16A and 17A**), suggesting that *CETL* does not influence the oscillator to a great extent. In contrast, the *elf3* mutant was found to be arrhythmic under LL conditions (**Covington et al., 2001**) and conditionally arrhythmic under DD conditions, depending on the reporter used (**Hicks et al., 1996, Covington et al., 2001, Thines and Harmon 2010**). These results suggest that CETL has a weaker influence on the oscillator than ELF3. The third difference is with respect to the regulation of clock-related Myb transcription factor genes (i.e., *LHY*/*CCA1* in *A. thaliana* and *ROC40* in *C. reinhardtii*). The *elf3* mutant shows lower *LHY/CCA1* levels than the WT (**Kikis et al., 2005**). ELF3 is also known to repress the gene expression of the *PSEUDO RESPONSE REGULATOR* 9 (PRR9) (**Dixon et al., 2011**), which is also one of the transcriptional repressors of *LHY/CCA1* (**Farré et al., 2005, Nakamichi et al., 2010**). It has therefore been proposed that ELF3 indirectly activates *LHY/CCA1* by repressing the gene expression of the *LHY/CCA1* repressors such as PRR9 (**Kolmos et al., 2011**, **Dixon et al., 2011**). In contrast, the *ROC40* expression was not greatly affected or was slightly upregulated in the *cetl-1* mutant (**Fig 25B**). In the mutant, the slightly higher level of expression of *ROC40* may be associated with the weak light-induced downregulation of *ROC40* mRNAs (**Figs 24 and 25B**), or possibly an indirect effect of the impaired light-induced degradation of ROC15 (**Figs 1 and 12**). These differences may be due to the potential differences between the circadian clock systems of *C. reinhardtii* and *A. thaliana*.

3.4. CONCLUSION

The possibility of the existence of an ELF3 homolog opens up many avenues of exploration that would enable further elucidation of the *C. reinhardtii* circadian clock. One such avenue is the existence of an EC in *C. reinhardtii*, since *C. reinhardtii* also has a potential homolog of the other EC component, ELF4 (**Mittag et al., 2005, Linde et al., 2017**). ELF3 has been shown to have thermo-sensing abilities due to a prion-like domain (**Jung et al., 2020**) and is shown to be involved in temperature entrainment of the *A. thaliana* clock (**Thines and Harmon 2010**). Therefore, another possibility is that *CETL* plays a role in the integration of temperature signals to the clock. In *C. reinhardtii*, the C1 and C3 subunits of the clock-related protein complex, CHLAMY1, can integrate temperature information into the circadian clock (**Voytsekh et al., 2008**). This may provide a gateway to study the involvement of CETL in temperature integration into the circadian clock. In conclusion, this study has revealed many pathways that could be explored to improve our understanding of temporal organization in *C. reinhardtii* and the evolution of circadian clocks in Viridiplantae.

4. CHAPTER 2

Role of the blue-light photoreceptor pCRY in the light induced degradation of ROC15

4.1. INTRODUCTION

Cryptochromes

The effects of different wavelengths and the input to the clock has been explored to identify photoreceptors involved in resetting. This brings into picture the photoreceptor Cryptochrome.

Cryptochromes (CRY) are known to mainly receive blue and UV-A light (**Ahmad and Cashmore, 1993**) and belong to the cryptochrome/photolyase super-family (**Kanai et al., 1997, Lin and Todo, 2005**). However, it shows no photolyase activity (**Lin et al., 1995**, **Hsu et al., 1996**, **Selby and Sancar 1999**) even though it shows sequence similarity to DNA photolyases (**Ahmad and Cashmore, 1993**). Most Cryptochromes are comprised of two domains: a chromophore binding domain called Photolyase-related (PHR) region and a carboxyl terminal domain that varies in length and is highly diverged (**Todo 1999, Cashmore et al., 1999**). The chromophore binding domain binds to two chromophores: Flavin adenine dinucleotide (FAD) and pterin (methenyltetrahydrofolate, MTHF) (**Lin et al., 1995**, **Malhotra et al., 1995, Hsu et al., 1996**)**.** FAD has three redox states and this governs the wavelength of light cryptochromes can absorb (**Sancar 2003**)**.** This photoreceptor is ubiquitous and is present in plants and animals, however, homology studies suggest that Cryptochromes in plants and animals are a result of independent evolutionary events (**Cashmore et al., 1999**). Based on this, Cryptochromes are mainly classified into two Sub-families: Animal Cryptochromes and Plant Cryptochromes. However, there are some CRYs that have maintained their DNA repair activity (**Selby and Sancar, 2006**, **Pokorny et al., 2008**). These are classified into a third sub-family: CRY-DASH (**Hitomi et al., 2000, Brudler et al., 2003**).

Cryptochromes and the Circadian clock

Cryptochromes have been identified to participate in the circadian clock of animals, plants and green algae like *C. reinhardtii*. However, the nature and extent of their involvement varies between organisms.

Animal Cryptochromes

Cryptochrome has been well studied in the fruit fly *D. melanogaster* and mammals such as mouse. In both organisms Cryptochrome has been shown to be involved in the circadian clock. In case of *D. melanogaster*, Cryptochrome's light dependent interaction with the clock protein TIM, resulting in the eventual degradation of TIM, is associated with resetting of the *D. melanogaster* circadian clock in response to light (**Myers et al., 1996, Ceriani et al., 1999**). It was

also identified however, that it might not be the only photoreceptor involved in resetting (**Stanewsky et al., 1998**). Additionally, it was also shown to play a role in the peripheral oscillators of *D. melanogaster* in a light independent manner (**Krishnan et al., 2001**).

In mammals, two Cryptochromes: CRY1 and CRY2 were identified in mice. Their involvement in the circadian clock was identified by the observation that the *cry1cry2* double knockout mice were arrhythmic in constant dark conditions (**Van Der Horst et al., 1999**). Both form a complex with the clock protein period (PER) to form the negative element of the transcription- translation feedback loop, inhibiting their own transcription by acting on the positive elements BMAL1 and CLOCK (**Griffin et al., 1999**). Their role in photic resetting of the clock was shown to be redundant with other photoreceptors (**Selby et al., 2000**).

Plant Cryptochromes

Three *CRY* genes were identified in the *A. thaliana* genome (*CRY1-3).* While both CRY1 and CRY2 are photoreceptors, CRY3 was identified to belong to the CRY-DASH sub-family and was found to also possess DNA repair properties (**Ahmad and Cashmore 1993**, **Kleine et al., 2003, Brudler et al., 2003, Selby and Sancar 2006, Pokorny et al., 2008**). Both CRY1 and CRY2 are involved in blue light responses, although, CRY1 was shown to mediate higher intensities of blue light than CRY2 (**Lin et al., 1998**). CRY1 was also shown to be more stable than CRY2 in response to green and UV-A light in addition to blue light (**Lin et al., 1998**). In contrast to the animal Cryptochromes, plant Cryptochromes appear not to be part of the circadian oscillator (**Devlin and Kay 2000**) although, the expression of both genes was found to be under circadian control (**Harmer et al., 2000**). CRY1 was implicated in the blue light signalling to the clock as the *cry1* mutant showed period lengthening under constant blue light conditions (**Somers et al., 1998, Devlin and Kay 2000**). In contrast, *cry2* mutation was shown not to have a major effect on the circadian rhythm under blue light (**Devlin and Kay 2000**). However, phase resetting in response to blue light was revealed to be impaired in the *cry1cry2* double mutant (**Yanovsky et al., 2001**). Plant Cryptochromes also appear to be involved in red light signalling to the clock through their interaction with the red light photoreceptors Phytochrome A and B (PHYA and PHYB) (**Devlin and Kay 2000, Màs et al., 2000**).

Cryptochromes in *C. reinhardtii*

C. reinhardtii shows the presence of mainly two Cryptochromes: animal CRY (aCRY) and plant CRY (pCRY) (**Beel et al., 2012**). A CRY-DASH homolog was also identified (**Beel et al., 2012**). *C. reinhardtii* CRYs appear to be different in many ways compared to other CRYs. The first point of difference is their wavelength specificity. CRYs are generally regarded as blue light and UV-A photoreceptors (**Ahmad and Cashmore, 1993**). However, pCRY also known as CPH1 was shown to undergo proteasome mediated degradation in response to both blue and red light (**Reisdorph and Small, 2004**) and aCRY was shown to be capable of absorbing red light in its neutral radical state *in vitro* in addition to absorbing blue light in its oxidized state (**Beel et al., 2012**). The second difference is their role in the circadian clock. In contrast to *A. thaliana* CRYs which are mainly involved in the light input to the clock (**Devlin and Kay 2000, Yanovsky et al., 2001**), *C. reinhardtii* pCRY appears to be associated with the circadian oscillator and light input to the clock due to the rhythm phenotype of the *pCRY* mutant in constant darkness and altered phase resetting of the mutant respectively (**Müller et al., 2017**). While, the exact nature of involvement of aCRY in

the circadian clock is unclear, it appears to regulate the mRNA levels of circadian clock associated genes such as C3 subunit of CHLAMY1, *ROC15* and *ROC55* in response to red and blue light (**Beel et.al., 2012**). Additionally, unlike CRYs in animals *C. reinhardtii* aCRY shows some photolyase activity (capable of repairing 6-4 photoproducts) (**Franz et al., 2018**).

In this second study, I chose a reverse genetics approach and aimed to further elucidate the role of pCRY, which has been identified to play a role in blue-light resetting (**Müller et al., 2017**), in the light induced degradation of ROC15.

4.2. RESULTS

Light induced degradation of ROC15 in a *pCRY* mutant

The relationship between pCRY and light induced ROC15 degradation was explored by observing the ROC15-LUC fusion protein in a *pCRY* mutant. This mutant was generated via CRISPR/Cas9 gene editing technique and possess an insertion of a hygromycin resistance gene in the second exon of the *pCRY* gene. The mutant was exposed to blue light at two intensities (0.2 µmol m^{-2} s^{-1} and 2 µmol m^{-2} s^{-1}). At an intensity of 0.2 µmol m^{-2} s^{-1}, the *pCRY* mutant did not show an acute decrease in ROC15 bioluminescence (**Fig 27A**)**.** Additionally, unlike the WT, the mutant did not show an acute decrease in ROC15 bioluminescence even in response to blue light of an intensity of 2 µmol m^{-2} s^{-1} (**Fig 27B**). The mutant was also exposed to other wavelengths of light (Violet, yellow and red) at two intensities (0.2 µmol m^{-2} s^{-1} and 2 µmol m^{-2} s^{-1}). Interestingly, an acute decrease in ROC15 bioluminescence was not observed in response to any of the wavelengths tested, at both intensities (**Fig 27**). From these results it appears that the *pCRY* mutant has an impaired ROC15 light response across a wide range of visible wavelengths.

Light induced ROC15 phosphorylation in the *pCRY* mutant

To further explore the nature of the relationship between pCRY and ROC15, the light induced phosphorylation of ROC15 was observed in the *pCRY* mutant. A genetic cross was performed to obtain a progeny harbouring *pCRY* mutation and expressing ROC15-HA. Light induced phosphorylation of ROC15 can be observed in the WT as an electrophoretic mobility shift of ROC15-HA (**Niwa et al., 2013**) (**Figs 15 and 28**). This shift was not observed in the *pCRY* mutant in response to both red and blue light (**Fig 28**). Additionally, ROC15-HA was detected in the *pCRY* mutant even 15 minutes after exposure to red and blue light pulses (**Fig 28**). These results suggest that *pCRY* is required for both, red and blue light induced phosphorylation of ROC15.

4.3. DISCUSSION

Light signaling pathway for ROC15 degradation

The results of pCRY from this study indicate that pCRY is also common to both red/violet and blue light signalling pathways (**Fig 27**) and plays a role upstream of light induced ROC15 phosphorylation (**Fig 28**). Taken together these results indicate that while red/violet and blue lights follow different pathways, they are possibly integrated downstream of CSL. While there exists a chance that the red/violet and blue light pathways integrate at CETL (**Fig 26A**), preliminary data [**Experiments performed by Cheng-Jen-Yin**] indicate that CSL is required for the red light induced mobility shift of pCRY, but not for its blue light dependent mobility shift.

This, along with the information that pCRY is a known blue light receptor and that CETL possess no recognizable chromophore binding domains (**Figs 4B and 7**), and that CETL appears to be stable in response to blue and red light (**Fig 11A**), makes the scenarios presented in **Figs 26B** and **26C** more likely compared to the scenario in **Fig 26A**. However, the nature of interaction between pCRY and CETL needs to be clarified to fully understand the light signalling pathway for ROC15 degradation.

Light resetting of *C. reinhardtii*

Blue light was found to be highly effective in resetting the clock of the CC-124 strain of *C. reinhardtii* (**Forbes-Stovall et al., 2014**). Phase resetting in response to blue light revealed that a *pCRY* mutant generated by RNAi was more sensitive to blue light than the WT, suggesting that pCRY might be a negative modulator for resetting (**Forbes-Stovall et al., 2014**). A later study involving a *pCRY* mutant generated by insertional mutagenesis also revealed that blue-light resetting of the clock was altered in the *pCRY* mutant. However, the ability to reset was not lost in this mutant (**Müller et al., 2017**). In the current study, while the resetting of the *pCRY* mutant has not been directly tested, the role of pCRY in one of the mechanisms for clock resetting was explored i.e. light induced degradation of ROC15 (**Niwa et. al., 2013**). As observed in **Fig 26,** the ROC15 degradation of the *pCRY* mutant was impaired in response to many wavelengths of light. Indicating that pCRY is required for the process. This result, together with the impaired light resetting of the *roc15* mutant (**Niwa et al., 2013**) makes it likely that phase resetting is also affected in the *pCRY* mutant used in the current study. Although, this is yet to be tested.

However, taking into consideration the prior investigations of pCRY (**Forbes-Stovall et al., 2014**, **Müller et al., 2017)** along with the results of the current investigation it appears that there might be more than one molecular mechanism for the light resetting of the *C. reinhardtii* circadian clock. It is also possible that multiple photoreceptors are involved in the response of a single wavelength.

4.4. CONCLUSION

This study revealed the role of the photoreceptor pCRY in one of the possible mechanisms for the light resetting in *C. reinhardtii* circadian clock i.e. light induced degradation of the clock protein ROC15 (**Niwa et al., 2013**). The results suggest that pCRY is essential for the process (**Figs 26 and 27**). The study has brought us one step closer to understanding the *C. reinhardtii* circadian clock. It is however necessary to explore not only the light induced phase shift of the *pCRY* mutant used in the current study, in addition to also exploring aspects such as light response of mRNA of clock related genes, resetting phenotype of the *aCRY* mutant and possibly an *aCRYpCRY* double mutant to fully understand the light resetting of the *C. reinhardtii* circadian clock.

5. GENERAL DISCUSSION

This study revealed two more participants of the light signalling pathway for ROC15 degradation i.e. CETL and pCRY. However, the interaction between CETL and pCRY is essential to understand the pathway completely. It is also interesting that pCRY appears to play a role downstream of CSL in the red light pathway, suggesting that the red light is initially received by another component. Additionally, the results of the *cetl-1* mutant and the phase resetting of the *pCRY* mutant (**Müller et al., 2017**), suggest it would be interesting to explore alternate mechanisms for light resetting of the *C. reinhardtii* clock. The absorption spectrum of the photoreceptor aCRY and its effect on mRNA levels of clock genes in response to light (**Beel et al., 2012**) make it an interesting gateway for further exploration of light resetting in *C. reinhardtii.*

Here, it is also intriguing to compare the roles of *C. reinhardtii* pCRY and *A. thaliana* CRYs. It appears that the *C. reinhardtii* pCRY resemble the *A. thaliana* CRYs in function. For example, its role downstream of CSL in the red light pathway suggests that red light is initially received by another photoreceptor. This resembles the red light signalling pathway in *Arabidopsis*. CRY1 was found to be required for red light signalling through the photoreceptor Phytochrome A (PhyA) (**Devlin and Kay 2000**). Similarly, PhyB was found to be required for the complete functioning of CRY2 (**Màs et al., 2000**). While *C. reinhardtii* has candidate red light photoreceptors such as aCRY (**Beel et al., 2012**), no known homolog Phytochrome has been identified (**Merchant et al., 2007, Li et al 2015**). Therefore, it would be interesting to explore the interaction between aCRY and pCRY in addition to using pCRY to identify the red-light photoreceptor.

While this similarity exists in the CRY function, the target of CRY in *C. reinhardtii* and *A. thaliana* is slightly different. This study showed that pCRY was involved in the light induced degradation of the LUX homolog ROC15. However, in *A. thaliana* there is no indication of LUX undergoing degradation in response to light and there is no indication of CRY affecting LUX in a similar manner (**Kozma-Bognár and Krisztina Káldi 2008, Oakenfull and Davis 2017**).

Additionally, deciphering the interaction between CETL and pCRY would be interesting when compared to the relationship between ELF3 and CRYs in *A. thaliana.* While, no direct interaction has been established between the two, ELF3 appears to be involved in the COP1 (an E3 ubiquitin ligase) mediated degradation of the clock associated protein GI and appears to play a role downstream of CRY2 in the process (**Yu et al., 2008**).

In conclusion, there are some similarities between the *C. reinhardtii* and *A. thaliana* clock regarding the function of CETL and pCRY such as their role in light input to the oscillator. However, the nature of involvement in the process and extent of participation in the circadian clock appears to be slightly different. In case of CETL, it appears to mediate light positively to the oscillator contrary to the antagonistic effect shown by ELF3 (**McWatters et al., 2000, Covington et al., 2001,**). Furthermore, unlike ELF3 it appears not play a critical role in the oscillator itself. In case of pCRY, its participation in the light induced degradation of the LUX homolog ROC15, is unique to *C. reinhardtii* in comparison to *A. thaliana.* These results therefore indicate a divergence in the light resetting and overall structure of the clock in Viridiplantae. Therefore, there are still a lot of questions that remain unanswered when it comes to the clocks of green algae and land plants. One of them being that the clock architecture is still not completely understood in many members of the sub-kingdom Viridiplantae. In the way exploring

the evolution of CRYs gave a hint to the nature of plant circadian clocks (**Cashmore et al., 1999**), elucidation of the light resetting in *Chlamydomonas* will further help deepen the understanding of the circadian clock and its evolutionary basis.

6. MATERIALS AND METHODS

Strains and media: I used the ROC15-LUC mating type $^{+}$ (mt^{+}) and mating type $^{-}$ (mt^{-}) (**Niwa et al., 2013**), CBR (mt^{+}) (**Matsuo et al., 2008**), BR (mt^{+}) (**Niwa et al., 2013**), *b19* (*cetl-2*) (mt^{+}) (**Kinoshita et al., 2017**), *csl* (mt^{+}) (**Kinoshita et al., 2017**), and ROC15-HA (mt^{+}) (**Niwa et al., 2013**) strains. The *pCRY* mutant was acquired from Dr. Simon Kelterborn and Dr. Peter Hegemann (Humboldt University, Berlin). The *pCRY* mutation was introduced into a *C. reinhardtii* strain possessing *ROC15-LUC* via CRISPR/Cas9 gene editing technique. BR is a reporter-less strain used to measure background noise during bioluminescence monitoring experiments. All strains were maintained on agar plates containing with Tris-acetate-phosphate (TAP) (**Gorman et al., 1965**) medium and stored in constant white light conditions (10-20 µmol m^{-2} s^{-1}) at 24 ˚C (storage culture). The storage cultures were re-plated every 1-1.5 months. A high-salt (HS) medium (**Sueoka 1960**) was also used in this study. All *C. reinhardtii* strains used in this study were derived from the CBR34 strain (**Matsuo et al., 2008**), which was obtained from a genetic cross between a CC2137-based reporter strain (*tufA* promoter-*lucCP*) (**Matsuo et al., 2006**) and the SAG11-32a WT strain.

Light sources: The light sources that were used in this study are detailed henceforth. LED tubes (red LED: LT20RS, 636 nm [full width at half maximum of 21 nm]; blue LED: LT20BS, 458 nm [21 nm], Beamtec, Saitama, Japan) were used for mutant screening (**Figs 1**, **2, 3, 6B and 10C**). LED panels (red LED: ISL-150×150-RR, 660 nm [24 nm], yellow LED: ISL-150×150-YY, blue LED: ISL-150×150-BB, 470 nm [27 nm], violet LED: ISL-150×150-VV, 405 nm [14 nm], CCS, Kyoto, Japan) were used for light pulse and wavelength specificity experiments (**Figs 1B, 1C, 2B, 2C, 6E, 6F, 10F, 10G, 12, 13, 15, 20, 26, 27**). The wavelength of the yellow LED was measured using a multi-channel spectrometer (MC2100, Otsuka Electronics, Osaka, Japan). The peak was detected at 570nm [11nm]. White LED panels (MLP-LSK2478DA5, Musashi Electric, Saitama, Japan) and white LED tubes (LT-40KY-III, Beamtec, Saitama, Japan) were used as background light during rhythm assays (**Figs 16A, 17A, 18, 19, 22, and 23**). Light intensity was measured with a light meter (LI-250 equipped with LI-190, LI-COR, NE, USA; LA-105, NK systems, Osaka, Japan). Blue LEDs were used as safety lights at lower intensities that were undetectable by the light meters. Fluorescent tubes (FL20SSW/18-B, Hitachi, Tokyo, Japan) were used for culturing and mRNA analysis (**Figs 9, 24, and 25**).

Culture conditions: The three main types of cultures used in the study are detailed below.
1. Unsynchronized TAP cultures: Cells from the storage cultures were inoculated into TAP medium and maintained at 24 °C in LL (30-40 µmol m^{-2} s^{-1}) for 3-4 days (starter culture). Cells from starter cultures were then inoculated into fresh TAP medium to achieve a final concentration of 1×10^5 cells/mL and maintained under the same conditions as the starter culture for 2 days.
2. LD-entrained and free-running HS cultures were prepared as previously described (**Matsuo et al., 2020**). Briefly, starter cultures were inoculated into fresh HS medium at a concentration of

2×10^5 cells/mL and maintained at 24 °C in LL (30-40 μmol m^{-2} s^{-1}) for 3 days. The temperature was then reduced to 17 °C, and lights turned off for 12 hours to synchronize the circadian clock. After the synchronization period, the LD-entrained cultures were maintained in a 12-hour light (10 μmol m^{-2} s^{-1})/12-hour dark cycle, and free-running cultures were kept in LL conditions (10 μmol m^{-2} s^{-1}).
3. Spot cultures for bioluminescence monitoring: Cells were cultured for 3 days in 96 well plates (Nunc MicroWell, Thermo Fisher Scientific, MA, USA) in 100 μL of TAP medium maintained at 24 °C in LL conditions (30-40 μmol m^{-2} s^{-1}). Following this, 5 μL of culture was spotted onto 1.5% HS agar plates (Agar BA-70, Ina Food Industry, Nagano, Japan was used for rhythm assays and Agar against dryness (LG), Kanto Chemical, Tokyo, Japan was used for light response assays). The spots were allowed to grow for 4 days at 24 °C in LL conditions (30-40 μmol m^{-2} s^{-1}).

Genetic crosses and TAIL-PCR Genetic crosses and TAIL-PCR were performed as described previously (**Matsuo et al., 2008**).

Plasmid construction: To obtain the pLaadA/CETL plasmid, the blunt-ended 11.9 kb SacI/BamHI fragment from a bacterial artificial chromosome containing the *CETL* gene— obtained from the C9 strain— was sub-cloned into the EcoRV-digested pLaadA plasmid (**Kinoshita et al., 2017**). This fragment also contained the 264 nucleotide insertion. To obtain pLaadA/HA-CETL plasmid, an EcoRV restriction site was introduced just after the second predicted start codon of CETL in the pLaadA/CETL plasmid by PCR-based mutagenesis. A codon adapted HA sequence (**10B Fig**) was inserted at the EcoRV site by using In-Fusion technology (TakaRa Bio, Shiga, Japan).

Bioluminescence monitoring: Cultures were transferred into 96 well white plates (Nunc F96 MicroWell, Thermo Fisher Scientific), 96 well black plates (STREIFEN-PLATTE [762076], Greiner Bio-One, Kremsmünster, Austria), or 24 well black plates (Krystal Microplates, Porvair Sciences, Norfolk, UK). In cases where spot cultures needed to be transferred, the spots on the agar were cut along with the agar and transferred into wells using a glass tube (inner diameter: 6 mm). Luciferase substrates were added to each well at a final concentration of 100 μM (liquid cultures) or approximately 200 μM (spot cultures). D-luciferin (Biosynth, Staad, Switzerland) was used unless specifically mentioned, and the luciferin analog Akalumine-HCL (FUJIFILM Wako Pure Chemical Corporation, Osaka, Japan) was used in some experiments (**Kuchimaru et al., 2016**). Bioluminescence was monitored at 24 °C using a custom-made automatic bioluminescence apparatus (**Okamoto et al., 2005a**) and commercially available instruments (CL24A-LIC and CL96S-4, Churitsu Electronic Corporation, Nagoya, Japan). In each cycle, bioluminescence was measured after at least 3.5 min of dark exposure to ensure a decrease in delayed light emission of chlorophyll. The results of bioluminescence monitoring were analyzed using the Rhythm analysis program, RAP (**Okamoto et al., 2005b**) and Kaiseki NINJA (Churitsu Electronic Corporation, Nagoya, Japan). Bioluminescence rhythm data were de-trended by dividing by the 24-hour moving average. The Cosinor-rhythmometry method was used to analyze bioluminescence rhythm data over 3-4 days. Data for which the curve fitting was obviously inaccurate or had a high error index (>0.055) were not considered for further analysis. For the analysis of the ROC15-LUC reporter, luminescence detected in empty wells or in cultures of the reporter-less BR strain was considered background noise and subtracted unless specifically mentioned.

Transformation: Transformation of *the C. reinhardtii* nuclear genome was achieved by electroporation, as described previously (**Shimogawara et al., 1998, Niwa et al., 2013**). For

mutagenesis, ROC15-LUC mt^+ was used as a host strain for transformation with the *aph7"* fragment. The *aph7"* fragment for mutagenesis was obtained by digesting the plasmid pHyg3 (**Berthold et al., 2002**) with the HindIII restriction endonuclease. The 1.7 kb fragment was purified after agarose gel electrophoresis, and 30 ng of DNA (/~3 × 10^7 cells) was used for the transformation. Transformants were selected on TAP agar plates with a final hygromycin concentration of 30 µg/mL. For complementation, the pLaadA/CETL plasmid was digested with the PacI restriction endonuclease. The resulting 14.3 kb fragment was purified after agarose gel electrophoresis. DNA fragments (300 ng /~3 × 10^7 cells) were used for transformation, and transformants were selected on TAP agar plates with a final spectinomycin concentration of 50 µg/mL.

Mutant/complement screening: The transformant colonies were inoculated into 100 µL of TAP medium and maintained in 96 well plates (Nunc MicroWell, Thermo Fisher Scientific) for 3 days at 24 °C in LL conditions (30-40 µmol m^{-2} s^{-1}). Following this, 5 µL of the culture was transferred into 100 µL of fresh TAP medium containing D-luciferin (final concentration, 100 µM) in 96 well white plates (Nunc F96 MicroWell, Thermo Fisher Scientific). The plates were maintained at 24 °C in LL conditions (30-40 µmol m^{-2} s^{-1}) for 1 day before bioluminescence monitoring. Bioluminescence was monitored using a custom-made automatic bioluminescence apparatus (**Okamoto et al., 2005a**).

Protein analysis: Western blot analysis was performed as previously described (**Niwa et al., 2013**). Polyacrylamide gel (12.5%) (e-PAGEL, ATTO Corporation, Tokyo, Japan) was used for the observation of light-induced phosphorylation of ROC15 (**Figs 15 and 27**) and 7.5% polyacrylamide gel (e-PAGEL, ATTO Corporation) was used for the detection of HA-CETL (**Figs 11A and 10E**). The transfer step was performed using a Qblot kit, EZ blot kit and EZFastBlot *HMW* kit (ATTO Corporation)). BLOCK ACE Powder (KAC, Kyoto, Japan) was used to block the membranes. Rat monoclonal anti-HA antibody was used as the primary antibody (1:10000, clone 3F10, Roche, Basel, Switzerland). Horseradish peroxidase-conjugated goat anti-rat IgG was used as a secondary antibody (1:25000, Merck KGaA, Darmstadt, Germany).

Immunocytochemistry was performed as described previously (**Niwa et al., 2013**). Rat monoclonal anti-HA (1:1000) and mouse monoclonal anti-NPC (1:1000, clone MAb414, Labcorp, NC, USA) were used as primary antibodies. Alexa Fluor 488-conjugated goat anti-rat IgG (Thermo Fisher Scientific) and Alexa Fluor 647-conjugated goat anti-mouse IgG (Thermo Fisher Scientific) were used as secondary antibodies. Fluorescence was observed using a laser scanning confocal fluorescence microscope (FV10i-DOC; Olympus, Tokyo, Japan).

RT-qPCR: RT-qPCR was performed as described previously (**Kinoshita et al., 2017**). The primers used for quantification of *ROC15, ROC40*, *ROC66, ROC75,* and *RCK1* transcripts are the same as previously described (**Matsuo et al., 2020**). Primers used for quantification of *CETL* transcript are listed in Table 1.

7.AKNOWLEDGEMENTS

I would like to thank Nagoya University for giving me the opportunity to pursue my Doctoral degree at their esteemed institution. I would also like to thank my advisor Dr. Matsuo Takuya for his constant support during extremely difficult times. I also want to thank him for the guidance and advice throughout and for always taking the time to clarify my doubts and concerns. I am truly grateful to have had the opportunity to work as his student.

Next, I would like to express my gratitude to all the other members of Dr. Matsuo's lab. Ms. Ohmura Ayumi, Ms. Ozawa Mariko and Ms. Tatsukawa Yayoi for their kind assistance with the experiments and for taking the time to clarify any doubts about how to perform experiments. I thank Mr. Imai Kohei for the endless discussions, his inputs on presentations and his ever so kind support during difficult and tiring times. I also thank Ms. Okumura Yu and Ms. Tishadas Shivvani for their assistance with experiments. I would also like to thank Mr. Cheng-Jen-Yin for his assistance in the Cryptochrome related experiments.

I would like to thank Dr. Simon Kelterborn (Humboldt University) and Dr. Perter Hegemann (Humboldt University) for providing the *pCRY* mutant used in this study. I would also like to thank Dr. Fukuzawa Hideya (Kyoto University) and Dr. Yamano Takashi (Kyoto University) for providing the BAC clone carrying the Cre07.g357500 fragment. Next, I would like to thank Kuroki Yoko (RIKEN), Toyoda Atsushi (National Institute of Genetics), Fujiyama Asao (National Institute of Genetics) and Kohara Yuji (National Institute of Genetics) for contributions to the BAC library construction and end – sequence database development. I want to extend my gratitude to the Japanese Ministry of Education, Culture, Sports, Science, and Technology (MEXT scholarship) (2016-2018) and the Sato Yo International Scholarship Foundation (SISF) (2018-2021) for financial support of living expenses during the term of the project.

I would also like to thank Dr. Sugiyama Shin for helping me during the tough pandemic years by giving me part time work which ended up giving me a way to organize my thoughts. I would also like to express my gratitude to Dr. Hori Hiroshi for helping me during the time I injured my leg. Last, but not least, I would express gratitude to my friends and my family for their constant support and guidance from many miles away.

8. REFERENCES

1. Ahmad M, Cashmore AR. HY4 gene of *A. thaliana* encodes a protein with characteristics of a blue-light photoreceptor. Nature. 1993;366: 162–166. doi:10.1038/366162a0

2. Arthur JM, Guthrie JD, Newell JM. Some Effects of Artificial Climates on the Growth and Chemical Composition of Plants. Am J Bot. 1930;17: 416–482. doi:10.2307/2435930

3. Aschoff J. Circadian rhythms in man. Science. 1965;148: 1427–1432. doi:10.1126/science.148.3676.1427

4. Aschoff J. Exogenous and endogenous components in circadian rhythms. Cold Spring Harb Symp Quant Biol. 1960;25: 11–28. doi:10.1101/sqb.1960.025.01.004

5. Beel B, Prager K, Spexard M, Sasso S, Weiss D, Müller N, et al. A flavin binding cryptochrome photoreceptor responds to both blue and red light in *Chlamydomonas reinhardtii.* Plant Cell. 2012;24: 2992–3008. doi:10.1105/tpc.112.098947

6. Berthold P, Schmitt R, Mages W. An engineered *Streptomyces hygroscopicus* aph 7" gene mediates dominant resistance against hygromycin B in *Chlamydomonas reinhardtii*. Protist. 2002;153: 401–412. doi:10.1078/14344610260450136

7. Bruce VG. Environmental Entrainment of Circadian Rhythms. Cold Spring Harb Symp Quant Biol. 1960;25: 29–48. doi:10.1101/SQB.1960.025.01.005

8. Bruce VG. The biological clock in *Chlamydomonas reinhardi*. J Protozool. 1970;17: 328–334. doi:10.1111/j.1550-7408.1970.tb02380.x

9. Brudler R, Hitomi K, Daiyasu H, Toh H, Kucho K-I, Ishiura M, et al. Identification of a new cryptochrome class. Structure, function, and evolution. Mol Cell. 2003;11: 59–67. doi:10.1016/s1097-2765(03)00008-x

10. Burki F. The eukaryotic tree of life from a global phylogenomic perspective. Cold Spring Harb Perspect Biol. 2014;6: a016147. doi:10.1101/cshperspect.a016147

11. Byrne TE, Wells MR, Johnson CH. Circadian rhythms of chemotaxis to ammonium and of methylammonium uptake in *chlamydomonas*. Plant Physiol. 1992;98: 879–886. doi:10.1104/pp.98.3.879

12. Cashmore AR, Jarillo JA, Wu YJ, Liu D. Cryptochromes: blue light receptors for plants and animals. Science. 1999;284: 760–765. doi:10.1126/science.284.5415.760

13. Ceriani MF, Darlington TK, Staknis D, Más P, Petti AA, Weitz CJ, et al. Light-dependent sequestration of TIMELESS by CRYPTOCHROME. Science. 1999;285: 553–556. doi:10.1126/science.285.5427.553

14. Covington MF, Panda S, Liu XL, Strayer CA, Wagner DR, Kay SA. ELF3 modulates resetting of the circadian clock in *Arabidopsis*. Plant Cell. 2001;13: 1305–1315. doi:10.1105/tpc.13.6.1305

15. Cs P. The circadian oscillation in *Drosophila pseudoobscura* pupae: a model for the photoperiodic clock. Z Pflanzenphysiol. 1966;54: 275–307. Available: https://ci.nii.ac.jp/naid/10030580177/

16. Daan S. Colin Pittendrigh, Jürgen Aschoff, and the Natural Entrainment of Circadian Systems. J Biol Rhythms. 2000;15: 195–207. doi:10.1177/074873040001500301

17. Daan S. Tonic and phasic effects of light in the entrainment of circadian rhythms. Ann N Y Acad Sci. 1977;290: 51–59. doi:10.1111/j.1749-6632.1977.tb39716.x

18. de Mairan JJ. Observation botanique. Histoire de l'Academie Royale des Sciences Paris. 1729 [cited 15 Dec 2022]. Available: https://ci.nii.ac.jp/naid/10021910265/

19. Devlin PF, Kay SA. Cryptochromes are required for phytochrome signaling to the circadian clock but not for rhythmicity. Plant Cell. 2000;12: 2499–2510. doi:10.1105/tpc.12.12.2499

20. Dixon LE, Knox K, Kozma-Bognar L, Southern MM, Pokhilko A, Millar AJ. Temporal repression of core circadian genes is mediated through EARLY FLOWERING 3 in *Arabidopsis*. Curr Biol. 2011;21: 120–125. doi:10.1016/j.cub.2010.12.013

21. Djouani-Tahri E-B, Christie JM, Sanchez-Ferandin S, Sanchez F, Bouget F-Y, Corellou F. A eukaryotic LOV-histidine kinase with circadian clock function in the picoalga *Ostreococcus.* Plant J. 2011;65: 578–588. doi:10.1111/j.1365-313X.2010.04444.x

22. Dunlap JC. Molecular bases for circadian clocks. Cell. 1999;96: 271–290. doi:10.1016/s0092-8674(00)80566-8

23. Dunlap JC, Loros JJ. The *neurospora* circadian system. J Biol Rhythms. 2004;19: 414–424. doi:10.1177/0748730404269116

24. Farré EM, Harmer SL, Harmon FG, Yanovsky MJ, Kay SA. Overlapping and distinct roles of PRR7 and PRR9 in the *Arabidopsis* circadian clock. Curr Biol. 2005;15: 47–54. doi:10.1016/j.cub.2004.12.067

25. Forbes-Stovall J, Howton J, Young M, Davis G. *Chlamydomonas reinhardtii* strain CC-124 is highly sensitive to blue light in addition to green and red light in resetting its circadian clock, with the blue-light …. Plant Physiol. 2014. doi:10.1016/j.plaphy.2013.12.002.

26. Franz S, Ignatz E, Wenzel S, Zielosko H, Putu EPGN, Maestre-Reyna M, et al. Structure of the bifunctional cryptochrome aCRY from *Chlamydomonas reinhardtii*. Nucleic Acids Res. 2018;46: 8010–8022. doi:10.1093/nar/gky621

27. Fuller KK, Hurley JM, Loros JJ, Dunlap JC. 6 Photobiology and Circadian Clocks in *Neurospora*. In: Nowrousian M, editor. Fungal Genomics. Berlin, Heidelberg: Springer Berlin Heidelberg; 2014. pp. 121–148. doi:10.1007/978-3-642-45218-5_6

28. Gorman DS, Levine RP. Cytochrome f and plastocyanin: their sequence in the photosynthetic electron transport chain of *Chlamydomonas reinhardi*. Proceedings of the National Academy of Sciences. 1965. pp. 1665–1669. doi:10.1073/pnas.54.6.1665

29. Griffin EA Jr, Staknis D, Weitz CJ. Light-independent role of CRY1 and CRY2 in the mammalian circadian clock. Science. 1999;286: 768–771. doi:10.1126/science.286.5440.768

30. Grigoriev IV, Hayes RD, Calhoun S, Kamel B, Wang A, Ahrendt S, et al. PhycoCosm, a comparative algal genomics resource. Nucleic Acids Res. 2021;49: D1004–D1011. doi:10.1093/nar/gkaa898

31. Hardin PE, Hall JC, Rosbash M. Feedback of the *Drosophila* period gene product on circadian cycling of its messenger RNA levels. Nature. 1990;343: 536–540. doi:10.1038/343536a0

32. Harmer SL, Hogenesch JB, Straume M, Chang HS, Han B, Zhu T, et al. Orchestrated transcription of key pathways in *Arabidopsis* by the circadian clock. Science. 2000;290: 2110–2113. doi:10.1126/science.290.5499.2110

33. Hastings JW, Sweeney BM. The action spectrum for shifting the phase of the rhythm of luminescence in *Gonyaulax polyedra*. J Gen Physiol. 1960;43: 697–706. doi:10.1085/jgp.43.4.697

34. Hicks KA, Albertson TM, Wagner DR. EARLY FLOWERING3 encodes a novel protein that regulates circadian clock function and flowering in *Arabidopsis*. Plant Cell. 2001;13: 1281–1292. doi:10.1105/tpc.13.6.1281

35. Hicks KA, Millar AJ, Carré IA, Somers DE, Straume M, Meeks-Wagner DR, et al. Conditional circadian dysfunction of the *Arabidopsis* early-flowering 3 mutant. Science. 1996;274: 790–792. doi:10.1126/science.274.5288.790

36. Highkin HR, Hanson JB. Possible Interaction between Light-dark Cycles and Endogenous Daily Rhythms on the Growth of Tomato Plants. Plant Physiol. 1954;29: 301–302. doi:10.1104/pp.29.3.301

37. Hillman WS. Injury of Tomato Plants by Continuous Light and Unfavorable Photoperiodic Cycles. Am J Bot. 1956;43: 89–96. doi:10.2307/2438816

38. Hirota T, Fukada Y. Resetting mechanism of central and peripheral circadian clocks in mammals. Zoolog Sci. 2004;21: 359–368. doi:10.2108/zsj.21.359

39. Hirschie Johnson C, Elliott JA, Foster R. Entrainment of Circadian Programs. Chronobiol Int. 2003;20: 741–774. doi:10.1081/CBI-120024211

40. Hitomi K, Okamoto K, Daiyasu H, Miyashita H, Iwai S, Toh H, et al. Bacterial cryptochrome and photolyase: characterization of two photolyase-like genes of *Synechocystis* sp. PCC6803. Nucleic Acids Res. 2000;28: 2353–2362. doi:10.1093/nar/28.12.2353

41. Hsu DS, Zhao X, Zhao S, Kazantsev A, Wang RP, Todo T, et al. Putative human blue-light photoreceptors hCRY1 and hCRY2 are flavoproteins. Biochemistry. 1996;35: 13871–13877. doi:10.1021/bi962209o

42. Hsu PY, Harmer SL. Wheels within wheels: the plant circadian system. Trends in Plant Science. 2014. pp. 240–249. doi:10.1016/j.tplants.2013.11.007

43. Huang H, Nusinow DA. Into the Evening: Complex Interactions in the *Arabidopsis* Circadian Clock. Trends Genet. 2016;32: 674–686. doi:10.1016/j.tig.2016.08.002

44. Huang H, Alvarez S, Bindbeutel R, Shen Z, Naldrett MJ, Evans BS, et al. Identification of Evening Complex Associated Proteins in *Arabidopsis* by Affinity Purification and Mass Spectrometry. Mol Cell Proteomics. 2016;15: 201–217. doi:10.1074/mcp.M115.054064

45. Hurley J, Loros JJ, Dunlap JC. Dissecting the mechanisms of the clock in *Neurospora*. Methods Enzymol. 2015;551: 29–52. doi:10.1016/bs.mie.2014.10.009

46. Jakubcakova V, Oster H, Tamanini F, Cadenas C, Leitges M, van der Horst GTJ, et al. Light entrainment of the mammalian circadian clock by a PRKCA-dependent posttranslational mechanism. Neuron. 2007;54: 831–843. doi:10.1016/j.neuron.2007.04.031

47. Johnson CH, Kondo T, Hastings JW. Action Spectrum for Resetting the Circadian Phototaxis Rhythm in the CW15 Strain of *Chlamydomonas*: II. Illuminated Cells. Plant Physiol. 1991;97: 1122–1129. doi:10.1104/pp.97.3.1122

48. Jones MA, Hu W, Litthauer S, Lagarias JC, Harmer SL. A Constitutively Active Allele of Phytochrome B Maintains Circadian Robustness in the Absence of Light. Plant Physiol. 2015;169: 814–825. doi:10.1104/pp.15.00782

49. Jung J-H, Barbosa AD, Hutin S, Kumita JR, Gao M, Derwort D, et al. A prion-like domain in ELF3 functions as a thermosensor in *Arabidopsis.* Nature. 2020;585: 256–260. doi:10.1038/s41586-020-2644-7

50. Kageyama H, Nishiwaki T, Nakajima M, Iwasaki H, Oyama T, Kondo T. Cyanobacterial circadian pacemaker: Kai protein complex dynamics in the KaiC phosphorylation cycle

in vitro. Mol Cell. 2006;23: 161–171. doi:10.1016/j.molcel.2006.05.039

51. Kanai S, Kikuno R, Toh H, Ryo H, Todo T. Molecular Evolution of the Photolyase–Blue-Light Photoreceptor Family. J Mol Evol. 1997;45: 535–548. doi:10.1007/PL00006258

52. Kikis EA, Khanna R, Quail PH. ELF4 is a phytochrome-regulated component of a negative-feedback loop involving the central oscillator components CCA1 and LHY. Plant J. 2005;44: 300–313. doi:10.1111/j.1365-313x.2005.02531.x

53. Kinoshita A, Niwa Y, Onai K, Yamano T, Fukuzawa H, Ishiura M, et al. CSL encodes a leucine-rich-repeat protein implicated in red/violet light signaling to the circadian clock in *Chlamydomonas.* PLoS Genet. 2017;13: e1006645. doi:10.1371/journal.pgen.1006645

54. Kleine T, Lockhart P, Batschauer A. An *Arabidopsis* protein closely related to *Synechocystis* cryptochrome is targeted to organelles. Plant J. 2003;35: 93–103. doi:10.1046/j.1365-313x.2003.01787.x

55. Klemm E, Ninnemann H. Detailed action spectrum for the delay shift in pupae emergence of *Drosophila pseudoobscura*. Photochem Photobiol. 1976;24: 369–371. doi:10.1111/j.1751-1097.1976.tb06838.x

56. Koh K, Zheng X, Sehgal A. JETLAG resets the *Drosophila* circadian clock by promoting light-induced degradation of TIMELESS. Science. 2006;312: 1809–1812. doi:10.1126/science.1124951

57. Kolmos E, Herrero E, Bujdoso N, Millar AJ, Tóth R, Gyula P, et al. A reduced-function allele reveals that EARLY FLOWERING3 repressive action on the circadian clock is modulated by phytochrome signals in *Arabidopsis*. Plant Cell. 2011;23: 3230–3246. doi:10.1105/tpc.111.088195

58. Kondo T, Johnson CH, Hastings JW. Action Spectrum for Resetting the Circadian Phototaxis Rhythm in the CW15 Strain of *Chlamydomonas*: I. Cells in Darkness. Plant Physiol. 1991;95: 197–205. doi:10.1104/pp.95.1.197

59. Kozma-Bognár L, Káldi K. Synchronization of the fungal and the plant circadian clock by light. Chembiochem. 2008;9: 2565–2573. doi:10.1002/cbic.200800385

60. Krishnan B, Levine JD, Lynch MK, Dowse HB, Funes P, Hall JC, et al. A new role for cryptochrome in a *Drosophila* circadian oscillator. Nature. 2001;411: 313–317. doi:10.1038/35077094

61. Kuchimaru T, Iwano S, Kiyama M, Mitsumata S, Kadonosono T, Niwa H, et al. A luciferin analogue generating near-infrared bioluminescence achieves highly sensitive deep-tissue imaging. Nat Commun. 2016;7: 1–8. doi:10.1038/ncomms11856

62. Leliaert F, Verbruggen H, Zechman FW. Into the deep: new discoveries at the base of the green plant phylogeny. Bioessays. 2011;33: 683–692. doi:10.1002/bies.201100035

63. Li F-W, Melkonian M, Rothfels CJ, Villarreal JC, Stevenson DW, Graham SW, et al. Phytochrome diversity in green plants and the origin of canonical plant phytochromes. Nature Communications. 2015. doi:10.1038/ncomms8852

64. Lin C, Yang H, Guo H, Mockler T, Chen J, Cashmore AR. Enhancement of blue-light sensitivity of *Arabidopsis* seedlings by a blue light receptor cryptochrome 2. Proc Natl Acad Sci U S A. 1998;95: 2686–2690. doi:10.1073/pnas.95.5.2686

65. Lin C, Robertson DE, Ahmad M, Raibekas AA, Jorns MS, Dutton PL, et al. Association of flavin adenine dinucleotide with the *Arabidopsis* blue light receptor CRY1. Science. 1995;269: 968–970. doi:10.1126/science.7638620

66. Lin C, Todo T. The cryptochromes. Genome Biol. 2005;6: 220. doi:10.1186/gb-2005-6-5-220

67. Linde A-M, Eklund DM, Kubota A, Pederson ERA, Holm K, Gyllenstrand N, et al. Early evolution of the land plant circadian clock. New Phytol. 2017;216: 576–590. doi:10.1111/nph.14487

68. Liu XL, Covington MF, Fankhauser C, Chory J, Wagner DR. ELF3 Encodes a Circadian Clock–Regulated Nuclear Protein That Functions in an *Arabidopsis* PHYB Signal Transduction Pathway. Plant Cell. 2001;13: 1293–1304. doi:10.1105/TPC.000475

69. Liu Y-G, Mitsukawa N, Oosumi T, Whittier RF. Efficient isolation and mapping of *Arabidopsis thaliana* T-DNA insert junctions by thermal asymmetric interlaced PCR. The Plant Journal. 1995. pp. 457–463. doi:10.1046/j.1365-313x.1995.08030457.x

70. Loros JJ. Principles of the animal molecular clock learned from *Neurospora*. Eur J Neurosci. 2020;51: 19–33. doi:10.1111/ejn.14354

71. Ma F, Salomé PA, Merchant SS, Pellegrini M. Single-cell RNA sequencing of batch *Chlamydomonas* cultures reveals heterogeneity in their diurnal cycle phase. Plant Cell. 2021;33: 1042–1057. doi:10.1093/plcell/koab025

72. Malhotra K, Kim ST, Batschauer A, Dawut L, Sancar A. Putative blue-light photoreceptors from *Arabidopsis thaliana* and *Sinapis alba* with a high degree of sequence homology to DNA photolyase contain the two photolyase cofactors but lack DNA repair activity. Biochemistry. 1995;34: 6892–6899. doi:10.1021/bi00020a037

73. Matsuo T, Iida T, Ohmura A, Gururaj M, Kato D, Mutoh R, et al. The role of ROC75 as a daytime component of the circadian oscillator in *Chlamydomonas reinhardtii*. PLoS Genet. 2020;16: e1008814. doi:10.1371/journal.pgen.1008814

74. Matsuo T, Onai K, Okamoto K, Minagawa J, Ishiura M. Real-time monitoring of chloroplast gene expression by a luciferase reporter: evidence for nuclear regulation of

chloroplast circadian period. Mol Cell Biol. 2006;26: 863–870. doi:10.1128/MCB.26.3.863-870.2006

75. Matsuo T, Okamoto K, Onai K, Niwa Y, Shimogawara K, Ishiura M. A systematic forward genetic analysis identified components of the *Chlamydomonas* circadian system. Genes Dev. 2008;22: 918–930. doi:10.1101/gad.1650408

76. McWatters HG, Bastow RM, Hall A, Millar AJ. The ELF3 zeitnehmer regulates light signalling to the circadian clock. Nature. 2000;408: 716–720. doi:10.1038/35047079

77. Merchant SS, Prochnik SE, Vallon O, Harris EH, Karpowicz SJ, Witman GB, et al. The *Chlamydomonas* Genome Reveals the Evolution of Key Animal and Plant Functions. Science. 2007 [cited 5 Nov 2021]. doi:10.1126/science.1143609

78. Mills JN. CIRCADIAN RHYTHMS DURING AND AFTER THREE MONTHS IN SOLITUDE UNDERGROUND. J Physiol. 1964;174: 217–231. doi:10.1113/jphysiol.1964.sp007483

79. Mittag M, Kiaulehn S, Johnson CH. The circadian clock in *Chlamydomonas reinhardtii*. What is it for? What is it similar to? Plant Physiol. 2005;137: 399–409. doi:10.1104/pp.104.052415

80. Mittag M. Conserved circadian elements in phylogenetically diverse algae. Proc Natl Acad Sci U S A. 1996;93: 14401–14404. doi:10.1073/pnas.93.25.14401

81. Mohawk JA, Green CB, Takahashi JS. Central and peripheral circadian clocks in mammals. Annu Rev Neurosci. 2012;35: 445–462. doi:10.1146/annurev-neuro-060909-153128

82. Myers MP, Wager-Smith K, Rothenfluh-Hilfiker A, Young MW. Light-induced degradation of TIMELESS and entrainment of the *Drosophila* circadian clock. Science. 1996;271: 1736–1740. doi:10.1126/science.271.5256.1736

83. Más P, Devlin PF, Panda S, Kay SA. Functional interaction of phytochrome B and cryptochrome 2. Nature. 2000;408: 207–211. doi:10.1038/35041583

84. Müller N, Wenzel S, Zou Y, Künzel S, Sasso S, Weiß D, et al. A Plant Cryptochrome Controls Key Features of the *Chlamydomonas* Circadian Clock and Its Life Cycle. Plant Physiol. 2017;174: 185–201. doi:10.1104/pp.17.00349

85. Nagoshi E, Saini C, Bauer C, Laroche T, Naef F, Schibler U. Circadian gene expression in individual fibroblasts: cell-autonomous and self-sustained oscillators pass time to daughter cells. Cell. 2004;119: 693–705. doi:10.1016/j.cell.2004.11.015

86. Nakajima M, Imai K, Ito H, Nishiwaki T, Murayama Y, Iwasaki H, et al. Reconstitution of circadian oscillation of cyanobacterial KaiC phosphorylation in vitro. Science. 2005;308: 414–415. doi:10.1126/science.1108451

87. Nakamichi N, Kiba T, Henriques R, Mizuno T, Chua N-H, Sakakibara H. PSEUDO-RESPONSE REGULATORS 9, 7, and 5 are transcriptional repressors in the *Arabidopsis* circadian clock. Plant Cell. 2010;22: 594–605. doi:10.1105/tpc.109.072892

88. Nishiwaki T, Satomi Y, Nakajima M, Lee C, Kiyohara R, Kageyama H, et al. Role of KaiC phosphorylation in the circadian clock system of *Synechococcus elongatus* PCC 7942. Proc Natl Acad Sci U S A. 2004;101: 13927–13932. doi:10.1073/pnas.0403906101

89. Niwa Y, Matsuo T, Onai K, Kato D, Tachikawa M, Ishiura M. Phase-resetting mechanism of the circadian clock in *Chlamydomonas reinhardtii*. Proc Natl Acad Sci U S A. 2013;110: 13666–13671. doi:10.1073/pnas.1220004110

90. Nohales MA, Kay SA. Molecular mechanisms at the core of the plant circadian oscillator. Nat Struct Mol Biol. 2016;23: 1061–1069. doi:10.1038/nsmb.3327

91. Nusinow DA, Helfer A, Hamilton EE, King JJ, Imaizumi T, Schultz TF, et al. The ELF4–ELF3–LUX complex links the circadian clock to diurnal control of hypocotyl growth. Nature. 2011;475: 398–402. doi:10.1038/nature10182

92. O'Neill JS, Reddy AB. Circadian clocks in human red blood cells. Nature. 2011;469: 498–503. doi:10.1038/nature09702

93. Oakenfull RJ, Davis SJ. Shining a light on the Arabidopsis circadian clock. Plant Cell Environ. 2017;40: 2571–2585. doi:10.1111/pce.13033

94. Okamoto K, Onai K, Furusawa T, Ishiura M. A portable integrated automatic apparatus for the real-time monitoring of bioluminescence in plants. Plant, Cell and Environment. 2005a. pp. 1305–1315. doi:10.1111/j.1365-3040.2005.01377.x

95. Okamoto K, Onai K, Ishiura M. RAP, an integrated program for monitoring bioluminescence and analyzing circadian rhythms in real time. Analytical Biochemistry. 2005b. pp. 193–200. doi:10.1016/j.ab.2004.11.007

96. Partch CL, Green CB, Takahashi JS. Molecular architecture of the mammalian circadian clock. Trends Cell Biol. 2014;24: 90–99. doi:10.1016/j.tcb.2013.07.002

97. Pittendrigh CS, Minis DH. Circadian systems: longevity as a function of circadian resonance in *Drosophila melanogaster*. Proc Natl Acad Sci U S A. 1972;69: 1537–1539. doi:10.1073/pnas.69.6.1537

98. Pokorny R, Klar T, Hennecke U, Carell T, Batschauer A, Essen L-O. Recognition and repair of UV lesions in loop structures of duplex DNA by DASH-type cryptochrome. Proc Natl Acad Sci U S A. 2008;105: 21023–21027. doi:10.1073/pnas.0805830106

99. Reisdorph NA, Small GD. The CPH1 gene of *Chlamydomonas reinhardtii* encodes two forms of cryptochrome whose levels are controlled by light-induced proteolysis. Plant Physiol. 2004;134: 1546–1554. doi:10.1104/pp.103.031930

100. Reppert SM, Weaver DR. Coordination of circadian timing in mammals. Nature. 2002;418: 935–941. doi:10.1038/nature00965

101. Salomé PA, Merchant SS. Co-expression networks in *Chlamydomonas* reveal significant rhythmicity in batch cultures and empower gene function discovery. Plant Cell. 2021;33: 1058–1082. doi:10.1093/plcell/koab042

102. Sancar A. Structure and function of DNA photolyase and cryptochrome blue-light photoreceptors. Chem Rev. 2003;103: 2203–2237. doi:10.1021/cr0204348

103. Sanchez SE, Rugnone ML, Kay SA. Light Perception: A Matter of Time. Mol Plant. 2020;13: 363–385. doi:10.1016/j.molp.2020.02.006

104. Sargent ML, Briggs WR. The effects of light on a circadian rhythm of conidiation in *neurospora*. Plant Physiol. 1967;42: 1504–1510. doi:10.1104/pp.42.11.1504

105. Schulze T, Prager K, Dathe H, Kelm J, Kiessling P, Mittag M. How the green alga *Chlamydomonas reinhardtii* keeps time? Protoplasma. 2010;244: 3–14. doi:10.1007/s00709-010-0113-0

106. Selby CP, Sancar A. A third member of the photolyase/blue-light photoreceptor family in *Drosophila*: a putative circadian photoreceptor. Photochem Photobiol. 1999;69: 105–107. doi:10.1111/j.1751-1097.1999.tb05313.x

107. Selby CP, Sancar A. A cryptochrome/photolyase class of enzymes with single-stranded DNA-specific photolyase activity. Proc Natl Acad Sci U S A. 2006;103: 17696–17700. doi:10.1073/pnas.0607993103

108. Selby CP, Thompson C, Schmitz TM, Van Gelder RN, Sancar A. Functional redundancy of cryptochromes and classical photoreceptors for nonvisual ocular photoreception in mice. Proc Natl Acad Sci U S A. 2000;97: 14697–14702. doi:10.1073/pnas.260498597

109. Shimogawara K, Fujiwara S, Grossman A, Usuda H. High-efficiency transformation of *Chlamydomonas reinhardtii* by electroporation. Genetics. 1998;148: 1821–1828. doi:10.1093/genetics/148.4.1821

110. Siffre M. Hors du temps: l'expérience du 16 juillet 1962 au fond du gouffre de Scarasson par celui qui l'a vécue. FeniXX; 1963.

111. Somers DE, Devlin PF, Kay SA. Phytochromes and cryptochromes in the entrainment of the *Arabidopsis* circadian clock. Science. 1998;282: 1488–1490. doi:10.1126/science.282.5393.1488

112. Stanewsky R, Kaneko M, Emery P, Beretta B, Wager-Smith K, Kay SA, et al. The cryb mutation identifies cryptochrome as a circadian photoreceptor in *Drosophila*. Cell. 1998;95: 681–692. doi:10.1016/s0092-8674(00)81638-4

113. Straley SC, Bruce VG. Stickiness to Glass: Circadian Changes in the Cell Surface of *Chlamydomonas reinhardi*. Plant Physiol. 1979;63: 1175–1181. doi:10.1104/pp.63.6.1175

114. Sueoka N. MITOTIC REPLICATION OF DEOXYRIBONUCLEIC ACID IN *CHLAMYDOMONAS REINHARDI*. Proc Natl Acad Sci U S A. 1960;46: 83–91. doi:10.1073/pnas.46.1.83

115. Swade RH. Circadian rhythms in fluctuating light cycles: toward a new model of entrainment. J Theor Biol. 1969;24: 227–239. doi:10.1016/s0022-5193(69)80048-2

116. Sweeney BM, Haxo FT. Persistence of a Photosynthetic Rhythm in Enucleated *Acetabularia.* Science. 1961;134: 1361–1363. doi:10.1126/science.134.3487.1361

117. Takahashi JS, DeCoursey PJ, Bauman L, Menaker M. Spectral sensitivity of a novel photoreceptive system mediating entrainment of mammalian circadian rhythms. Nature. 1984;308: 186–188. doi:10.1038/308186a0

118. Thines B, Harmon FG. Ambient temperature response establishes ELF3 as a required component of the core *Arabidopsis* circadian clock. Proc Natl Acad Sci U S A. 2010;107: 3257–3262. doi:10.1073/pnas.0911006107

119. Thommen Q, Pfeuty B, Schatt P, Bijoux A, Bouget F-Y, Lefranc M. Probing entrainment of *Ostreococcus tauri* circadian clock by green and blue light through a mathematical modeling approach. Front Genet. 2015;6: 65. doi:10.3389/fgene.2015.00065

120. Todo T. Functional diversity of the DNA photolyase/blue light receptor family. Mutat Res. 1999;434: 89–97. doi:10.1016/s0921-8777(99)00013-0

121. Van der Horst GT, Muijtjens M, Kobayashi K, Takano R, Kanno S, Takao M, et al. Mammalian Cry1 and Cry2 are essential for maintenance of circadian rhythms. Nature. 1999;398: 627–630. doi:10.1038/19323

122. Voytsekh O, Seitz SB, Iliev D, Mittag M. Both subunits of the circadian RNA-binding protein CHLAMY1 can integrate temperature information. Plant Physiol. 2008;147: 2179–2193. doi:10.1104/pp.108.118570

123. Yanovsky MJ, Mazzella MA, Whitelam GC, Casal JJ. Resetting of the circadian clock by phytochromes and cryptochromes in *Arabidopsis*. J Biol Rhythms. 2001;16: 523–530. doi:10.1177/074873001129002213

124. Yu J-W, Rubio V, Lee N-Y, Bai S, Lee S-Y, Kim S-S, et al. COP1 and ELF3 control circadian function and photoperiodic flowering by regulating GI stability. Mol Cell. 2008;32: 617–630. doi:10.1016/j.molcel.2008.09.026

125. Zheng B, Albrecht U, Kaasik K, Sage M, Lu W, Vaishnav S, et al. Nonredundant roles of the mPer1 and mPer2 genes in the mammalian circadian clock. Cell. 2001;105: 683–694. doi:10.1016/s0092-8674(01)00380-4

9. TABLES

Primer set	Primer name	Sequence (5' -->3')	Target	Purpose
I	UPI	CGCCGCCTCCAAGCTGTACACAC	Upstream of *aph7"* insertion (M1 (*cetl-1*))	Insertion check in the *CETL* gene from *cetl-1* mutant.
	DPI	GGTGCATGTGCGGGTGCATACTGG	Downstream of *aph7"* insertion (M1(*cetl-1*))	
II	m19-F	AGCCGAGGCCCGCGTCGGAAATG	Upstream of *aph7"* insertion (*b19* (*cetl-2*))	Insertion check in the *CETL* gene from *cetl-2* mutant.
	m19-R	GGCAGTAGCGGTCAGGGCGGTG	Downstream of *aph7"* insertion (*b19* (*cetl-2*))	
III	RTP4(I)	GCGCGGGTGCAACAGGTCATCTGGTC	First exon junction of the *CETL* transcript	Insertion check in the *CETL* transcript from the *cetl-1* mutant.
	RTP3(II)	GGGCGGCGGCATAAGGAGAGCTGAC	Exon immediately downstream of insertion locus in the *CETL* transcript	
IV	qPCR1	TGGACCCACAGGCCCTGGGCAACAC	Fifth and seventh exon junction of the *CETL* transcript (Cre07.g357500)	Quantification of *CETL* mRNA.
	qPCR2	TGCCGGGGGGGCACCGTCTTGAATG		

Table 1. Details of primers used for insertion check and RT-qPCR.

S. No	Genome	Repository/portal	Protein ID	Transcript ID	Supporting references
1.	*Chlamydomonas reinhardtii* CBR strain	DDBJ/GenBank/EMBL-EBI		LC664050	
2.	*Chlamydomonas incerta* SAG 7. 73	PhycoCosm	16158	16158	[1]
3.	*Chlamydomonas schloesseri* CCAP 11/173	PhycoCosm	12441	12441	
4.	*Edaphochlamys debaryana* CCAP 11/70	PhycoCosm	11184	11184	
5.	*Volvox carteri* v2.1	PhycoCosm	12823	12823	[2]
6.	*Gonium pectorale* NIES- 2863	PhycoCosm	14005	14005	
7.	*Gonium pectorale* NIES- 2863	PhycoCosm	14004	14004	
8.	*Chlamydomonas eustigma* NIES-2499	PhycoCosm	8338	8338	[4]
9.	*Dunaliella salina* CCAP 19/18	PhycoCosm	13574	13574	[5]
10.	*Chromochloris zofingiensis* v5.2.3.2	Phytozome		Cz15g15170.t1	[6]
11.	*Raphidocelis subcapitata* NIES-35	PhycoCosm	7428	7428	[7]
12.	*Enallax costatus* CCAP 276/31 v1.1	PhycoCosm	6729302	6730092	[8]
13.	*Scenedesmus Sp.* NREL 46B-D3 v1.0	PhycoCosm	1642377	1643679	[9]
14.	*Tetradesmus obliquus* UTEX B 72 v1.1	PhycoCosm	1123993	1124339	[8]
15.	*Asterochloris glomerata* Cgr/DA1 pho v2.0	PhycoCosm	5319	5319	[10]
16.	*Bortryococcus braunii* Showa v2.1	PhycoCosm	20297	20297	[11]
17.	*Symbiochloris reticulata* Spain reference genome v1.0	PhycoCosm	838596	838660	[8]
18.	*Picochlorum renovo*	PhycoCosm	29125	29169	[12]
19.	*Micractinium conductrix* SAG 241.80	PhycoCosm	5015	5015	[13]
20.	*Chlorella variabilis* NC64A	PhycoCosm	52115	52115	[14]
21.	*Chlorella sorokiniana* UTEX 1602	PhycoCosm	5130	5130	[13]
22.	*Micromonas commoda* NOUM17(RCC299)	PhycoCosm	7934	7934	[15]
23.	*Klebsormidium nitens* NIES-2285	*Klebsormidium nitens* NIES-2285 genome project	kfl00240_0090_v1.1		[16]
24.	Chara braunii	ORCAE	g6559.t1		[17]
25.	*Marchantia polymorpha* v3.1	Phytozome		Mapoly0014s0139.1	[18]
26.	*Physcomitrium patens* v3.3	Phytozome		Pp3c11_14750V3.4	[19]
27.	*Selaginella moellendorfii* v1.0	Phytozome		415241	[20]
28.	*Selaginella moellendorfii* v1.0	Phytozome		411196	
29.	*Sorghum bicolor*	PhycoCosm	5010261	5239448	[21]
30.	*Oryza sativa*	rap-db	Os01t0566100-02		[22]
31.	*Oryza sativa*	rap-db	Os06t0142600-01		
32.	*Populus trichocarpa* v4.1	Phytozome		Potri.006G233800.1	[23]
33.	*Arabidopsis thaliana*	TAIR	AT2G25930.1		[24]

34.	*Solanum lycopersicum* ITAG4.0	Phytozome		Solyc08g065870 .4.1	[25]
35.	*Zea mays* B84 v1.2	Phytozome		ZmB84.06G283 200.1.p	[26]

Table 2. Accession details for the sequences used in the protein sequence alignment (**Figs 4B, 4C, 7, and 8 Figs**)

11. SUPPORTING REFERENCES

These are the references for the sequences used for protein sequence alignment

1. Craig RJ, Hasan AR, Ness RW, Keightley PD. Comparative genomics of 923 Chlamydomonas. Plant Cell. 2021;33: 1016–1041. DOI: 10.1093/plcell/koab026. 924

2. Prochnik SE, Umen J, Nedelcu AM, Hallmann A, Miller SM, Nishii I, et al. Genomic 925 Analysis of Organismal Complexity in the Multicellular Green Alga Volvox carteri. 926 Science. 2010; Volume 329: 223–226. DOI: 10.1126/science.1188800. 927

3. Hanschen ER, Marriage TN, Ferris PJ, Hamaji T, Toyoda A, Fujiyama A, et al. The 928 Gonium pectorale genome demonstrates co-option of cell cycle regulation during 929 the evolution of multicellularity. Nat Commun. 2016;7: 11370. DOI: 930 10.1038/ncomms11370. 931

4. Hirooka S, Hirose Y, Kanesaki Y, Higuchi S, Fujiwara T, Onuma R, et al. Acidophilic 932 green algal genome provides insights into adaptation to an acidic environment. 933 Proc Natl Acad Sci U S A. 2017; Volume 114: E8304–E8313. DOI: 934 10.1073/pnas.1707072114. 935

5. Polle JEW, Barry K, Cushman J, Schmutz J, Tran D, Hathwaik LT, et al. Draft Nuclear 936 Genome Sequence of the Halophilic and Beta-Carotene-Accumulating Green Alga 937 Dunaliella salina Strain CCAP19/18. Genome Announc. 2017;5. 938 doi:10.1128/genomeA.01105-17. 939

6. Roth MS, Cokus SJ, Gallaher SD, Walter A, Lopez D, Erickson E, et al. Chromosome940 level genome assembly and transcriptome of the green alga Chromochloris 941 zofingiensis illuminates astaxanthin production. Proc Natl Acad Sci U S A. 2017;114: 942 E4296–E4305. DOI: 10.1073/pnas.1619928114. 943

7. Suzuki S, Yamaguchi H, Nakajima N, Kawachi M. Raphidocelis subcapitata 944 (=Pseudokirchneriella subcapitata) provides an insight into genome evolution and 945

environmental adaptations in the Sphaeropleales. Sci Rep. 2018; Volume 8: 8058. 946
DOI: 10.1038/s41598-018-26331-6. 947

8. Grigoriev IV, Hayes RD, Calhoun S, Kamel B, Wang A, Ahrendt S, et al. PhycoCosm, 948
a comparative algal genomics resource. Nucleic Acids Res. 2021;49: D1004–D1011. 949
DOI: 10.1093/nar/gkaa898. 950

9. Calhoun S, Bell TAS, Dahlin LR, Kunde Y, LaButti K, Louie KB, et al. A multi-omic 951
characterization of temperature stress in a halotolerant Scenedesmus strain for 952
algal biotechnology. Commun Biol. 2021;4: 333. DOI: 10.1038/s42003-021-01859- 953
y. 954

10. Armaleo D, Müller O, Lutzoni F, Andrésson ÓS, Blanc G, Bode HB, et al. The lichen 955
symbiosis re-viewed through the genomes of Cladonia grayi and its algal partner 956
Asterochloris glomerata. BMC Genomics. 2019;20: 605. DOI: 10.1186/s12864-019- 957
5629-x. 958

11. Browne DR, Jenkins J, Schmutz J, Shu S, Barry K, Grimwood J, et al. Draft Nuclear 959
Genome Sequence of the Liquid Hydrocarbon-Accumulating Green Microalga 960
Botryococcus braunii Race B (Showa). Genome Announc. 2017;5. 961
doi:10.1128/genomeA.00215-17. 962

12. Dahlin LR, Gerritsen AT, Henard CA, Van Wychen S, Linger JG, Kunde Y, et al. 963
Development of a high-productivity, halophilic, thermotolerant microalga 964
Picochlorum renovo. Commun Biol. 2019;2: 388. DOI: 10.1038/s42003-019-0620-2. 965

13. Arriola MB, Velmurugan N, Zhang Y, Plunkett MH, Hondzo H, Barney BM. Genome 966
sequences of Chlorella sorokiniana UTEX 1602 and Micractinium conductrix SAG 967
241.80: implications to maltose excretion by a green alga. Plant J. 2018;93: 566– 968
586. DOI: 10.1111/tpj.13789. 969

14. Blanc G, Duncan G, Agarkova I, Borodovsky M, Gurnon J, Kuo A, et al. The Chlorella 970
variabilis NC64A genome reveals adaptation to photosymbiosis, coevolution with 971
viruses, and cryptic sex. Plant Cell. 2010;22: 2943–2955. DOI: 972
10.1105/tpc.110.076406. 973

15. Worden AZ, Lee JH, Mock T, Rouzé P, Simmons MP, Aerts AL, et al. Green evolution 974
and dynamic adaptations revealed by genomes of the marine picoeukaryotes 975
Micromonas. Science. 2009;324: 268–272. DOI: 10.1126/science.1167222. 976

16. Hori K, Maruyama F, Fujisawa T, Togashi T, Yamamoto N, Seo M, et al. 977
Klebsormidium flaccidum genome reveals primary factors for plant terrestrial 978
adaptation. Nat Commun. 2014;5: 3978. DOI: 10.1038/ncomms4978. 979

17. Nishiyama T, Sakayama H, de Vries J, Buschmann H, Saint-Marcoux D, Ullrich KK, et 980 al. The Chara Genome: Secondary Complexity and Implications for Plant 981 Terrestrialization. Cell. 2018;174: 448–464.e24. DOI: 10.1016/j.cell.2018.06.033. 982

18. Bowman JL, Kohchi T, Yamato KT, Jenkins J, Shu S, Ishizaki K, et al. Insights into 983 Land Plant Evolution Garnered from the Marchantia polymorpha Genome. Cell. 984 2017;171: 287–304.e15. DOI: 10.1016/j.cell.2017.09.030. 985

19. Lang D, Ullrich KK, Murat F, Fuchs J, Jenkins J, Haas FB, et al. The Physcomitrella 986 patens chromosome-scale assembly reveals moss genome structure and evolution. 987 Plant J. 2018;93: 515–533. DOI: 10.1111/tpj.13801 988

20. Banks JA, Nishiyama T, Hasebe M, Bowman JL, Gribskov M, dePamphilis C, et al. 989 The Selaginella genome identifies genetic changes associated with the evolution of 990 vascular plants. Science. 2011;332: 960–963. DOI: 10.1126/science.1203810. 991

21. Paterson AH, Bowers JE, Bruggmann R, Dubchak I, Grimwood J, Gundlach H, et al. 992 The Sorghum bicolor genome and the diversification of grasses. Nature. 2009;457: 993 551–556. DOI: 10.1038/nature07723. 994

22. Sakai H, Lee SS, Tanaka T, Numa H, Kim J, Kawahara Y, et al. Rice Annotation 995 Project Database (RAP-DB): An Integrative and Interactive Database for Rice 996 Genomics. Plant Cell Physiol. 2013;54: e6–e6. DOI: 10.1093/pcp/pcs183. 997

23. Tuskan GA, Difazio S, Jansson S, Bohlmann J, Grigoriev I, Hellsten U, et al. The 998 genome of black cottonwood, Populus trichocarpa (Torr. & Gray). Science. 999 2006;313: 1596–1604. DOI: 10.1126/science.1128691. 1000

24. Berardini TZ, Reiser L, Li D, Mezheritsky Y, Muller R, Strait E, Huala E. The 1001 Arabidopsis information resource: making and mining the “gold standard” 1002 annotated reference plant genome. genesis. 2015; 53: 474-85.DOI: 1003 10.1002/dvg.22877. 1004

25. Hosmani PS, Flores-Gonzalez M, van de Geest H, Maumus F, Bakker LV, Schijlen E, 1005 et al. An improved de novo assembly and annotation of the tomato reference 1006 genome using single-molecule sequencing, Hi-C proximity ligation and optical 1007 maps. Cold Spring Harbor Laboratory. 2019. doi:10.1101/767764 1008

26. Bornowski N, Michel KJ, Hamilton JP, Ou S, Seetharam AS, Jenkins J, et al. Genomic 1009 variation within the maize stiff-stalk heterotic germplasm pool. Plant Genome. 1010 2021;14: e20114. doi:10.1002/tpg2.20114

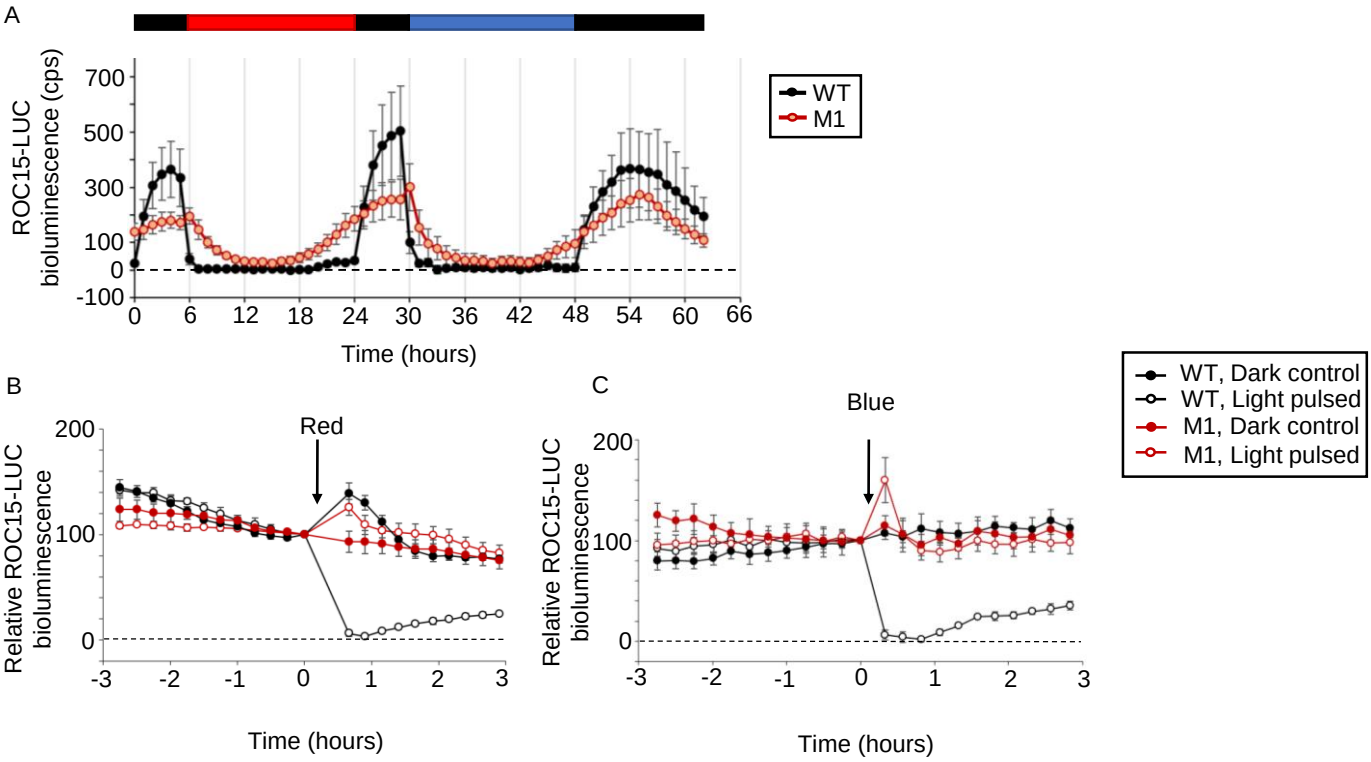

Fig 1. Representative bioluminescence traces of the M1 mutant. A. ROC15-LUC bioluminescence pattern of M1 under diurnal conditions. The red, blue, and black bars above the graph represent red light (8 µmol m^{-2} s^{-1}), blue light (20 µmol m^{-2} s^{-1}), and darkness, respectively. Cells were prepared for the screening as described in Materials and Methods. Mean ± standard deviation (SD) of 32-36 biological replicates are plotted. **B** and **C.** Representative trace of the ROC15-LUC bioluminescence response to light pulses in M1 mutant. Unsynchronized TAP cultures were transferred into 24 well black plates, maintained in darkness for at least 6 hours to allow for the accumulation of ROC15-LUC, and exposed to a 5 min pulse of red light (**B**, 10 µmol m^{-2} s^{-1}) or blue light (**C**, 20 µmol m^{-2} s^{-1}). Bioluminescence has been calculated relative to that at the time point just before light pulse (Time 0). Background was not subtracted. Mean ± SD of 6 biological replicates are shown. Arrows indicate the approximate time points of light pulses. The increase in bioluminescence levels after the light pulse probably corresponds to the disturbance of the plate during the experiment.

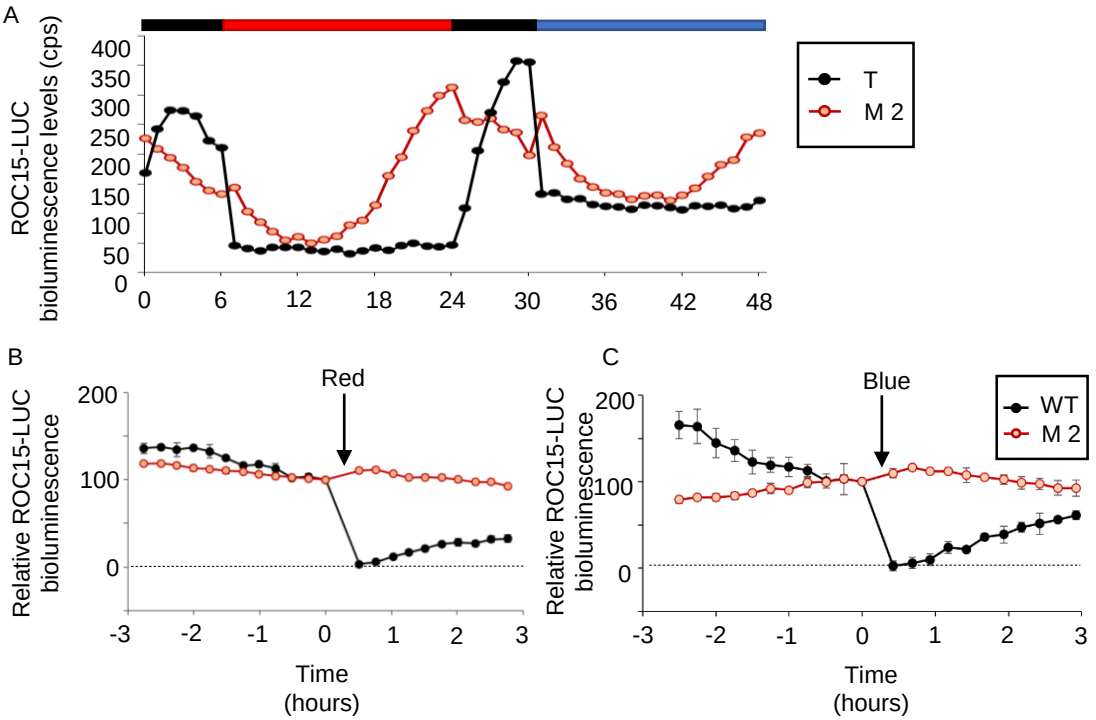

Fig 2. ROC15 light response of the M2 mutant. A. ROC15-LUC bioluminescence pattern of the M2 mutant, observed under diurnal conditions. The red, blue, and black bars above the graph represent red light (8 µmol m^{-2} s^{-1}), blue light (20 µmol m^{-2} s^{-1}), and dark conditions, respectively. Cells were prepared as described in Materials and Methods (mutant/complement screening). The results of the initial screening are shown. The trace of a transformant (T), exhibiting a WT response, is shown for comparison. The background was not subtracted. **B** and **C.** ROC15 bioluminescence response to light pulses in the M2 mutant. Unsynchronized TAP cultures were transferred into 24 well black plates, and their bioluminescence was monitored. Cells were kept in darkness for at least 4-6 hours to allow for the accumulation of ROC15-LUC, and then exposed to a 5-min pulse of red (**B**, 10 µmol m^{-2} s^{-1}) and blue (**C**, 5 µmol m^{-2} s^{-1}) light. Bioluminescence has been calculated relative to the time point just before the light pulse (Time 0). Mean ± SD of 4 biological replicates are shown. Arrows indicate approximate time of light pulses.

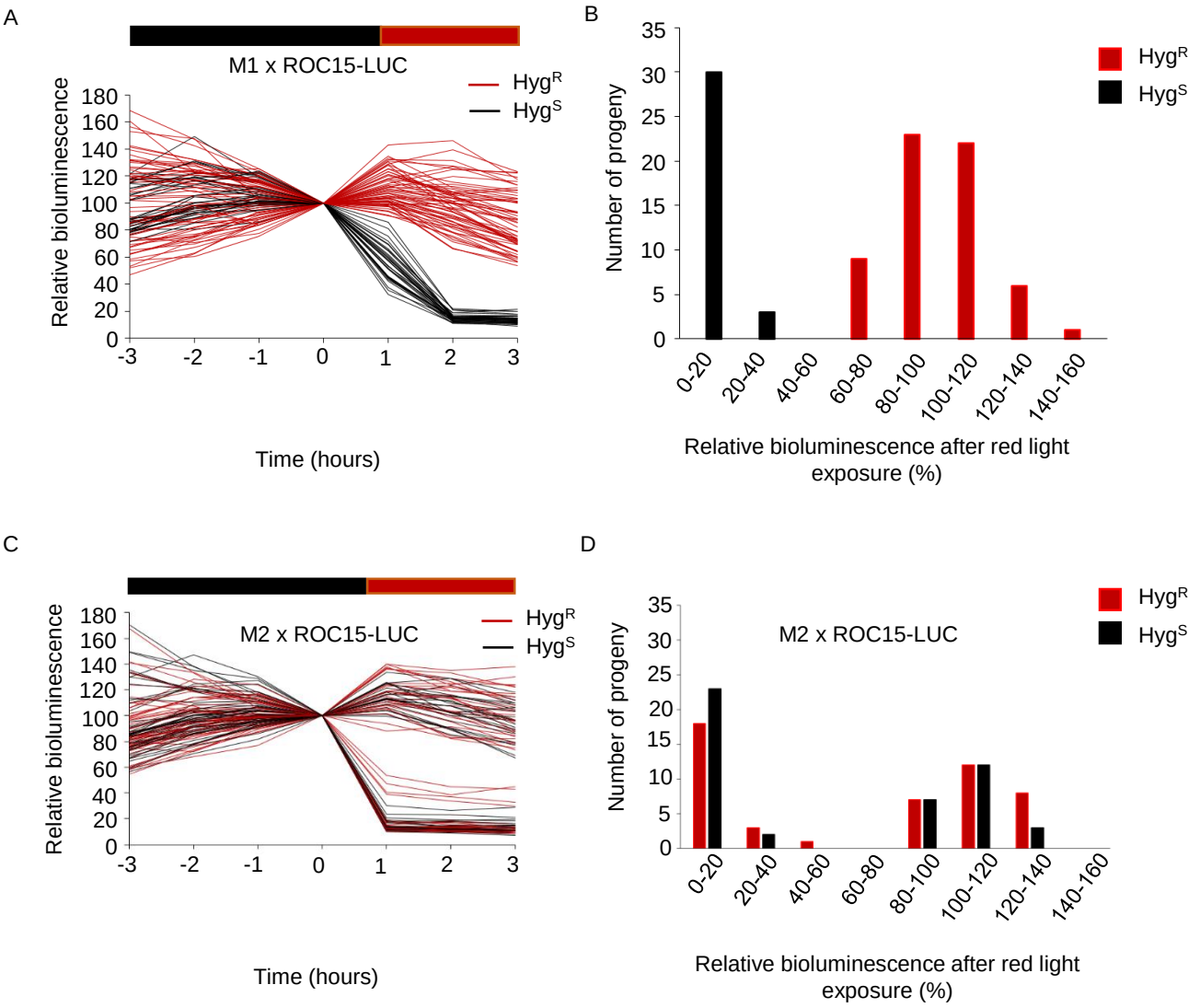

Fig 3. Genetic linkage analysis of M1 and M2. M1 and M2 mutants were backcrossed with the parental ROC15-LUC reporter strain. The progeny were subjected to hygromycin resistance screening and ROC15 bioluminescence monitoring in response to red light (8 µmol m^{-2} s^{-1}). **A** and **C.** Bioluminescence trace of the progeny in response to light, along with the approximate light schedule used. Cells were prepared as described in Materials and Methods (mutant/complement screening). All values were calculated relative to that at the time point (0-hour) just before the start of light phase. The background was not subtracted. Results of 94-96 individual progeny have been plotted. **B** and **D.** Distribution of the numbers of progeny showing hygromycin sensitivity, and their relative bioluminescence levels after exposure to light (corresponding to hour 2 in **A** and **C**).

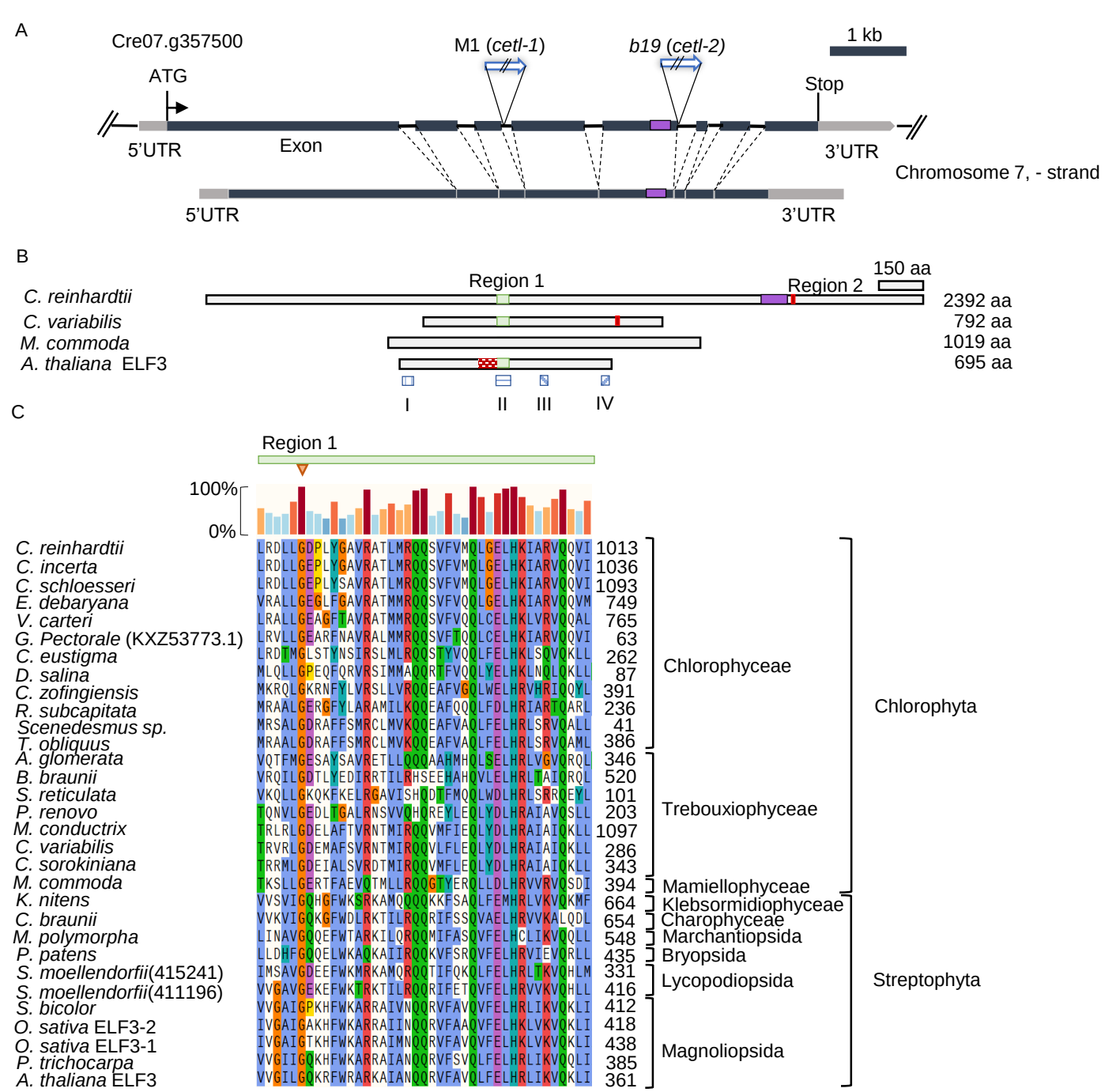

Fig 4. Gene responsible for the mutant phenotype. A. Schematic representation of Cre07.g357500 and its corresponding transcript. 5'UTR and 3'UTR ends of the transcript are illustrated based on information from the database (*C. reinhardtii* v5.6, Joint Genome Institute). This gene corresponds to Cre07.g800875 in the latest version (v6.1). The N-terminus appears to be missing in the gene prediction of this version. M1 (*cetl-1*) and *b19* (*cetl-2*) indicate the insertion loci of *aph7"* in the mutants. The purple box indicates the location of the additional 264 nucleotides present in our laboratory strain. The location of these additional nucleotides in the transcript and the location of the corresponding amino acids in the encoded protein are also indicated by a purple box. **B.** Protein sequence alignment**.** A schematic depiction of amino acid sequences, representing the sequences from the two phyla used for alignment. The two regions of similarity (Region 1 and Region 2) are also shown. The patterned red box on the *Arabidopsis* ELF3 sequence represents the region that was shown to be responsible for interaction with ELF4 (**Jung et al., 2020**). The patterned blue boxes beneath the *Arabidopsis* ELF3 sequence represents the regions identified as Block I, II, III and IV (**Liu et al., 2001**). **C.** Alignment of the amino acid sequences at Region 1. The amino acids have been colored according to the Clustal X-scheme i.e. according to their properties and conservation. The red inverted triangle indicates conservation at the Glycine residue, which was found to be substituted in the *elf3-12* mutant (**Kolmos et al., 2011**). The colored bars above the alignment indicate the percentage of conservation. Sequences were aligned using MAFFT multiple sequence alignment program (MAFFT 7.471, SnapGene). The details of the amino acid sequences used for the alignment are listed in **Table 2**.

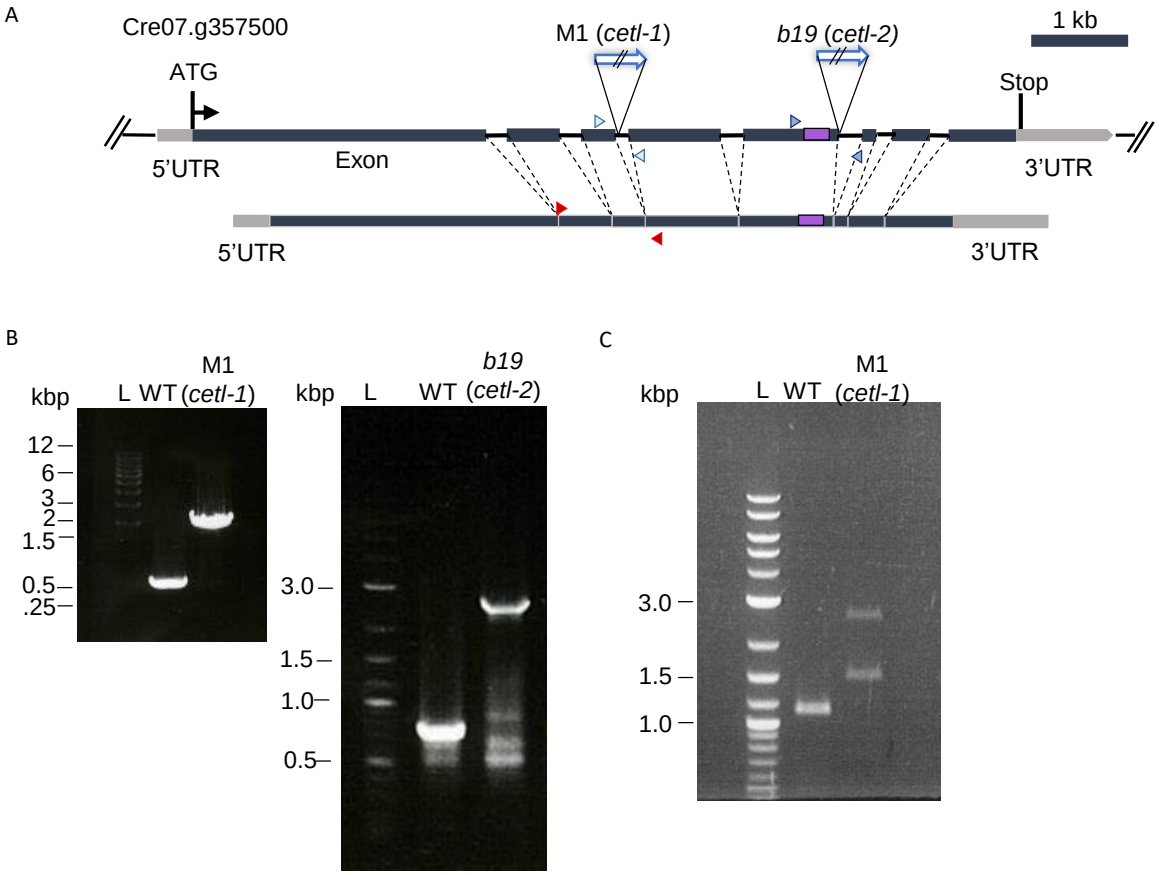

Fig 5. Confirmation of the *aph7"* insertion. Primer binding sites and PCR confirmation of the insertion of the hygromycin resistance gene (*aph7"*). **A.** Schematic representation of the Cre07.g357500 gene and its transcript. Blue triangles around the insertion loci indicate the binding sites of the primers used for PCR confirmation in the genomic DNA. The red triangles indicate the binding sites of the primers used for PCR confirmation in the cDNA. **B.** PCR was performed on the wild type (WT) and mutant genomic DNA with primers targeted around the insertion loci (depicted in A). The amplified products were visualized on an agarose gel. **C.** RT-PCR was performed on the Cre07.g357500 transcript in the WT and mutant with primers targeted to the loci depicted in A. The amplified products were visualized on an agarose gel. The primers used are listed in **Table 1**.

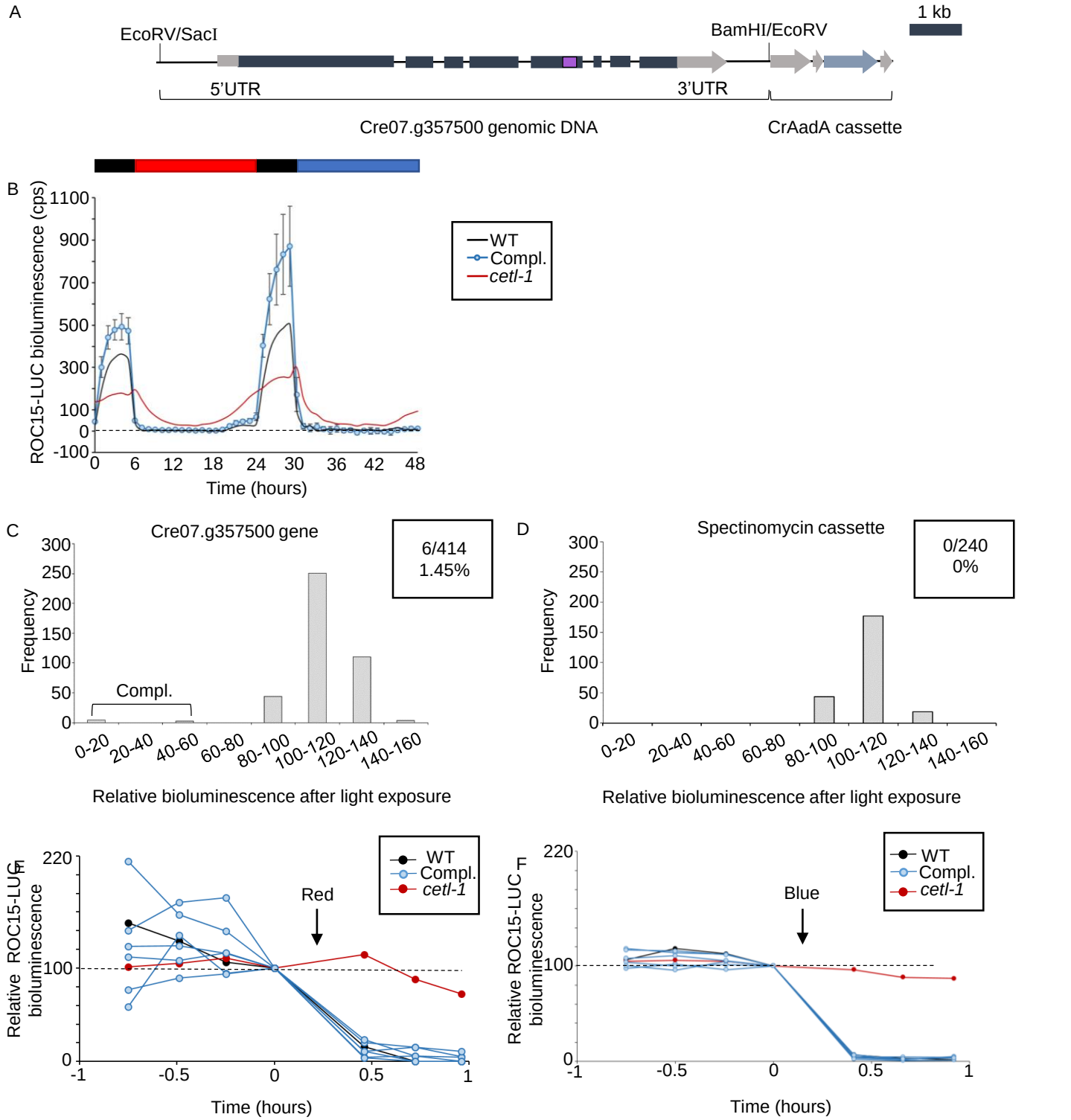

Fig 6. Complementation by the Cre07.g357500 gene. A. Schematic representation of the gene fragment used for complementation. WT genomic DNA fragment of Cre07.g357500 gene ligated to the spectinomycin resistance cassette (*aadA)* was used for complementation. **B.** A representative ROC15-LUC bioluminescence pattern of one of the six complements. Culture preparation and light conditions were the same as in **Fig 1A**. Mean ± SD of 8 biological replicates of the complement (Compl.) have been plotted. The bioluminescence trace of the WT and M1 from **Fig 1A** have been plotted for comparison. **C** and **D**. Histograms of the distribution of transformants with respect to the relative bioluminescence levels after exposure to red light (8 µmol m^{-2} s^{-1}). The bioluminescence values at the first time point after the start of red light exposure were taken relative to the values just before the start of red light exposure. Transformants with only *aadA* are shown as a negative control. **E** and **F.** Representative trace of the light-pulse response of the six isolated complements. Unsynchronized TAP cultures were transferred into 24 well black plates and their bioluminescence was monitored as described in the Materials and Methods. Cells were kept in darkness for at least 3 hours before being exposed to a 5-min pulse of red light (**E**, 10 µmol m^{-2} s^{-1}) and blue light (**F**, 10 µmol m^{-2} s^{-1}). Bioluminescence values have been calculated relative to the time point just before the light pulse (Time 0). Background was not subtracted. Arrows indicate the approximate time of the light pulse.

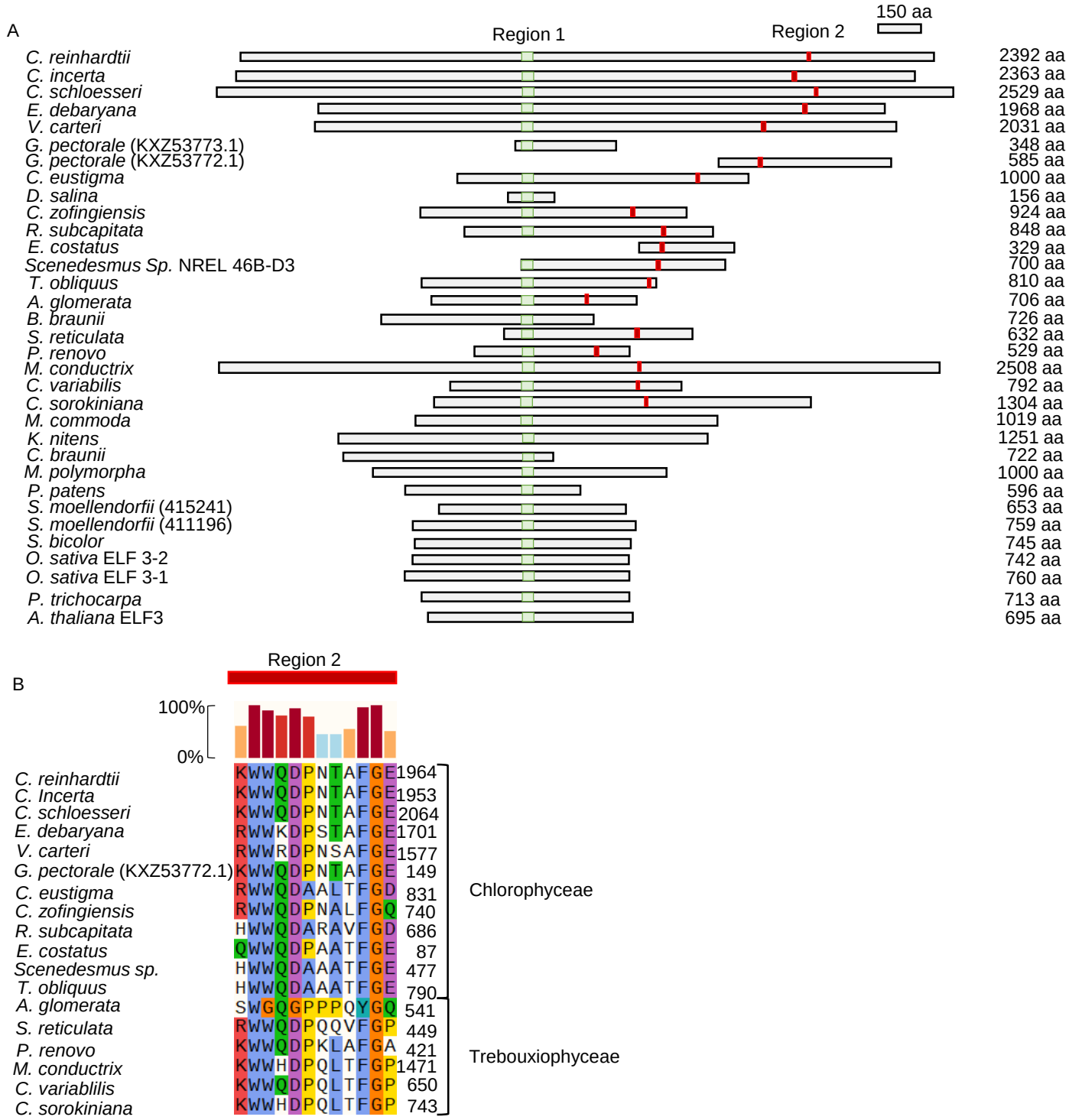

Fig 7. A. Schematic representation of all the protein sequences used in the alignment and the two regions of similarity (Region 1 and Region 2). **B.** Alignment of the sequences at Region 2. Amino acids have been colored according to their properties and conservation (Clustal X color scheme). Percentage of conservation at each site is indicated by colored bars above the alignment. Sequences were aligned in the same manner as in **Fig 4**. Amino acid sequences used for the alignment are the same as those used in **Fig 4**.

Aligned using MAFFT

```
C. reinhardtii      MGPDNQMPAGSGAVGKSQLAVPKQPQGGLPAGSGPHLGQSAGAPQVFAPGLAGATAAAAA  60
O. sativa           -----MATRGGGGGGGGK----------------------EAKGKVMGP----------  22
A. thaliana         ------MKRGK----------------------------DEEKILEP----------  13
S. lycopersicum     ------MKRGK----------------------------GEEKVMGP----------  13
Z. mays             ------MRRGATKDDA-------------------------APDKVMGP----------  18
                          :.:*.                              . .::..*  Block I

C. reinhardtii      MLGQLQSSGAML-SGPQPQLPLAAPAAQQHQQALQQYLLQQTQQLQQQLQQQQQQQQQQQ  119
O. sativa           LFPRLHVNDAAKGGGPR--------APPRNKMALYEQFTVPSHRFSG-------------  61
A. thaliana         MFPRLHVNDADK-GGPR--------APPRNKMALYEQLSIPSQRFG--------------  50
S. lycopersicum     MFPRLHVNDTDK-GGPR--------APPRNKMALYEQLSIPSQRFN--------------  50
Z. mays             LFPRLHVNDTLK-GGPR--------APPRNKMALYEQFSVPSHRYS--------------  55
                    ::::*::::: . :**:Block I *::::::**::::..:::::.

C. reinhardtii      RLQLAAGQGGGGVAPCISPVLQHLQLHRQLQAAAAGTSQTSQNSLSLGPGGQMQLLPPSF  179
O. sativa           ----GGGGGGVGGSP-----------------AHSTSAASQSQSQSQVYGRDSSLFQP--  98
A. thaliana         ------DHGTMNSRS-----------------NNTSTLVHPGPSSQPCGVERNL-----  81
S. lycopersicum     -------SGVLPLDP-----------------NNTSKMAPPSSSQGSGHDRSGYLP--  82
Z. mays             --------AAVPPAPSPAPPW----------GAQRPASAVPSTSASQVGGGDRPIFPL--  95
                           :. . .:                 .... . . : *:. * ....  .

C. reinhardtii      PQMPGRYPQLPGLVQAPQQAAAASGALMALSSLMAAGGVAGPVPGLAPPGVHGVPSGGMR  239
O. sativa           -------------FNVPSNR-------------------------------------  105
A. thaliana         -------------------------------------------------------  81
S. lycopersicum     -------------IQHPPSRRLAD--------------------------------  93
Z. mays             -------------FRVPSTE-------------------------------------  102
                                .

C. reinhardtii      PMGPGQLPLAAAPLLASTGRPGMPQPGAAGPPFFGGPGGPVPGVGGLQVPLPVPYGGGRP  299
O. sativa           -------------------------------------------------------  105
A. thaliana         -------------------------------------------------------  81
S. lycopersicum     ----------------------------------------------------KP  95
Z. mays             -------------------------------------------------------  102


C. reinhardtii      PGHMALGPGGGSAAGGGDSAVA----LLQQWQLQQLQQLQQQALLPGLPPAAASAFLNGA  355
O. sativa           PGHSTEKINSDKINKKISGSRKELGMLSSQTKGMDIYASRSTA-----------------  148
A. thaliana         SVQHLDSSAANQATEK----------FVSQMSFME--NVRSSA-----------------  112
S. lycopersicum     PGHSSDPST-----------------LLQQYE-----------------------------  110
Z. mays             PVRSSDQTNANSNGQGANGTIAESG---RQRQSTHLKSKDTNA-----------------  142
                    :.:... ..                 . .* .          .

C. reinhardtii      MLGAGMQQQQQQPALSGHKPPLQQPLQYALPQPSLVRRPVAVAAGGSPSLQLPPPQAEGG  415
O. sativa           ----------------------------------------------------EAPQRRAENT  158
A. thaliana         ----------------------------------------------------QHDQ------  116
S. lycopersicum     -------------------------------------------------------  110
Z. mays             ----------------------------------------------AGPPAEGNNS  152


C. reinhardtii      MARSAPAAQAPAVKPESSRQVGDMATAAAAAAAAAGDHYRNGSGSG-DRHGP--------  466
O. sativa           IKSS---------SGKRLADDDEFMVPSVFNSRFPQYSTQENAGVQ-DQSTPLVAANPHK  208
A. thaliana         --------------RKMVREEEDFAVPVYINSRRSQSHGRTKSGIEKEKHTPMVA-----  157
S. lycopersicum     --------------LKKRTEEDDFTVPIFVNSKLGQAHGSHNVNME--KLS---------  145
Z. mays             V-------------GKKLANDDDFTVPSVLYSGMPPHSSQE-------KLTLFPTTSPCK  192
                                 :  ....::.::.  .:. .. . ..  .    :...

C. reinhardtii      --PSPQQ--QRQPLPQPSRQLQAPQVQQTSGESYSTVTEGSTEASSGATSAGCSPPGAGG  522
O. sativa           S-PSTVSKSSTKCYNTVSKKLE--RIHVSDVKSRTPLKDKEMEA---------------  249
A. thaliana         --PSSHH----------SIRFQ--EVNQTGSKQNVCLATCSKP----------------  186
S. lycopersicum     --PSGQL-------FCPNKELE--GVTHLTLRQQRNSQNKE-----------------  175
Z. mays             SVPAKYS-------STDKRRLE--GMDASDVKSKGPSGIKEKEP---------------  227
                      *: .           ...::  .:  .. ..   .  ..

C. reinhardtii      TTEAASPRQYDKSLGGGGTGSPPSGGRRLAGPAHPAGAAGVRADGYKRRRDDWEEEEEVG  582
O. sativa           ----------------------------------------------AQTSKNVE-VEKSS  262
A. thaliana         ---------------------------------------------EVRDQVKANARSG  199
S. lycopersicum     --------------------------------------------NLKCTLARREKTT  188
Z. mays             ------------------------------------------VQVRINLEDKETTP  241
                                                               . . ...  :...
```

```
C. reinhardtii      PPHCAKALEAAAVAAGATPGGPLDGSETSGGLASGGGGGVTGADGN---GSGGSTTLGAP  639
O. sativa           SFHASKDM-FESRHAKVYPKMDKTGIINDSDEPHGGNSGHQATSRN-----GGSMKFQNP  316
A. thaliana         GFVI-------SLDVSVTEEIDLEKSASSHDRVNDYNASLRQESRNRLYRDGGKTRLKDT  252
S. lycopersicum     SNSA-------SKECRLDPQV--------------------------------GCSSIPEP  210
Z. mays             SFQVLNDK-TWSPDPKLSSHMDRL------KKQHAEAESYQIRTRN-----ENAVETQSP  289
                    .. .       : .... . .                       ..     .:.. .  :

C. reinhardtii      AQRRSLSDEVAAARAARAEDARQQQRQRAGRSGTSDA-GSGSRENASSGMRDVQLAEGGS  698
O. sativa           PMRRN-----EISSNPSSENTDRHYN----------LPQGGIEETGTKRKRLLEQH----  357
A. thaliana         DNGA--------ESHLATENHSQEGHGSP-----EDI----DNDREYSKSR---------  286
S. lycopersicum     VKGTY-----DGSSYPRKEFVSEEQLTA------NDL----VNDTESQEDR---------  246
Z. mays             PKNGV-----SLLSKPY---VDREQNGD------SDLLGHGLRETGEKRKR---------  326
                     ...         : .  .  ....          ..     .:.. .. *

C. reinhardtii      NGGAAAGSDAMQVDMRWQQTQAPTAAQAQTQAQQAGRGSAGSAGGGRGEVRGYGREAGRR  758
O. sativa           ---DAEKSD-------------------------------------------------  363
A. thaliana         ----ACAS--------------------------------------------------  290
S. lycopersicum     ----AHKS--------------------------------------------------  250
Z. mays             ------------------------------------------------------------  326
                        .  .

C. reinhardtii      GEPDTDMAEAEGEGEGQSETECSDTPLTSSSSQSQSQSQQRGAASQRQQHQGGPAGMQAG  818
O. sativa           -----DVSRLLEQHDAENIDDVSDSS-VECITGWE-------------------------  392
A. thaliana         ----------LQQINEEASDDVSDDSMVDSISSID-------------------------  315
S. lycopersicum     ----------LQTGNLDRGDDLSETSRVESISGTD-------------------------  275
Z. mays             ----------SHHDVEQNDDLSDSS-VESLPGME-------------------------  349
                             .. . :  ::.*:.: :.:... .

C. reinhardtii      GRGFREGEGEGGRMGASPLPASEAAVGAAGADDGVARAGGGSRDGSGGVAFPTRGNDGTT  878
O. sativa           ---------------ISP-------------DKIVG-----------------------  400
A. thaliana         ---------------VSP-------------DDVVG-----------------------  323
S. lycopersicum     ---------------ISP-------------DDIVG-----------------------  283
Z. mays             ---------------ISP-------------DDVVS-----------------------  357
                                  .**             *:.*.          Block II

C. reinhardtii      AAAAAAVTAAAAGLSLRAAPPQPWGEQAQLPPQFQPHQLQHQQHQQPMFSPPPPGGHMMM  938
O. sativa           ------------------------------------------------------------  400
A. thaliana         ------------------------------------------------------------  323
S. lycopersicum     ------------------------------------------------------------  283
Z. mays             ------------------------------------------------------------  357
                                          Block II

C. reinhardtii      PPPPAFPPGAGPVGPGGPLPPPPPGPPAPAGGPALRDLLGDPLYGAVRATLMRQQSVFVM  998
O. sativa           ------------------------------------AIGTKHFWKARRAIMNQQRVFAV  423
A. thaliana         ------------------------------------ILGQKRFWRARKAIANQQRVFAV  346
S. lycopersicum     ------------------------------------IIGLKRFWKARRAIVNQQRVFAI  306
Z. mays             ------------------------------------AIGPKHFWKARRAIVNQQRVFAV  380
                                  Block II                .:* :.::.:*.::.:**:**::

C. reinhardtii      QLGELHKIARVQQVIWSEMLVVDPAGLQAACMEAGFAGAGPAGPILRLPPPPAPGQQQQQ  1058
O. sativa           QVFELHKLVKVQKLI-------------------------AASPHVLIESDPCLGNALLG  458
A. thaliana         QLFELHRLIKVQKLI-------------------------AASPDLLLDEISFLGKVSAK  381
S. lycopersicum     QVFELHRLIKVQRLI-------------------------AGSPNSSLEDPAYLGKPLKS  341
Z. mays             QVFELHRLIKVQKLI-------------------------AASPHVLIEGDPCLGKSLAV  415
                    *:.***::.:**::*          Block II            :::* ..:.  ..:*. .

C. reinhardtii      QQQQRPLTPQPHMGLGTATPESQEGGGVAAGEQQHQRQRPGLASVAGAAEAGYQLTSATT  1118
O. sativa           SK--NKL---------------------------------------------------VEE  466
A. thaliana         SYPVKKL---------------------------------------------------LPS  391
S. lycopersicum     SS-IKRLP--------------------------------------------------LDCIV  353
Z. mays             SK--KRLA--------------------------------------------------GDVET  426
                    :   ..*                                                     .

C. reinhardtii      AHEAQA--GSVVASAAVEAAGGYGGGAGTSSQPHHGAQRSAPAAPPPPAAPPLSREELRV  1176
O. sativa           NLKAQP-----LLVATIDD------VEPSLQQPEVSKENTEDSPPSPH------------  503
A. thaliana         EFLVKPPLPHVVVKQRGDS----------EKTDQHKMESSAENVVGR-------------  428
S. lycopersicum     R-ESQS-----VLKRKHDS----------EKPHFRMEHTAESNVGK-------------  383
Z. mays             QLES----------AKNDDG-----VRP--KQLEHSKEKTEANQPSP-------------  456
                      ...      .  .. :.          ...... :.:... ...
```

```
C. reinhardtii      RLLGDMQLLFNLPRGLRERVLRSVPPEQLVRPAVPPPPAPRPAATMVGGGGGLGGGGNAV  1236
O. sativa           ------------------------------------------------------------  503
A. thaliana         ------------------------------------------------------------  428
S. lycopersicum     ------------------------------------------------------------  383
Z. mays             ------------------------------------------------------------  456

C. reinhardtii      VRPAASKLYTLMDGDEGPADSEQPTVVQKVVAQATARAAAAAAEKQRNNGGSGGGSVAGG  1296
O. sativa           ------------------------------------DTGLGSGQRDQAATNGVSKSNR  525
A. thaliana         ----------------------------------------LSNQ------GHHQQSNY  440
S. lycopersicum     ------------------------------------ASLSTVQ------NGSQLSSH  398
Z. mays             ----------------------------------------SQDEQAATNGAVAASM  472
                                                           *      .: . :.

C. reinhardtii      PNGGIPAAVGQAGPFRQQPTAAPPSPHAAQPATRLGLPDGAAAAVPSPHQVLPPFPPHGM  1356
O. sativa           R-------------------ATPVA-------------------------------  531
A. thaliana         M------------PFANNPPASP---------------------------------  451
S. lycopersicum     K------------PFSGTPLPTPVT-------------------------------  411
Z. mays             H--------------------TP---------------------------------  475
                                    ..*

C. reinhardtii      PQRPQASALLMPPPSMHPHMHPPSPAAAFGLPPHALPAGPGLAQPHALLGGMPPAAAAAA  1416
O. sativa           ----------------------SDNKQNNWGVQL--------------------------  543
A. thaliana         ------------------------APNGYCFPP----------------------------  460
S. lycopersicum     ----------------------NDSNAGPWCFQ----------------------------  422
Z. mays             ----------------------SDNKQKSWCI----------------------------  485
                                         .. ...

C. reinhardtii      GLAVGPPPHGMGAAGAAAAATAGAGAGAFGSPGSSFRAPPHPAQPGQPLHMDLPPQWSGPAM  1476
O. sativa           ----QPPQN-----------------------------------------------QWLVPVM  555
A. thaliana         ----QPPPSG--------------------------NH-------------QQWLIPVM  476
S. lycopersicum     ----QPPGH-----------------------------------------------QWLIPVM  434
Z. mays             ----PAPPS-----------------------------------------------QWLIPVM  497
                        .:*..                          Block III          **:.*:*

C. reinhardtii      -PQHG--HLPLHGQLPPHMHMAMPLHGQLPPGMAGPLGALPAR--GPLQGGAPGAPPPGG  1531
O. sativa           SPLEGLVYKPYSGPCPPAGSILAPFYANCTP------LSLPSTA-GDFMNSAYGV-----  603
A. thaliana         SPSEGLIYKPHPGM-------------------------AHTGHYGGYYGHYMPT-----  506
S. lycopersicum     SPSEGLVYKPFPGP-----GFTSPICGSGPP------GSSPTM--GNFFAPTYGV-----  476
Z. mays             SPSEGLVYKPYTGHCPPVGSLLAPPFFASYP------TSSSSTAGGDFMSSACGA-----  546
                    .*.:*..:.*..*          .      .       ....   *.: ... :.
                    Block III

C. reinhardtii      APMAVAAGGPRGPLQQPQQPQPLVRPPGVPPPLVGTPPLPMPQPGPSAAAPVPHLDAAGT  1591
O. sativa           ------------------------------------PMPH-QPQ-HMGAPGP-------  617
A. thaliana         ------------------------------------PMVMPQYHPGMGFP---------  520
S. lycopersicum     ------------------------------------PAPNPHYQ-GMGVPFA-------  491
Z. mays             ------------------------------------RL--------MSAP---------  552
                                                       :..  .    :..*

C. reinhardtii      SQPQSAAAPAPTPAAPVPGGGFGGVLPPALPVLFSSRQGAGVGAGGTKVPPVLRPPGVPA  1651
O. sativa           ---------------PSMPMNY---FPP-----FSI--------------PVMNPTAPA-  639
A. thaliana         ----------------PPGNGY---FPP-----YGMM------------PTIMNPYCSSQ  544
S. lycopersicum     ---------------PPTGHGY---FRQ-----YGM--------------PAMNPPISS-  513
Z. mays             ---------------------VY---FPS-----FSM--------------PAVSGSA---  567
                                  . .:   ::.     ::.              :.:.:

C. reinhardtii      PAIPVPRPVASIDPHEAWFARHVAGAGAGAQPAAAQPAAATPAAAAEAAGAAGPAAGAVG  1711
O. sativa           ------------------------------------------------------------  639
A. thaliana         ------------------------------------------------------------  544
S. lycopersicum     ------------------------------------------------------------  513
Z. mays             ------------------------------------------------------------  567

C. reinhardtii      SRQAQAQAPSQGLGSRPGSLQRIASTERVVGGGGGSAAAVTGTGALQQPPERQSQPQQRQ  1771
O. sativa           -----PVVEQGRHPSMPQPYGNF---------------------------------EQQS  661
A. thaliana         QQQQQQPNEQMNQFGHPGNLQNT-----------------------------------QQQQ  571
S. lycopersicum     -----TASEESNQYTMPGLQHQFSGVVDDV-----------------------NIQHQD  544
Z. mays             -------VEQVSHVAASQHKRN---------------------------------------  582
                           .:. .. . :.  ..                                  ...
```

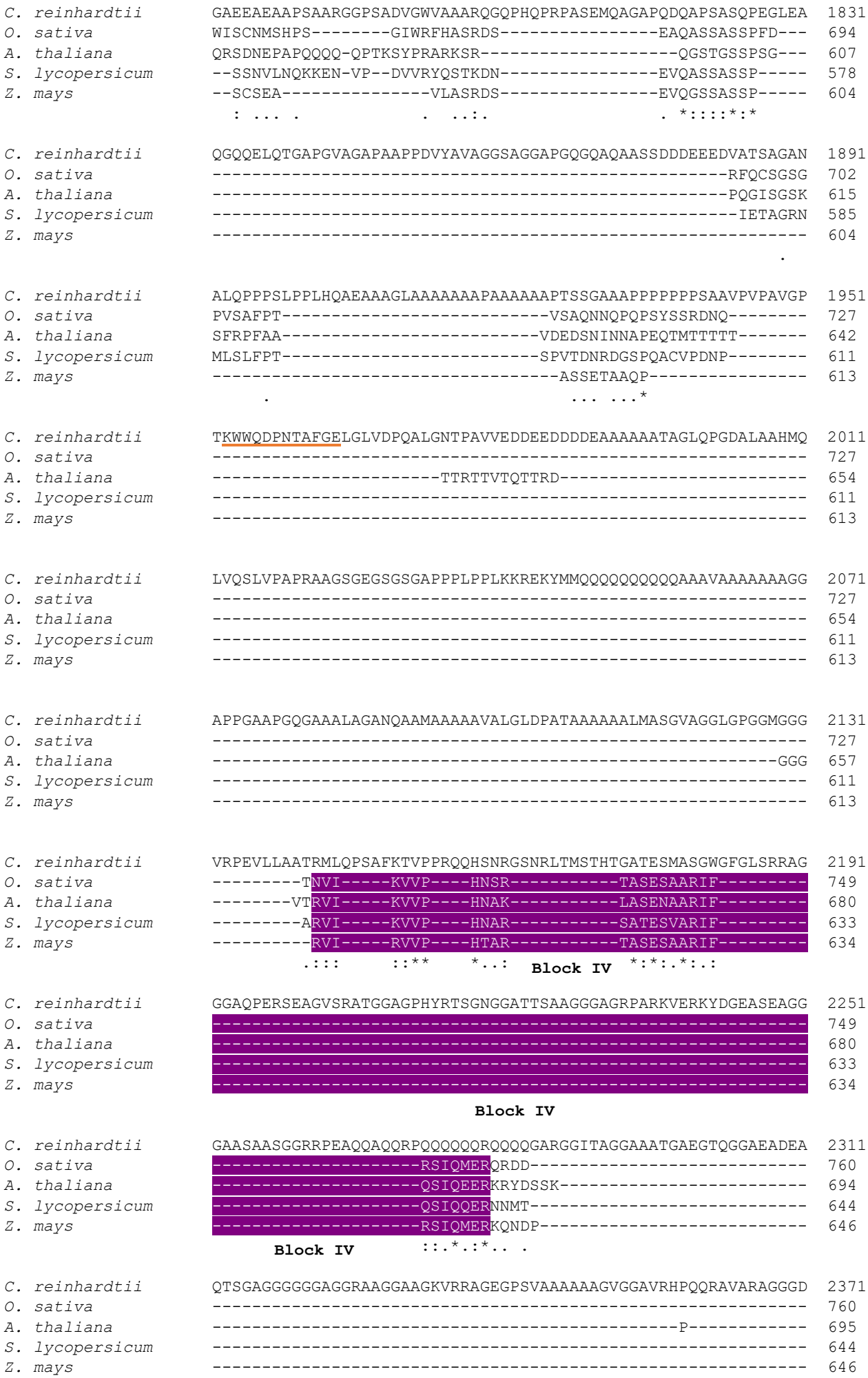
C. reinhardtii GAEEAEAAPSAARGGPSADVGWVAAARQGQPHQPRPASEMQAGAPQDQAPSASQPEGLEA 1831
O. sativa WISCNMSHPS--------GIWRFHASRDS----------EAQASSASSPFD--- 694
A. thaliana QRSDNEPAPQQQQ-QPTKSYPRARKSR----------QGSTGSSPSG--- 607
S. lycopersicum --SSNVLNQKKEN-VP--DVVRYQSTKDN----------EVQASSASSP----- 578
Z. mays --SCSEA----------VLASRDS----------EVQGSSASSP----- 604
C. reinhardtii QGQQELQTGAPGVAGAPAAPPDVYAVAGGSAGGAPGQGQAQAASSDDDEEEDVATSAGAN 1891
O. sativa ----------RFQCSGSG 702
A. thaliana ----------PQGISGSK 615
S. lycopersicum ----------IETAGRN 585
Z. mays ---------- 604
C. reinhardtii ALQPPPSLPPLHQAEAAAGLAAAAAAAPAAAAAAPTSSGAAAPPPPPPSAAVPVPAVGP 1951
O. sativa PVSAFPT----------VSAQNNQPQPSYSSRDNQ-------- 727
A. thaliana SFRPFAA----------VDEDSNINNAPEQTMTTTTT------- 642
S. lycopersicum MLSLFPT----------SPVTDNRDGSPQACVPDNP-------- 611
Z. mays ----------ASSETAAQP---------- 613
C. reinhardtii TKWWQDPNTAFGELGLVDPQALGNTPAVVEDDEEDDDDEAAAAAATAGLQPGDALAAHMQ 2011
O. sativa ---------- 727
A. thaliana ----------TTRTTVTQTTRD---------- 654
S. lycopersicum ---------- 611
Z. mays ---------- 613
C. reinhardtii LVQSLVPAPRAAGSGEGSGSGAPPPLPPLKKREKYMMQQQQQQQQQQAAAVAAAAAAAGG 2071
O. sativa ---------- 727
A. thaliana ---------- 654
S. lycopersicum ---------- 611
Z. mays ---------- 613
C. reinhardtii APPGAAPGQGAAALAGANQAAMAAAAAVALGLDPATAAAAAALMASGVAGGLGPGGMGGG 2131
O. sativa ---------- 727
A. thaliana ----------GGG 657
S. lycopersicum ---------- 611
Z. mays ---------- 613
C. reinhardtii VRPEVLLAATRMLQPSAFKTVPPRQQHSNRGSNRLTMSTHTGATESMASGWGFGLSRRAG 2191
O. sativa ---------TNVI-----KVVP----HNSR----------TASESAARIF--------- 749
A. thaliana --------VTRVI-----KVVP----HNAK----------LASENAARIF--------- 680
S. lycopersicum ---------ARVI-----KVVP----HNAR----------SATESVARIF--------- 633
Z. mays ----------RVI-----RVVP----HTAR----------TASESAARIF--------- 634
Block IV
C. reinhardtii GGAQPERSEAGVSRATGGAGPHYRTSGNGGATTSAAGGGAGRPARKVERKYDGEASEAGG 2251
O. sativa ---------- 749
A. thaliana ---------- 680
S. lycopersicum ---------- 633
Z. mays ---------- 634
Block IV
C. reinhardtii GAASAASGGRRPEAQQAQQRPQQQQQQRQQQQGARGGITAGGAAATGAEGTQGGAEADEA 2311
O. sativa ----------RSIQMERQRDD---------- 760
A. thaliana ----------QSIQEERKRYDSSK---------- 694
S. lycopersicum ----------QSIQQERNNMT---------- 644
Z. mays ----------RSIQMERKQNDP---------- 646
Block IV
C. reinhardtii QTSGAGGGGGGAGGRAAGGAAGKVRRAGEGPSVAAAAAAGVGGAVRHPQQRAVARAGGGD 2371
O. sativa ---------- 760
A. thaliana ----------P---------- 695
S. lycopersicum ---------- 644
Z. mays ---------- 646

C. reinhardtii	DVGEVSSGAVEAAEAEDGMSE	2392
O. sativa	----------	760
A. thaliana	----------	695
S. lycopersicum	----------	644
Z. mays	----------	646

Aligned using MUSCLE

```
C. reinhardtii      MGPDNQMPAGSGAVGKSQLAVPKQPQGGLPAGSGPHLGQSAGAPQVFAPGLAGATAAAAA  60
O. sativa           ------------------------------------------------------------  0
A. thaliana         ------------------------------------------------------------  0
S. lycopersicum     ------------------------------------------------------------  0
Z. mays             ------------------------------------------------------------  0

C. reinhardtii      MLGQLQSSGAMLSGPQPQLPLAAPAAQQHQQALQQYLLQQTQQLQQQLQQQQQQQQQQQR  120
O. sativa           ------------------------------------------------------------  0
A. thaliana         ------------------------------------------------------------  0
S. lycopersicum     ------------------------------------------------------------  0
Z. mays             ------------------------------------------------------------  0

C. reinhardtii      LQLAAGQGGGGVAPCISPVLQHLQLHRQLQAAAAGTSQTSQNSLSLGPGGQMQLLPPSFP  180
O. sativa           ---MATRGGGGGGG--------------------------------GKEAKGKVMGPLFP  25
A. thaliana         ----MKRGKD------------------------------------EEKILEPMFP  16
S. lycopersicum     ----MKRGKG------------------------------------EEKVMGPMFP  16
Z. mays             ----MRRGATK-----------------------------------DDAAPDKVMGPLFP  21
                        ..:*..                                      . :::.*.**
                                                                      Block I
C. reinhardtii      QMPGRYPQLPGLVQAPQQAAAASGALMALSSLMAAGGVAGPVPGLAPPGVHGVPSGGMRP  240
O. sativa           RLH-------------------------------------------------------  28
A. thaliana         RLH-------------------------------------------------------  19
S. lycopersicum     RLH-------------------------------------------------------  19
Z. mays             RLH-------------------------------------------------------  24
                    :::                      Block I

C. reinhardtii      MGPGQLPLAAAPLLASTGRPGMPQPGAAGPPFFGGPGGPVPGVGGLQVPLPVP---YGGG  297
O. sativa           -------------VNDAAKG-------------GGPRAPPRNKMALYEQFTVPSHRFSGG  62
A. thaliana         -------------VNDADK--------------GGPRAPPRNKMALYEQLSIPSQRFGDH  52
S. lycopersicum     -------------VNDTDK--------------GGPRAPPRNKMALYEQLSIPSQRFNSG  52
Z. mays             -------------VNDTLK--------------GGPRAPPRNKMALYEQFSVPSHRYSAA  57
                               :::: :    Block I     ***::*::::..:*::::.:*...:...

C. reinhardtii      RPPGHMALGPGGGSAAGGGDSAVALLQQWQLQQLQQLQQQALLPGLPPAAASAFLNGAML  357
O. sativa           GGGGGVGGSP--AHST------------------------------------------  76
A. thaliana         G-----TMNSRSNNTS------------------------------------------  63
S. lycopersicum     V----LPLDP--NNTS------------------------------------------  62
Z. mays             VPPAPSPAPPWGAQRP------------------------------------------  73
                          .  :  ....

C. reinhardtii      GAGMQQQQQQPALSGHKPPLQQPLQYALPQPSLVRRPVAVAAGGSPSLQLPPPQAEGGMA  417
O. sativa           -SAASQSQSQSQVYGRDSSLFQPFNV-------------------------PSNRPGHST  110
A. thaliana         -TLVHPGPSSQPC-GVERNL--SVQH---------------------------------  85
S. lycopersicum     -KMAPPSSSQGS--GHDRSGYLPIQH-------------------------PPSR-----  89
Z. mays             -ASAVPSTSASQVGGGDRPIFPLFRV-------------------------PSTEP---V  104
                     . . ...:...  * ....  ....                          .

C. reinhardtii      RSAPAAQAPAVKPESSRQVGDMATAAAAAAAAAGDHYRNGSGSGDRHGPPSPQQQRQPLP  477
O. sativa           EKINSDKINKKISGSRKELGMLSSQTKGMDIYASRSTAEAPQRRAENTIKSSSGKRLA--  168
A. thaliana         --LDSSAANQATEKFVSQMSFMENVRSSAQ----------------------HDQRKMV  120
S. lycopersicum     ------RLADKPPGHSSDPSTLLQQYE-------------------------LKKRT--  115
Z. mays             RSSDQTNANSNGQGANGTIAESGRQRQSTHLKSKDTNAAGPPAEGNNSV----GKKLA--  158
                           ..   ..  .... .  .                            ....

C. reinhardtii      QPSRQLQAPQVQQTSGESYSTVTEGSTEASSGATSAGCSPPGAGGTTEAASPRQYDKSLG  537
O. sativa           -DDDEFMVP-----------SVFNSRFPQYSTQENAGVQDQST--PLVAANPHKSPSTVS  214
A. thaliana         REEEDFAVP-----------VYINSRRSQSHGRTKSGIEKEKHT-PMVAPSSHHS-----  163
S. lycopersicum     -EEDDFTVP-----------IFVNSKLGQAHGSHNVNMEKLSPSGQLFCPNK--------  155
Z. mays             -NDDDFTVP-----------SVLYSGMPPHSSQEKLTLFPTTSPCKSVPAKYSSTDKR--  204
                     ....: :*           ....:.  .........  . .   ....:.

C. reinhardtii      GGGTGSPPSGGRRLAGPAHPAGAAGVRADGYKRRRDDWEEEEEVGPPHCAKALEAAAVAA  597
O. sativa           KSSTKCYNTVSKKL---------ERIHVSDVKSRTPLKDKEMEAAQTSKN----------  255
A. thaliana         --------I---RF---------QEVNQTGSKQNVCLATCSKP--EVRDQ----------  191
S. lycopersicum     ------------EL---------EGVTHLTLRQQRNSQNKE----NLKCT----------  180
Z. mays             ------------RL---------EGMDASDVKSKGPSGIKEKEPVQVRIN----------  233
                             ::         ..:   . :..     .:    ... .
```

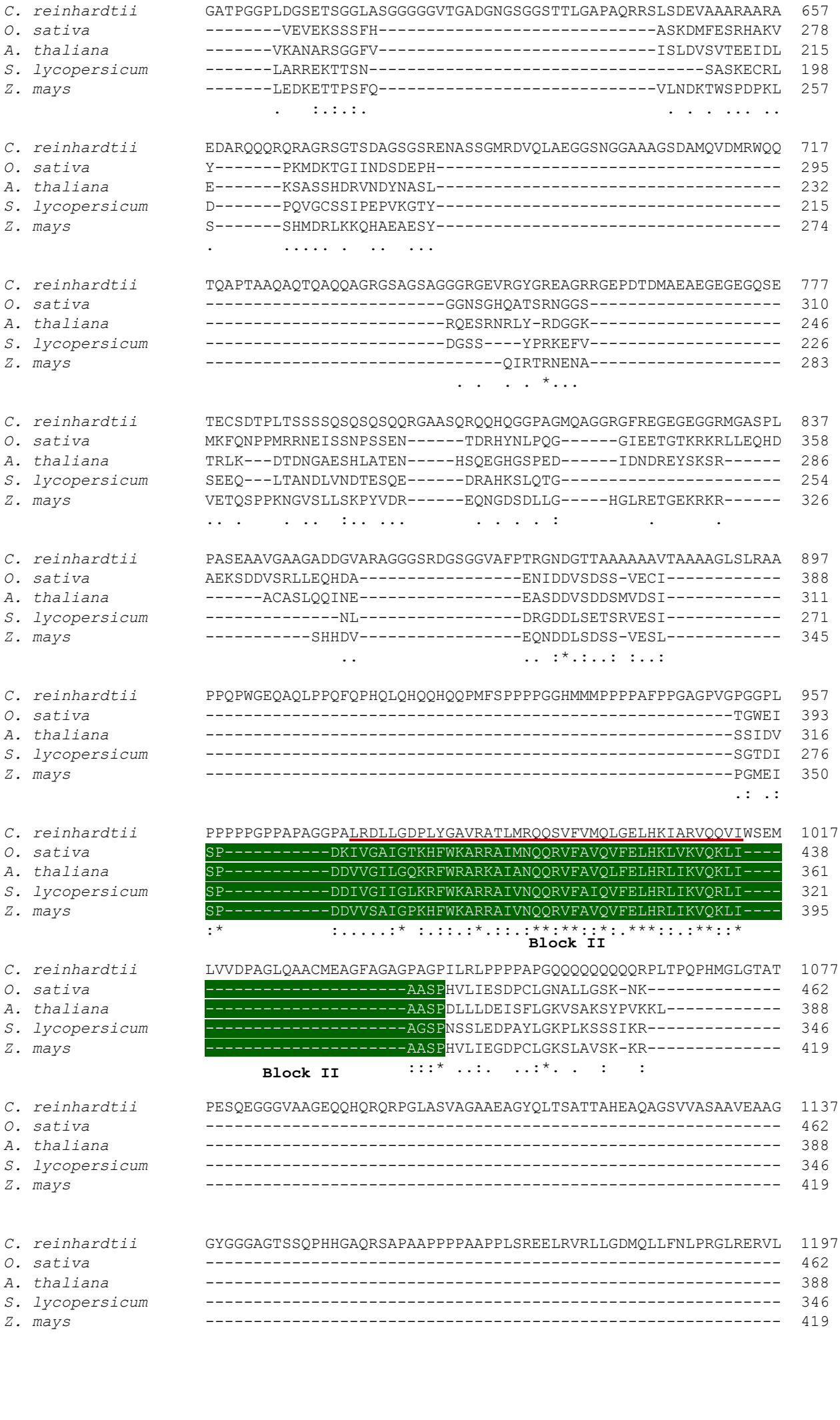
C. reinhardtii GATPGGPLDGSETSGGLASGGGGGVTGADGNGSGGSTTLGAPAQRRSLSDEVAAARAARA 657
O. sativa --------VEVEKSSSFH----------ASKDMFESRHAKV 278
A. thaliana -------VKANARSGGFV----------ISLDVSVTEEIDL 215
S. lycopersicum -------LARREKTTSN----------SASKECRL 198
Z. mays -------LEDKETTPSFQ----------VLNDKTWSPDPKL 257
C. reinhardtii EDARQQQRQRAGRSGTSDAGSGSRENASSGMRDVQLAEGGSNGGAAAGSDAMQVDMRWQQ 717
O. sativa Y-------PKMDKTGIINDSDEPH---------- 295
A. thaliana E-------KSASSHDRVNDYNASL---------- 232
S. lycopersicum D-------PQVGCSSIPEPVKGTY---------- 215
Z. mays S-------SHMDRLKKQHAEAESY---------- 274
C. reinhardtii TQAPTAAQAQTQAQQAGRGSAGSAGGGRGEVRGYGREAGRRGEPDTDMAEAEGEGEGQSE 777
O. sativa ----------GGNSGHQATSRNGGS---------- 310
A. thaliana ----------RQESRNRLY-RDGGK---------- 246
S. lycopersicum ----------DGSS----YPRKEFV---------- 226
Z. mays ----------QIRTRNENA---------- 283
C. reinhardtii TECSDTPLTSSSSQSQSQSQQRGAASQRQQHQGGPAGMQAGGRGFREGEGEGGRMGASPL 837
O. sativa MKFQNPPMRRNEISSNPSSEN------TDRHYNLPQG------GIEETGTKRKRLLEQHD 358
A. thaliana TRLK---DTDNGAESHLATEN-----HSQEGHGSPED------IDNDREYSKSR------ 286
S. lycopersicum SEEQ---LTANDLVNDTESQE------DRAHKSLQTG---------- 254
Z. mays VETQSPPKNGVSLLSKPYVDR------EQNGDSDLLG-----HGLRETGEKRKR------ 326
C. reinhardtii PASEAAVGAAGADDGVARAGGGSRDGSGGVAFPTRGNDGTTAAAAAAVTAAAAGLSLRAA 897
O. sativa AEKSDDVSRLLEQHDA----------ENIDDVSDSS-VECI---------- 388
A. thaliana ------ACASLQQINE----------EASDDVSDDSMVDSI---------- 311
S. lycopersicum ----------NL----------DRGDDLSETSRVESI---------- 271
Z. mays ----------SHHDV----------EQNDDLSDSS-VESL---------- 345
C. reinhardtii PPQPWGEQAQLPPQFQPHQLQHQQHQQPMFSPPPPGGHMMMPPPPAFPPGAGPVGPGGPL 957
O. sativa ----------TGWEI 393
A. thaliana ----------SSIDV 316
S. lycopersicum ----------SGTDI 276
Z. mays ----------PGMEI 350
C. reinhardtii PPPPPGPPAPAGGPALRDLLGDPLYGAVRATLMRQQSVFVMQLGELHKIARVQQVIWSEM 1017
O. sativa SP----------DKIVGAIGTKHFWKARRAIMNQQRVFAVQVFELHKLVKVQKLI---- 438
A. thaliana SP----------DDVVGILGQKRFWRARKAIANQQRVFAVQLFELHRLIKVQKLI---- 361
S. lycopersicum SP----------DDIVGIIGLKRFWKARRAIVNQQRVFAIQVFELHRLIKVQRLI---- 321
Z. mays SP----------DDVVSAIGPKHFWKARRAIVNQQRVFAVQVFELHRLIKVQKLI---- 395
Block II
C. reinhardtii LVVDPAGLQAACMEAGFAGAGPAGPILRLPPPPAPGQQQQQQQQQRPLTPQPHMGLGTAT 1077
O. sativa ----------AASPHVLIESDPCLGNALLGSK-NK---------- 462
A. thaliana ----------AASPDLLLDEISFLGKVSAKSYPVKKL---------- 388
S. lycopersicum ----------AGSPNSSLEDPAYLGKPLKSSSIKR---------- 346
Z. mays ----------AASPHVLIEGDPCLGKSLAVSK-KR---------- 419
Block II
C. reinhardtii PESQEGGGVAAGEQQHQRQRPGLASVAGAAEAGYQLTSATTAHEAQAGSVVASAAVEAAG 1137
O. sativa ---------- 462
A. thaliana ---------- 388
S. lycopersicum ---------- 346
Z. mays ---------- 419
C. reinhardtii GYGGGAGTSSQPHHGAQRSAPAAPPPPAAPPLSREELRVRLLGDMQLLFNLPRGLRERVL 1197
O. sativa ---------- 462
A. thaliana ---------- 388
S. lycopersicum ---------- 346
Z. mays ---------- 419

```
C. reinhardtii      RSVPPEQLVRPAVPPPPAPRPAATMVGGGGGLGGGGNAVVRPAASKLYTLMDGDEGPADS  1257
O. sativa           --LVEENL--KAQPLLVATI----------------------------------------DD  480
A. thaliana         --LPSEFLVKPPLPHVVVKQ----------------------------------------RGDS  410
S. lycopersicum     --LPLDCIVRESQSVLKRKH----------------------------------------DS  366
Z. mays             --LAGD-V--ETQLESAKND----------------------------------------DG  436
                      :. : :  .... . .                                          *.

C. reinhardtii      EQPTVVQKVVAQATARAAAAAAAEKQRNNGGSGGGSVAGGPNGGIPAAVGQAGPFRQQPTA  1317
O. sativa           VEPSLQQPEVSKENTEDSPPSPHDTGLGSGQRDQAATNGVSKSNRRATPVASDNKQNNWG  540
A. thaliana         EKTDQHKMESSAENVVGRLSN--------QGHHQQSNYMPFANNPPASPAPNGY-----C  457
S. lycopersicum     EKPH-FRMEHTAESNVGKASLSTV-----QNGSQLSSHKPFSGTPLPTPVTNDSNAGPWC  420
Z. mays             VRP--KQLEHSKEKTEANQPSP-------SQDEQAATNGAVAASMHT---PSDNKQKSWC  484
                    ..:   : : ..:.. . ..         ... : .. .. .... .   ...  .   .

C. reinhardtii      APPSPHAAQPATRLGLPDGAAAAVPSPHQVLPPFPPHGMPQRPQASALLMPPPSMHPHMH  1377
O. sativa           VQLQP----PQNQWLVP----VMSPLEGLVYKPYSGPC----PPAGSILA-P--------  579
A. thaliana         FPPQPPPSGNHQQWLIP----VMSPSEGLIYKPHPGMA----------HTGH--------  495
S. lycopersicum     FQ-QP----PGHQWLIP----VMSPSEGLVYKPFPGPG----------FTSP--------  453
Z. mays             IP-AP----PS-QWLIP----VMSPSEGLVYKPYTGHC----PPVGSLLAPP--------  522
                    .. .*    :  ::.:*    :::*:::::::*:.:..          .. :
                                Block III
C. reinhardtii      PPSPAAAFGLPPHALPAGPGLAQPHALLGGMPPAAAAAAGLAVGPPPHGMGAAGAAAAAT  1437
O. sativa           ---------------------------FYANCTPLSLPSTAGDFMNSAYG-----------  602
A. thaliana         ---------------------------YGGYY---------GHYMPTPMV-----------  509
S. lycopersicum     ---------------------------ICGSGPPGSSPTM-GNFFAPTYG-----------  475
Z. mays             ---------------------------FFASYPTSSSSTAGGDFMSSACG-----------  545
                                              . :  .. .     ........:

C. reinhardtii      AGAGAFGSPGSSFRAPPHPAQPGQPLHMDLPPQWSGPAMPQHGHLPLHGQLPPHMHMAMP  1497
O. sativa           ------------------------------------------------------------VP  604
A. thaliana         ------------------------------------------------------------MP  511
S. lycopersicum     ------------------------------------------------------------VP  477
Z. mays             ------------------------------------------------------------AR  547
                                                                                 .:

C. reinhardtii      LHGQLPPGMAGPLGALPARGPLQGGAPGAPPPGGAPMAVAAGGPRGPLQQPQQPQPLVRP  1557
O. sativa           MPHQ-PQHM---------------GAPGPPSMPMNYF-----------------------  625
A. thaliana         QYHP---GM---------------GFP---PPGNGYF-----------------------  527
S. lycopersicum     APNPHYQGM---------------GVPFAPPTGHGYF-----------------------  499
Z. mays             L-------M---------------SAP-------VYF-----------------------  555
                    .      .*              :.*   . . ..:

C. reinhardtii      PGVPPPLVGTPPLP-MPQPGPSAAAPVPHLDAAGTSQPQSAAAPAPTPAAPVPGGGFGGV  1616
O. sativa           ----------PPFS-IPVMNPTAPAPV--------------VEQGRHPSMPQPYGNF---  657
A. thaliana         ----------PPYGMMPTIMNPYCSSQ--------------QQQQQQPNEQMNQFGHPGN  563
S. lycopersicum     ----------RQYG-MPAMNPPISSTA--------------SEESNQYTMPGLQHQFSGV  534
Z. mays             ----------PSFS-MPAVSGSA------------------VEQVSHVAASQHKRN----  582
                             :... :*.. ...                    ..  .....    ..

C. reinhardtii      LPPALPVLFSSRQGAGVGAGGTKVPPVLRPPGVPAPAIPVPRPVASIDPHEAWFARHVAG  1676
O. sativa           ------------------------------------------------------------  657
A. thaliana         L-----------------------------------------------------------  564
S. lycopersicum     V-----------------------------------------------------------  535
Z. mays             ------------------------------------------------------------  582

C. reinhardtii      AGAGAQPAAAQPAAATPAAAAEAAGAAGPAAGAVGSRQAQAQAPSQGLGSRPGSLQRIAS  1736
O. sativa           ------------------------------------------------------------  657
A. thaliana         ------------------------------------------------------------  564
S. lycopersicum     ------------------------------------------------------------  535
Z. mays             ------------------------------------------------------------  582

C. reinhardtii      TERVVGGGGGSAAAVTGTGALQQPPERQSQPQQRQGAEEAEAAPSAARGGPSADVGWVAA  1796
O. sativa           ---------------------------------------EQQSWISCNMSHPSGIWRFHAS  679
A. thaliana         ------------------------------QNTQQQQQRSDNEPAPQQQQQPTKS-YPRA  593
S. lycopersicum     ------------------------------DDVNIQHQDSSNVLNQKKENVPDVVRYQST  565
Z. mays             ---------------------------------------------SCSEA-------VLAS  591
                                                                  .          . ..
```

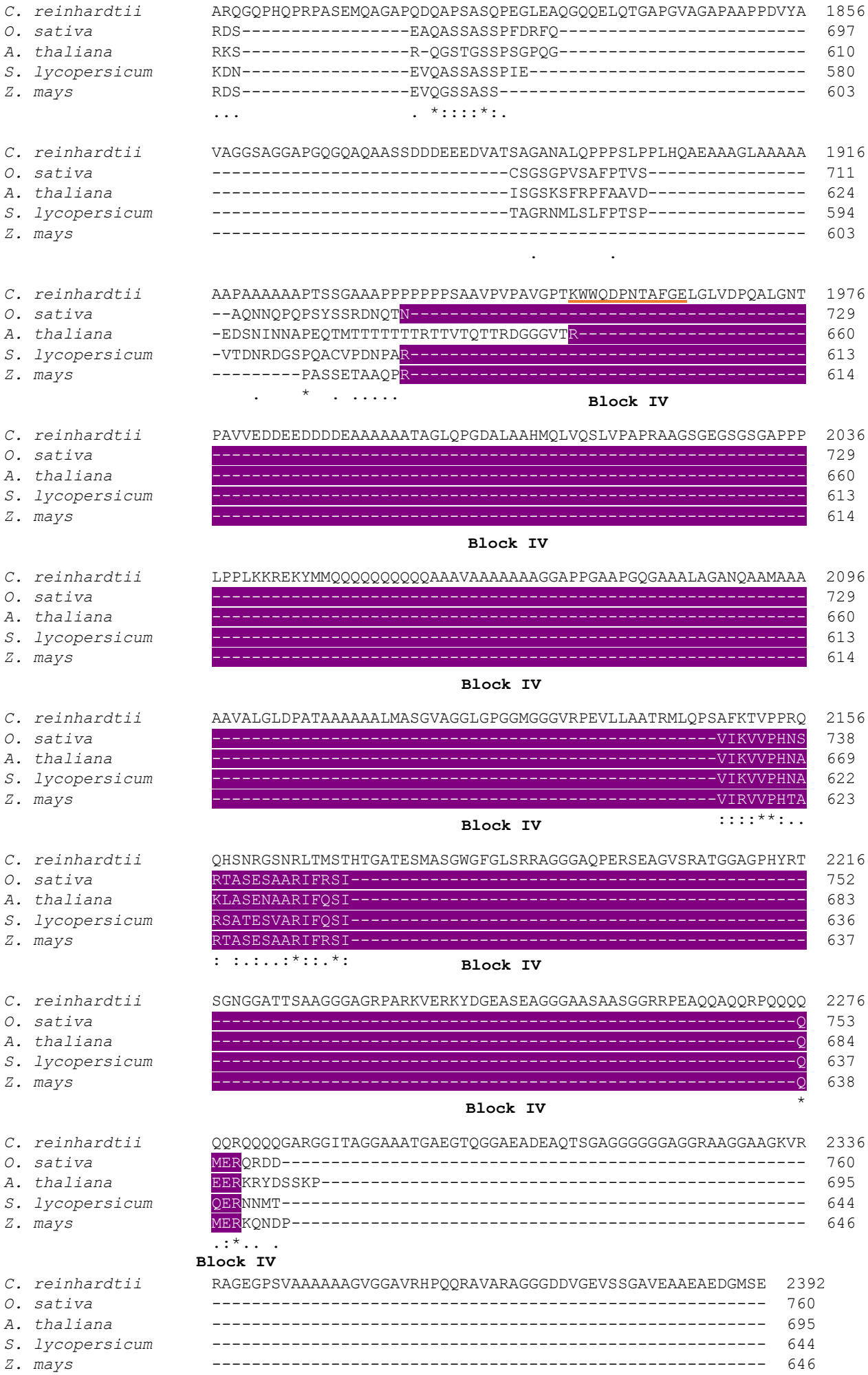
C. reinhardtii ARQGQPHQPRPASEMQAGAPQDQAPSASQPEGLEAQGQQELQTGAPGVAGAPAAPPDVYA 1856
O. sativa RDS----------EAQASSASSPFDRFQ---------- 697
A. thaliana RKS----------R-QGSTGSSPSGPQG---------- 610
S. lycopersicum KDN----------EVQASSASSPIE---------- 580
Z. mays RDS----------EVQGSSASS---------- 603
C. reinhardtii VAGGSAGGAPGQGQAQAASSDDDEEEDVATSAGANALQPPPSLPPLHQAEAAAGLAAAAA 1916
O. sativa ----------CSGSGPVSAFPTVS---------- 711
A. thaliana ----------ISGSKSFRPFAAVD---------- 624
S. lycopersicum ----------TAGRNMLSLFPTSP---------- 594
Z. mays ---------- 603
C. reinhardtii AAPAAAAAAPTSSGAAAPPPPPPPSAAVPVPAVGPTKWWQDPNTAFGELGLVDPQALGNT 1976
O. sativa --AQNNQPQPSYSSRDNQTN---------- 729
A. thaliana -EDSNINNAPEQTMTTTTTTTRTTVTQTTRDGGGVTR---------- 660
S. lycopersicum -VTDNRDGSPQACVPDNPAR---------- 613
Z. mays ---------PASSETAAQPR---------- 614
Block IV
C. reinhardtii PAVVEDDEEDDDDEAAAAAATAGLQPGDALAAHMQLVQSLVPAPRAAGSGEGSGSGAPPP 2036
O. sativa ---------- 729
A. thaliana ---------- 660
S. lycopersicum ---------- 613
Z. mays ---------- 614
Block IV
C. reinhardtii LPPLKKREKYMMQQQQQQQQQQAAAVAAAAAAAGGAPPGAAPGQGAAALAGANQAAMAAA 2096
O. sativa ---------- 729
A. thaliana ---------- 660
S. lycopersicum ---------- 613
Z. mays ---------- 614
Block IV
C. reinhardtii AAVALGLDPATAAAAAALMASGVAGGLGPGGMGGGVRPEVLLAATRMLQPSAFKTVPPRQ 2156
O. sativa ----------VIKVVPHNS 738
A. thaliana ----------VIKVVPHNA 669
S. lycopersicum ----------VIKVVPHNA 622
Z. mays ----------VIRVVPHTA 623
Block IV
C. reinhardtii QHSNRGSNRLTMSTHTGATESMASGWGFGLSRRAGGGAQPERSEAGVSRATGGAGPHYRT 2216
O. sativa RTASESAARIFRSI---------- 752
A. thaliana KLASENAARIFQSI---------- 683
S. lycopersicum RSATESVARIFQSI---------- 636
Z. mays RTASESAARIFRSI---------- 637
Block IV
C. reinhardtii SGNGGATTSAAGGGAGRPARKVERKYDGEASEAGGGAASAASGGRRPEAQQAQQRPQQQQ 2276
O. sativa ----------Q 753
A. thaliana ----------Q 684
S. lycopersicum ----------Q 637
Z. mays ----------Q 638
Block IV
C. reinhardtii QQRQQQQGARGGITAGGAAATGAEGTQGGAEADEAQTSGAGGGGGGAGGRAAGGAAGKVR 2336
O. sativa MERQRDD---------- 760
A. thaliana EERKRYDSSKP---------- 695
S. lycopersicum QERNNMT---------- 644
Z. mays MERKQNDP---------- 646
Block IV
C. reinhardtii RAGEGPSVAAAAAAGVGGAVRHPQQRAVARAGGGDDVGEVSSGAVEAAEAEDGMSE 2392
O. sativa ---------- 760
A. thaliana ---------- 695
S. lycopersicum ---------- 644
Z. mays ---------- 646

Fig 8. Protein sequence alignment with only angiosperm ELF3. Protein encoded by Cre07. g357500 was aligned with *A. thaliana* ELF3 and its homologs from *O. sativa* (ELF3-1)*, S. lycopersicum* and *Z. mays* using MAFFT (MAFFT 7.471, SnapGene) and MUSCLE (MUSCLE 3.8.1551, SnapGene) multiple sequence alignment algorithms. Block I, II, III, and IV are highlighted according to the regions recognized as Blocks in *A. thaliana* ELF3 (**Liu et al., 2001**). Conserved and similar amino acids are represented in the Clustal format. Region 1 and Region 2 are underlined in red and orange respectively, in both alignments. Details of the amino acid sequences can be found in **Table 2**.

A

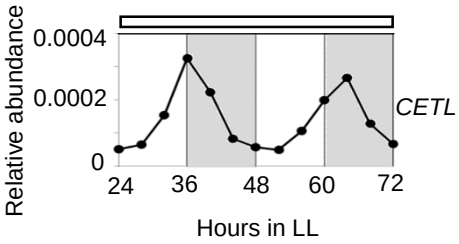

Fig 9. *CETL* gene expression pattern in LL conditions. *CETL* mRNA rhythm in LL conditions. A free-running high-salt culture of the wild type (WT; ROC15-LUC mt^{+}) was used. Cells were harvested every 4 hours between 24-72 hours in LL conditions and then subjected to RT-qPCR analysis. A representative trace of *CETL* mRNA levels (normalized by *RCK1* mRNA levels) is shown. The white bar above the graph represents the light conditions (i.e., LL conditions). The alternating white and grey background in the graph represents the subjective day and subjective night, respectively, that is expected from the light conditions prior to LL.

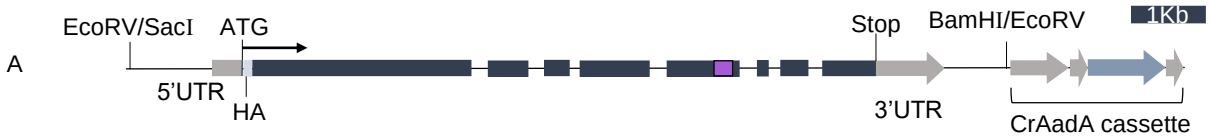
A
EcoRV/SacI
ATG
Stop
BamHI/EcoRV
1Kb
5'UTR
HA
3'UTR
CrAadA cassette

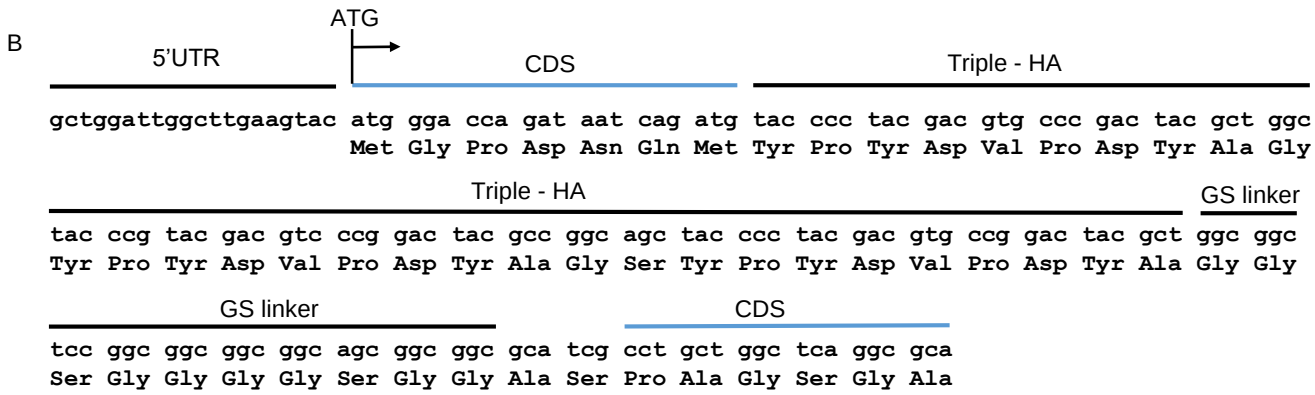
B
ATG
5'UTR
CDS
Triple - HA
gctggattggcttgaagtac atg gga cca gat aat cag atg tac ccc tac gac gtg ccc gac tac gct ggc
Met Gly Pro Asp Asn Gln Met Tyr Pro Tyr Asp Val Pro Asp Tyr Ala Gly
Triple - HA
GS linker
tac ccg tac gac gtc ccg gac tac gcc ggc agc tac ccc tac gac gtg ccg gac tac gct ggc ggc
Tyr Pro Tyr Asp Val Pro Asp Tyr Ala Gly Ser Tyr Pro Tyr Asp Val Pro Asp Tyr Ala Gly Gly
GS linker
CDS
tcc ggc ggc ggc ggc agc ggc ggc gca tcg cct gct ggc tca ggc gca
Ser Gly Gly Gly Gly Ser Gly Gly Ala Ser Pro Ala Gly Ser Gly Ala

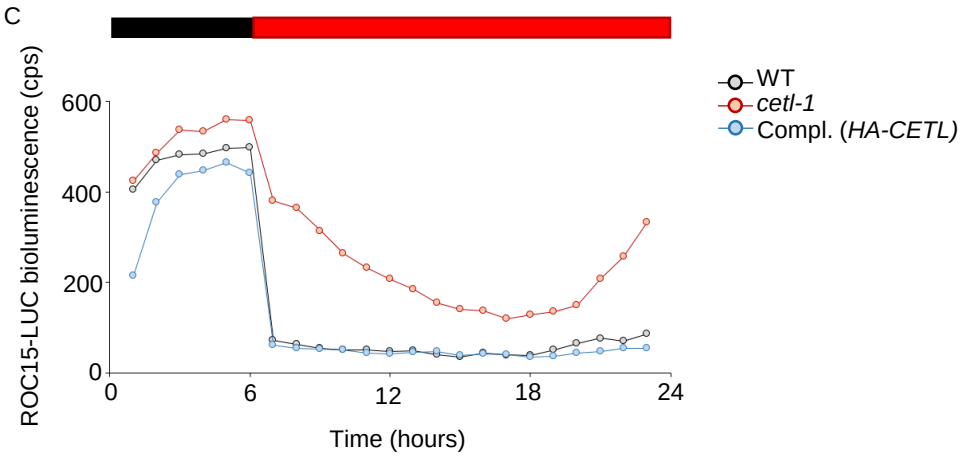
C
ROC15-LUC bioluminescence (cps)
600
400
200
0
0
6
12
18
24
Time (hours)
WT
cetl-1
Compl. (HA-CETL)

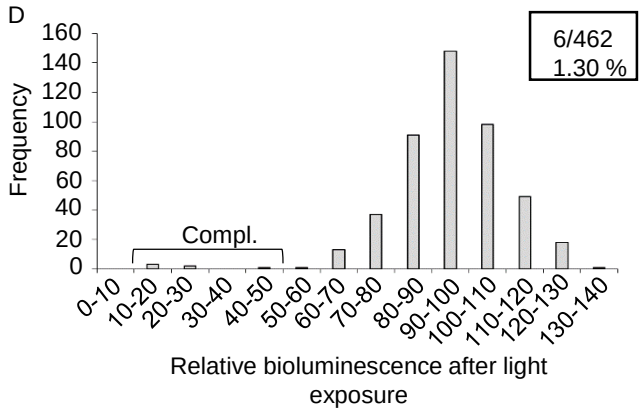
D
Frequency
160
140
120
100
80
60
40
20
0
6/462
1.30 %
Compl.
0-10
10-20
20-30
30-40
40-50
50-60
60-70
70-80
80-90
90-100
100-110
110-120
120-130
130-140
Relative bioluminescence after light exposure

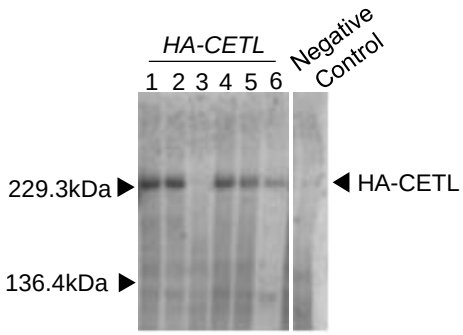
E
HA-CETL
1 2 3 4 5 6
Negative Control
229.3kDa
136.4kDa
HA-CETL

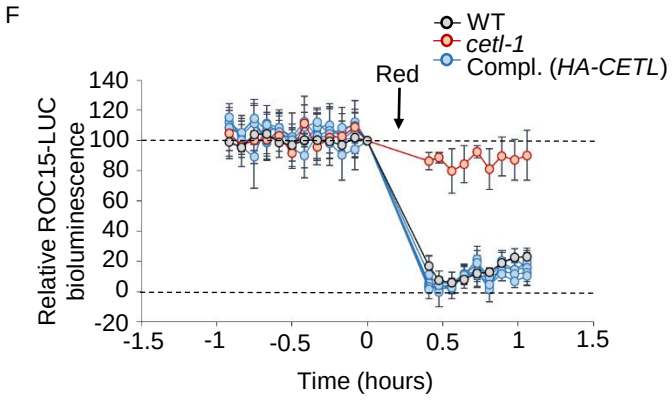
F
WT
cetl-1
Compl. (HA-CETL)
Red
Relative ROC15-LUC bioluminescence
140
120
100
80
60
40
20
0
-20
-1.5
-1
-0.5
0
0.5
1
1.5
Time (hours)

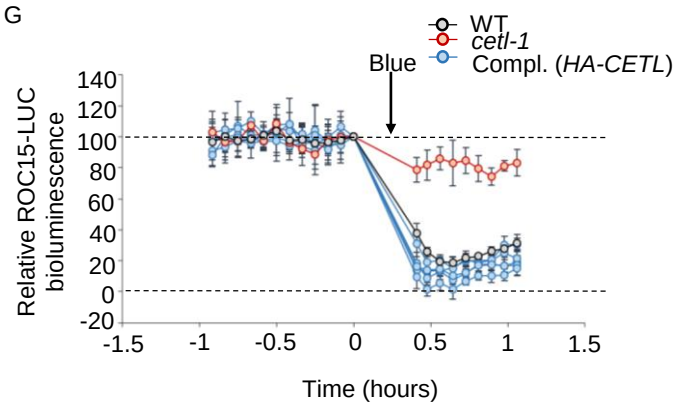
G
WT
cetl-1
Compl. (HA-CETL)
Blue
Relative ROC15-LUC bioluminescence
140
120
100
80
60
40
20
0
-20
-1.5
-1
-0.5
0
0.5
1
1.5
Time (hours)

Fig 10. Complementation by *HA-CETL* gene. A. Schematic representation of the gene fragment used for complementation. An HA tag, codon adapted for the *C. reinhardtii* nuclear genome was incorporated after the second predicted start codon of the *CETL* gene that was ligated to *aadA*. **B.** The codon adapted sequences of the HA tag and a flexible GS linker. **C.** Representative trace of the ROC15-LUC bioluminescence pattern of one of six complements. Culture preparations were the same as in **Fig 1A**. Cultures were subjected to 6 h dark /18 h red light (2 µmol m^{-2} s^{-1}) cycle. The representative trace of one of the six complements is shown in comparison to the traces of the WT and *cetl-1* (n=1). **D.** Histogram showing the distribution of the transformants with respect to the ROC15 bioluminescence levels at the first time point after red light exposure. Bioluminescence levels were calculated relative to the value just before light exposure. **E.** Western blot analysis of the complemented strains. Unsynchronized TAP cultures were maintained in darkness for 6 hours. Western blot was performed on whole protein extracts from cells harvested in darkness. The WT BR mt^+ strain was used as the negative control. **F** and **G.** Light pulse response of five of the six complements. Spot cultures on high-salt agar were transferred to 96 well black plates, and bioluminescence was monitored as described in Materials and Methods. Akalumine was used as substrate. Cells were in darkness for at least 6 hours before being exposed to 5-min pulses of red (**F**, 5 µmol m^{-2} s^{-1}) and blue light (**G**, 10 µmol m^{-2} s^{-1}). Bioluminescence values were calculated relative to the value just before the light pulse (Time 0). Mean ± SD of four biological replicates is shown. Arrows indicate approximate time of the light pulse.

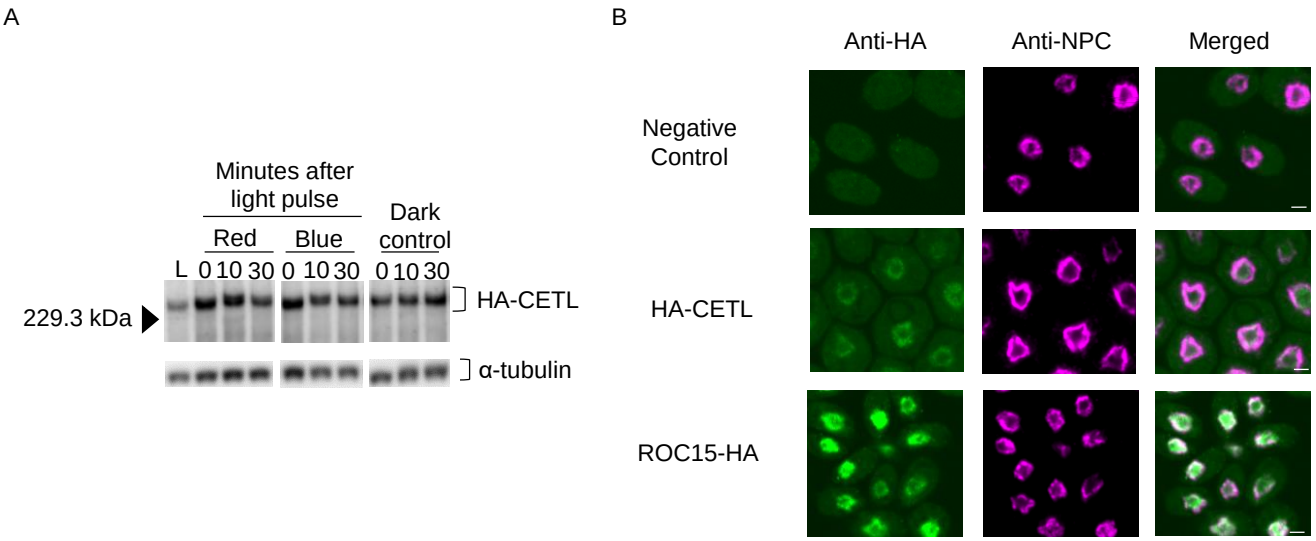

Fig 11. CETL protein light response and subcellular localization. A. CETL light response. High-salt cultures of complemented cells expressing HA-CETL were used. Cultures were maintained in LD conditions and exposed to 5 min pulses of red (10 µmol m^{-2} s^{-1}) and blue (20 µmol m^{-2} s^{-1}) light at ZT18. Western blot analysis was performed on whole protein extracts of cells harvested at ZT6 during the light phase (L), in the darkness before light pulse (0 min), and, 10 and 30 minutes after exposure to light pulses. Dark control was sampled at the same time points as the light pulsed samples. α-tubulin was used as loading control. **B.** CETL subcellular localization in comparison to ROC15 localization. Unsynchronized TAP cultures were maintained in darkness for 6 hours before cells were harvested in darkness and subjected to immunocytochemistry. The nuclear pore complex (NPC) was stained as a marker for the nuclear membrane. The ROC15-HA strain was used to observe ROC15 localization. The BR mt^{+} strain was used as a negative control. Results for a representative strain are shown. Scale bar: 2µm.

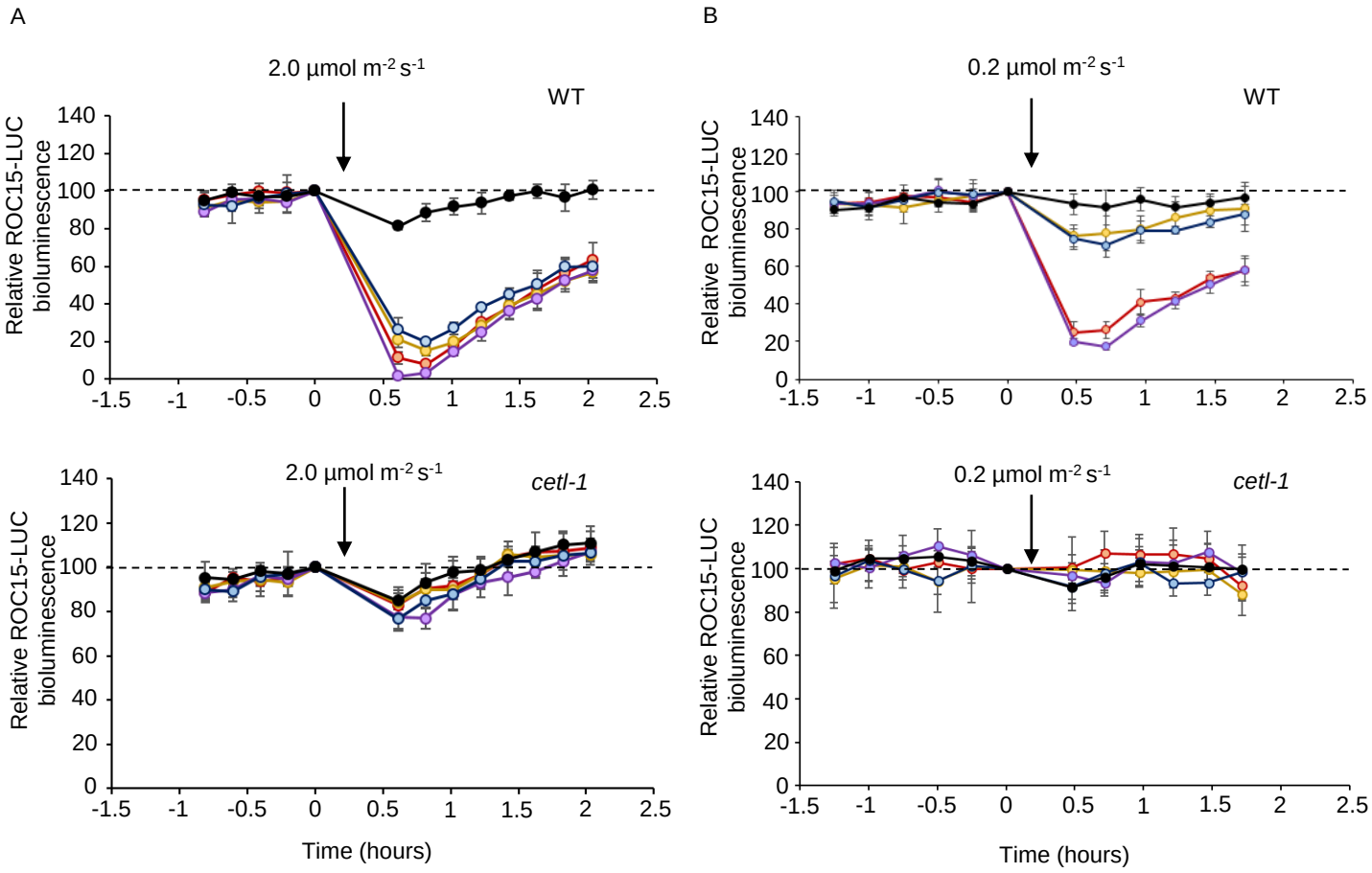

Fig 12. ROC15-LUC light response at different wavelengths in the *cetl-1* mutant. Spot cultures on high-salt agar were transferred to 96 well black plates, and bioluminescence was monitored as described in Materials and Methods. Akalumine was used as substrate. Cultures were maintained in darkness for at least 3 hours to allow for the build-up of ROC15-LUC, and then exposed to a 5-minute light pulse (violet, blue, yellow, or red) at two different intensities. **A** and **B**. Representative traces of ROC15-LUC bioluminescence in response to light pulses at intensities of 2 µmol m^{-2} s^{-1} and 0.2 µmol m^{-2} s^{-1}, respectively, in WT (top panel) and *cetl-1* (bottom panel). Bioluminescence values have been calculated relative to those at the time point just before the light pulse. Mean ± SD of 4 biological replicates are shown. Arrows refer to the approximate time of the light pulse. Each color represents the wavelength of light to which the sample was exposed.

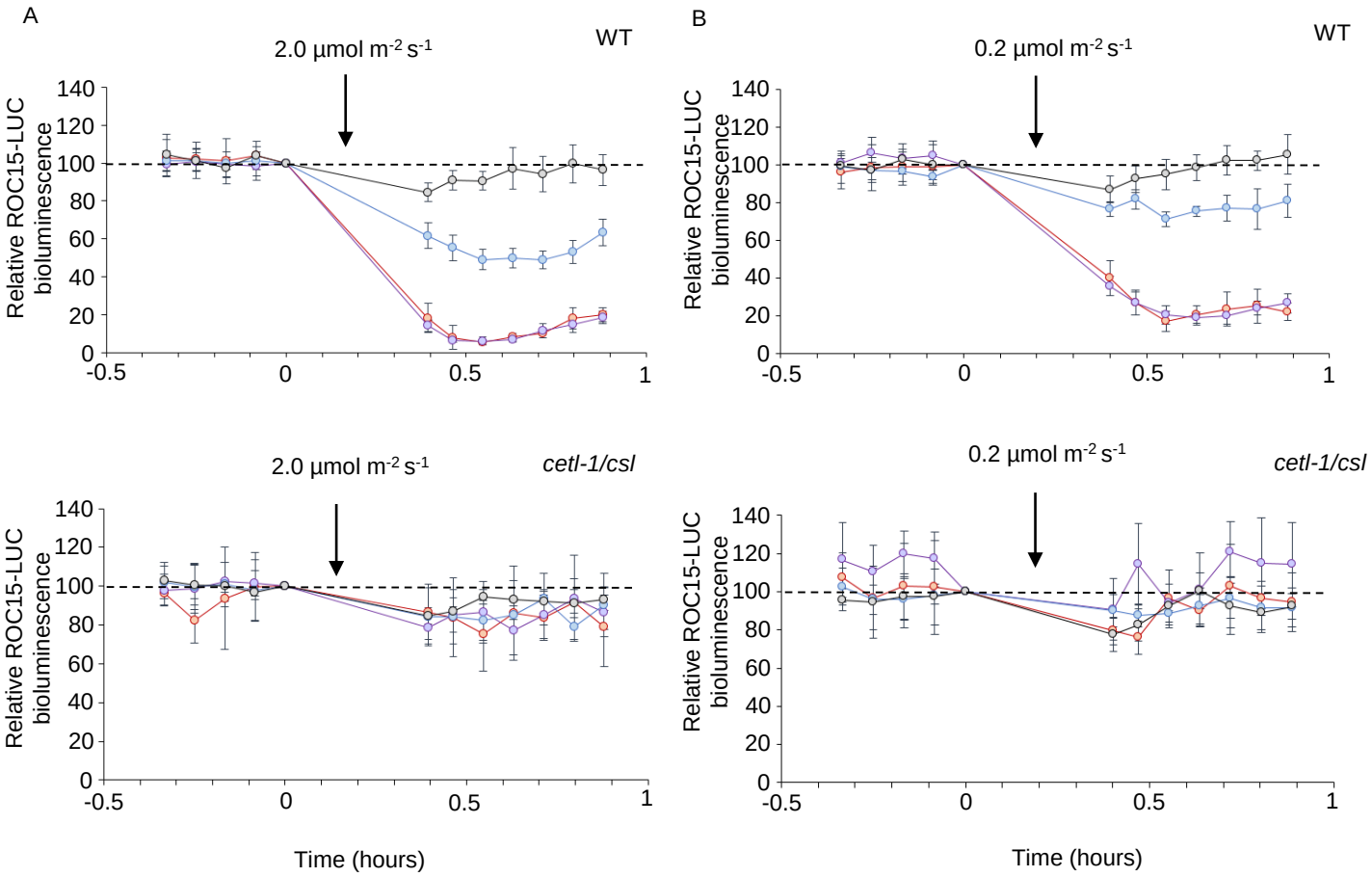

Fig 13. ROC15-LUC light response at different wavelengths in *cetl-1/csl* double mutant. The *cetl-1* (mt^-) mutant was crossed with *csl* mutant (mt^+) to obtain progenies that inherited *cetl-1* mutation, *csl* mutation and *ROC15-LUC*. Progenies were selected by antibiotic resistance testing and genomic PCRs. Spot cultures were prepared as described in **Fig 12**. Cultures were maintained in darkness for at least 6 hours before being exposed to 5-min pulses of red, blue and violet light **A** and **B.** Representative traces of WT (top) and *cetl-1/csl* double mutant (bottom) ROC15-LUC response to lights of different wavelength at intensities of 2 µmol m^{-2} s^{-1} (**A**) and 0.2 µmol m^{-2} s^{-1} (**B**). ROC15-LUC bioluminescence values have been calculated relative to the value just before exposure to the light pulse (Time 0). Mean ± SD of five biological replicates are shown. Arrows indicate the approximate time of the light pulse.

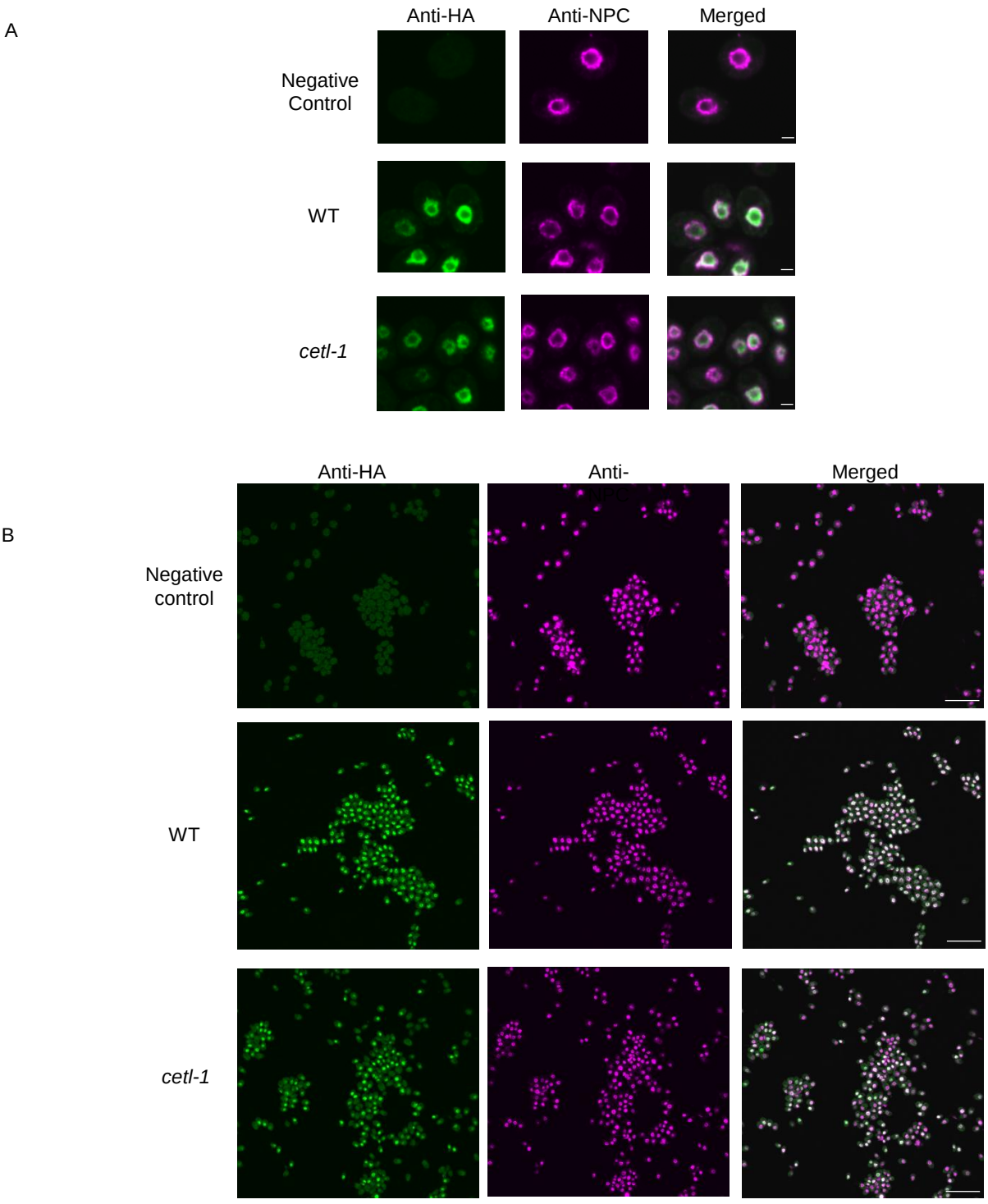

Fig 14. Subcellular localization of the ROC15 protein in the *cetl-1* mutant. The complement (**Fig 6**) was crossed with the ROC15-HA strain (wild type [WT]) to obtain progenies that inherited *ROC15-HA* (but not *ROC15-LUC*) along with the *cetl-1* mutation (*cetl-1*). Progenies were selected by antibiotic screening and genomic PCRs. **A.** ROC15 localization in the mutant. Unsynchronized TAP cultures were maintained in darkness for at least 6 hours to allow for accumulation of ROC15-HA. Cells were harvested in darkness and then subjected to immunocytochemistry. The NPC was counterstained as a marker for the nuclear membrane. The BR mt^+ strain was used as a negative control. Scale bar: 2μm. **B.** ROC15 sub-cellular localization in the *cetl-1* mutant at a lower magnification. Cultures were prepared in the same manner as described in **A**. Cultures were maintained in 6 hours of darkness and immunocytochemistry was performed on cells harvested in darkness. NPC was counterstained as a marker for the nuclear membrane. The BR mt^+ strain was used as the negative control. Cells were observed at a lower magnification of 10x. Scale bar: 30μm.

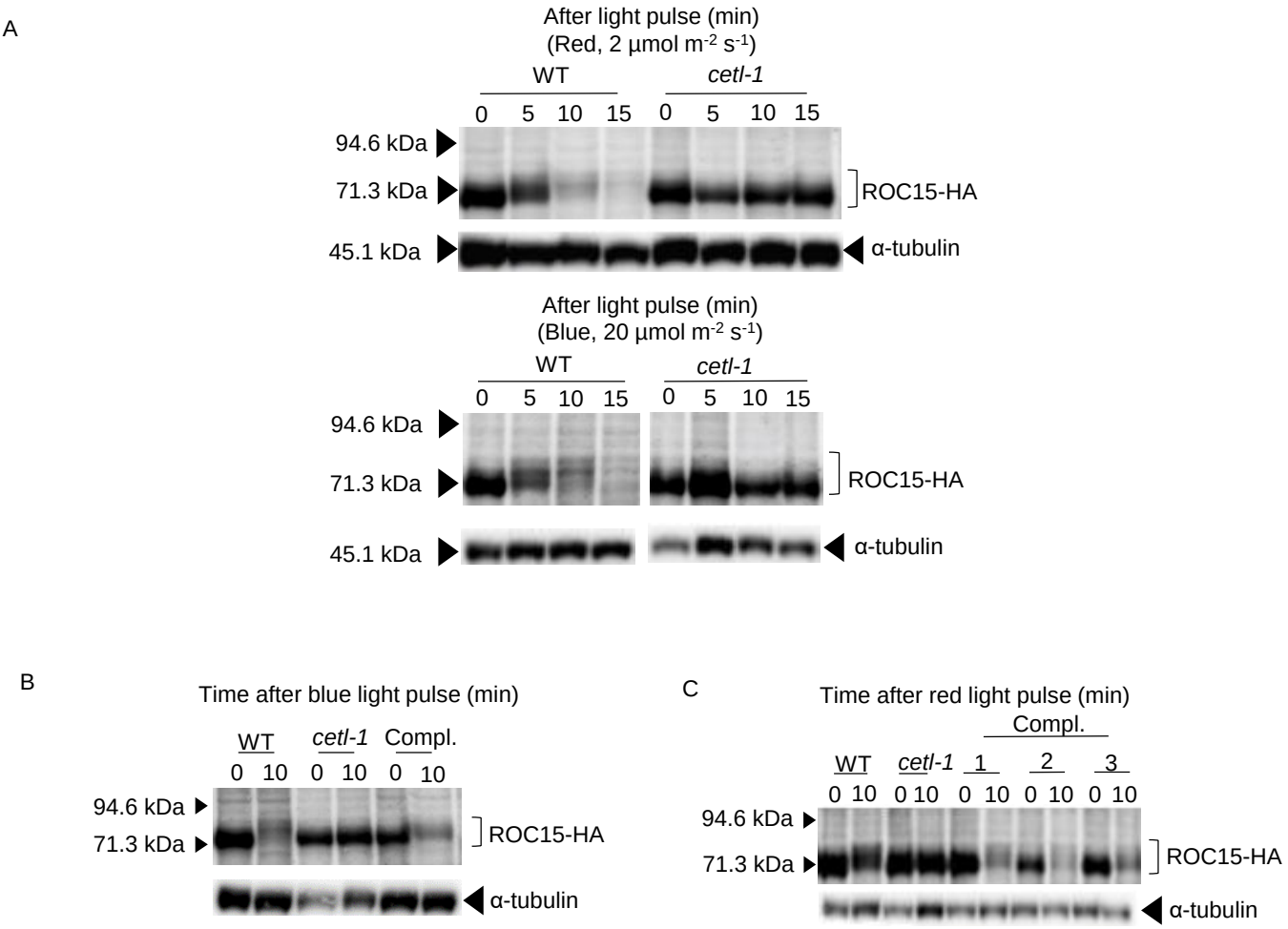

Fig 15. Light induced phosphorylation of the ROC15 protein in the *cetl-1* mutant. Strains in this experiment were obtained from the cross described in **Fig 14**. **A.** Absence of light-induced ROC15 phosphorylation in the mutant. Cells in LD-entrained high-salt cultures were exposed to a 0.5-min light pulse of red (2 µmol m^{-2} s^{-1}) and blue (20 µmol m^{-2} s^{-1}) wavelengths at midnight (between ZT14 and ZT17). Western blot analysis was performed on whole protein extracts from cells sampled before the light pulse and at approximately 5, 10, and 15 minutes after the light pulse. The 0 min data corresponds to the sample just before the light pulse. **B** and **C.** Light induced phosphorylation of ROC15 in complemented strains **B.** Cultures were prepared as described in **A**, and exposed to 0.5-min light pulse of blue (**B**, 20 µmol m^{-2} s^{-1}) wavelength at midnight (between ZT14 and ZT17). **C.** Unsynchronized TAP cultures were maintained in darkness for 4 hours and exposed to a 0.5-min pulse of red light (**C**, 2 µmol m^{-2} s^{-1}). Western blot was performed on whole protein extracts from cells sampled before the light pulse and at 10 minutes after the light pulse. The 0-minute data corresponds to the time point just before samples were exposed to a light pulse. Results of three complemented progenies (1-3) are shown for the red light pulse experiment (**C**). WT in this experiment refers to the wild type sibling from the cross described in **Fig 14**. α-tubulin was used as the loading control.

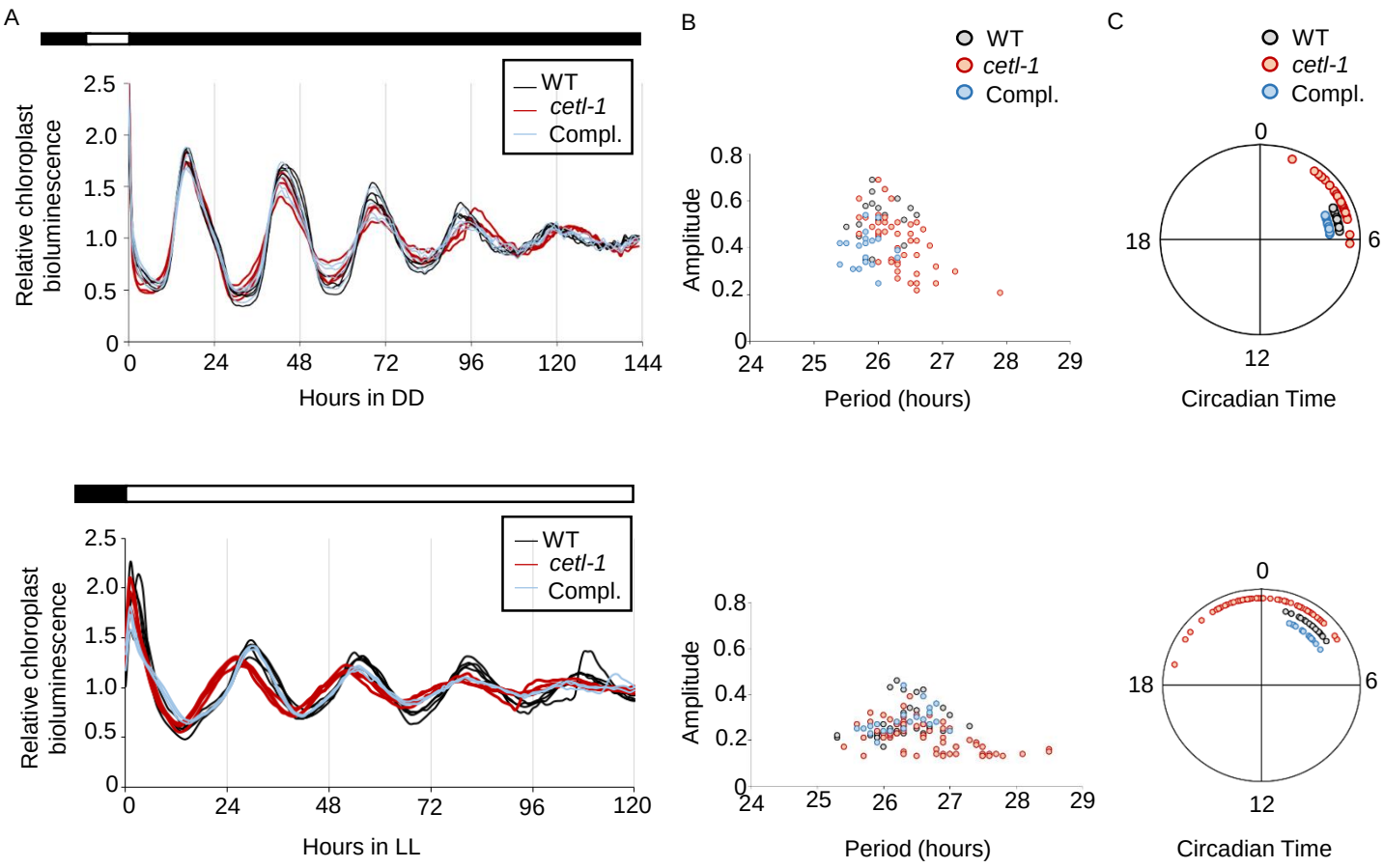

Fig 16. Circadian rhythm under DD and LL conditions. The mating type^{-} (mt^{-}) strain of the *cetl-1* mutant (**Fig 3**) and the complement (**Fig 6**) were crossed with the CBR strain (mt^{+}) (wild type [WT]) to obtain progenies that inherited the chloroplast luciferase reporter (but not the *ROC15-LUC*) along with *cetl-1* mutation (1-3), or along with both the *cetl-1* mutation and the *CETL* transgene (Compl.). These progenies were selected by antibiotic screening and genomic PCRs. Spot cultures of these progenies were synchronized by a 12-hour dark/12-hour light or 12-hour darkness before release into DD or LL conditions (2 μmol m^{-2} s^{-1}), respectively. **A.** Representative traces of chloroplast bioluminescence rhythm in the *cetl-1* mutant under DD (top) and LL (bottom) conditions. Data of 3-5 biological replicates of the WT, a *cetl-1* progeny, and a complemented progeny from a single trial are shown. The light regime used is also depicted above the graphs. **B** and **C.** The period and amplitude (B) and phase diagram indicating the circadian phases (C) of the rhythms under DD (top) and LL (bottom) conditions. Data points correspond to the results of biological replicates of the WT and three *cetl-1* progenies across four trials, and of three complemented progenies from two trials (Refer to **Fig 18** for the phase diagrams of individual *cetl-1* progeny from four different trials). The circadian times (CT) at the beginning of the DD and LL conditions were set to 12 and 0, respectively.

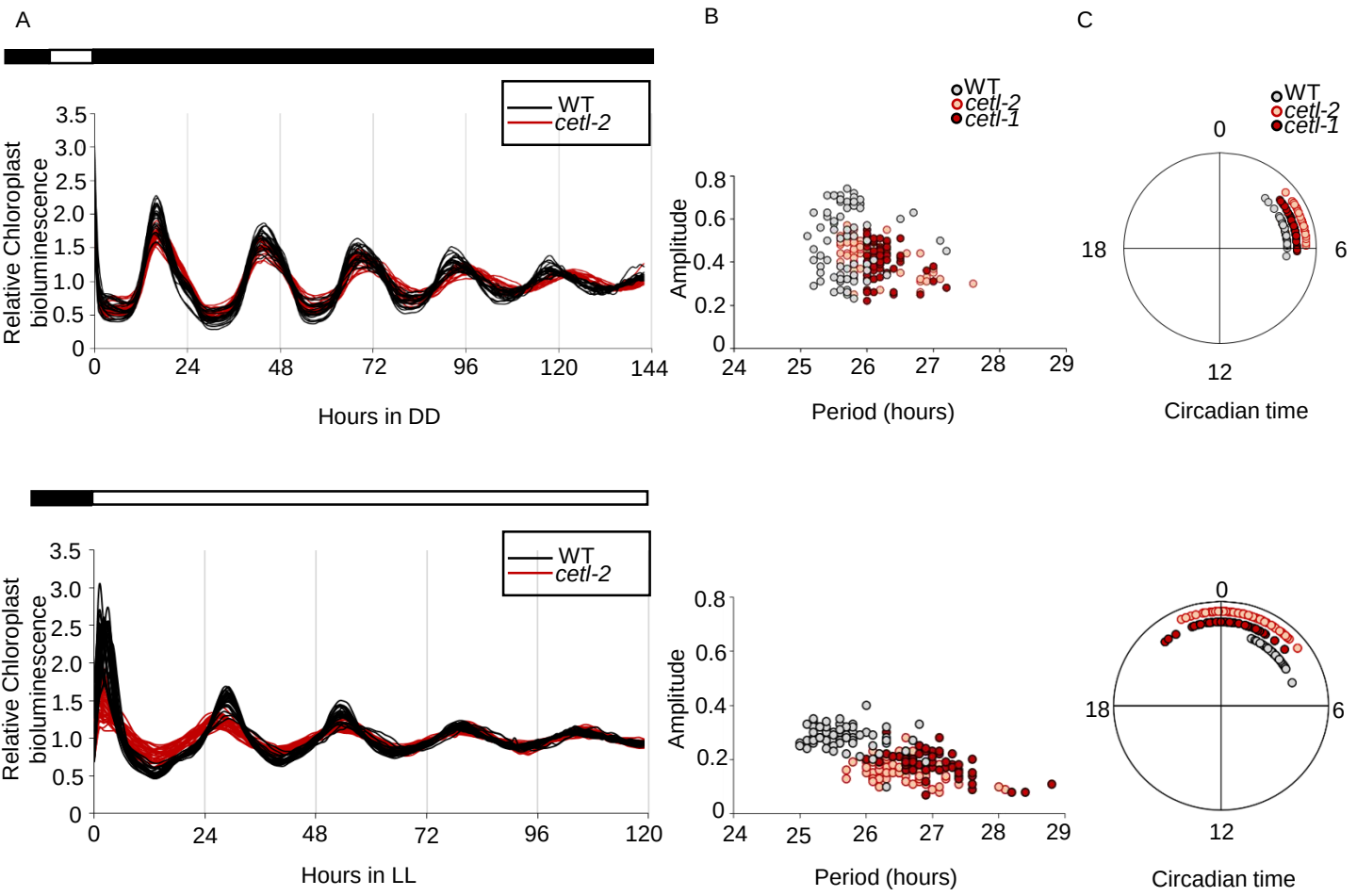

Fig 17. Circadian rhythm of the *cetl-2* mutant under LL and DD conditions. The *cetl-2* mutant (mt^-) was crossed with the CBR strain ([mt^+], WT) to obtain progenies with *cetl-2* mutation and chloroplast luciferase reporter. Progenies were selected based on antibiotic resistance and genomic PCRs. Spot cultures were prepared in the same manner as in **Fig 16. A.** Representative chloroplast bioluminescence rhythm of the *cetl-2* mutant under DD (top) and LL (bottom) conditions. Results from a single trial are shown. 22-25 biological replicates of the WT and 24-30 biological replicates of the *cetl-2* mutant were used for the experiments. Light schedules used are also depicted. **B** and **C.** Distribution of period and amplitude (**B**) and phase diagram of the circadian phases (**C**) of the chloroplast bioluminescence rhythm of the *cetl-2* mutant under DD (top) and LL (bottom) conditions. Data points correspond to the chloroplast bioluminescence rhythm of one *cetl-2* progeny from three trials (74-80 biological replicates). Data points have been shown in comparison to one *cetl-1* progeny and WT from three trials (61-72 and 67-69 biological replicates respectively). *cetl-1* was included in these experiments for comparison. The CT at the beginning of LL was set to 0 and at the beginning of DD was set to 12.

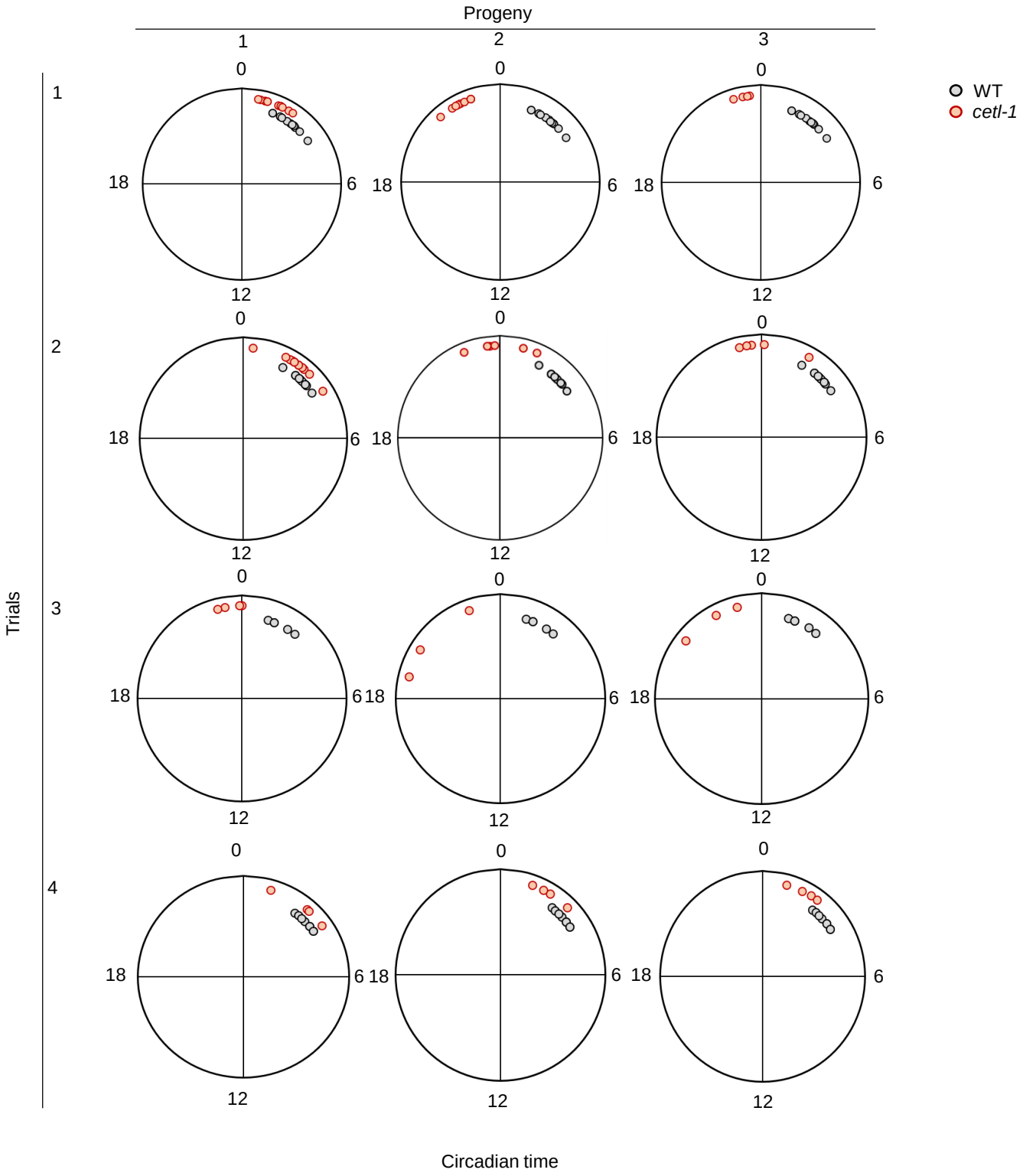

Fig 18. Circadian phases of individual *cetl-1* progeny from different trials under LL conditions. The phase diagram shown in **Fig 16C** (bottom) has been separated to show the data of individual *cetl-1* progeny (1-3) from different trials. As all three *cetl-1* progenies were analyzed at the same time in every trial, the circadian phases of the *cetl-1* progenies within a single trial are compared to the same WT data points. 5-12 biological replicates of WT and 3-12 biological replicates of *cetl-1* progenies were used for the experiment.

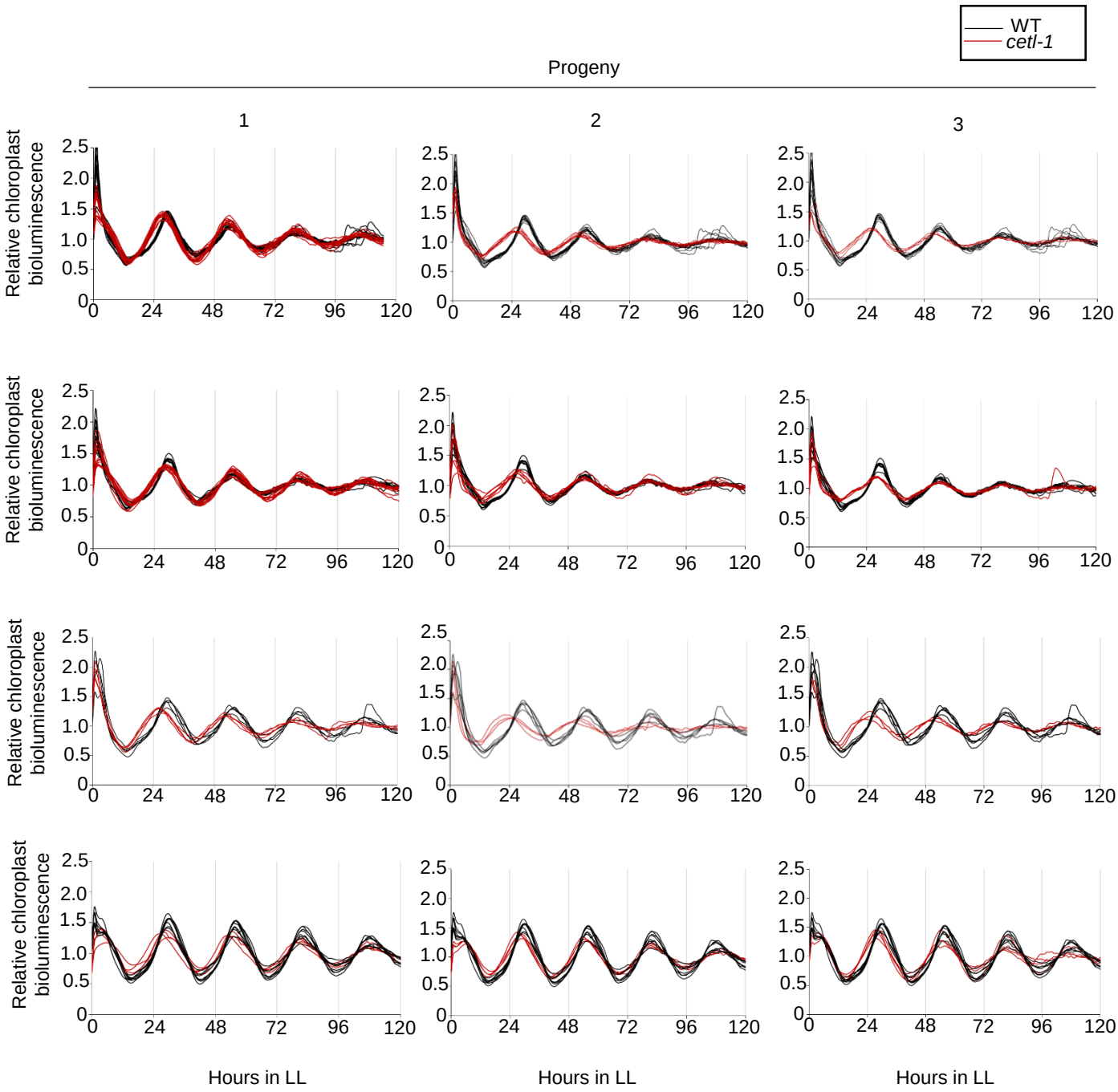

Fig 19. Chloroplast bioluminescence rhythms of individual *cetl-1* progeny from different trials under LL conditions. The chloroplast bioluminescence rhythms corresponding to the phase diagrams in **Fig 18**. The chloroplast bioluminescence traces of *cetl-1* and WT from **Fig 16A** are included in the figure for easy comparison. Since all three *cetl-1* progenies were monitored at the same time in a given trial, the bioluminescence traces of the progenies within a trial are compared to the same WT bioluminescence traces. Each row corresponds to a single trial. 5-12 biological replicates of the WT and 3-12 biological replicates of the *cetl-1* progenies were used in the experiments.

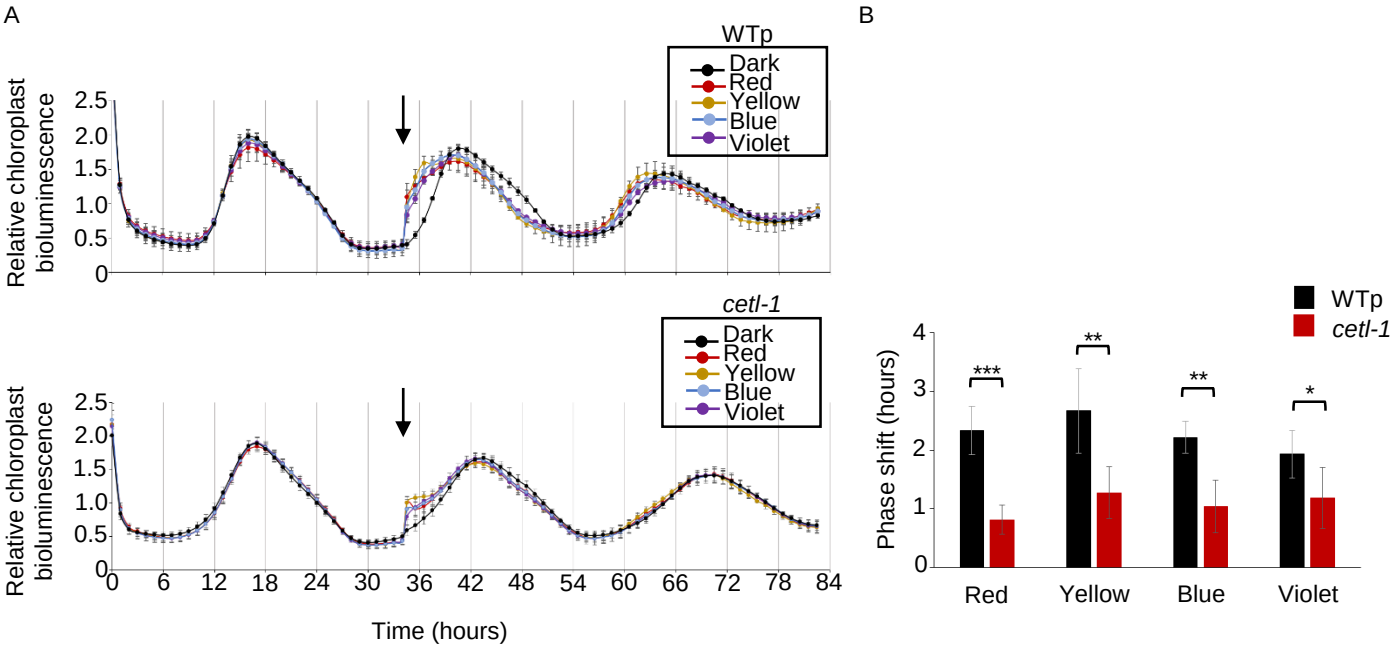

Fig 20. Light - induced phase resetting of the *cetl-1* mutant. The strains used in this experiment were obtained from the same cross as described in **Fig 16**. Representative bioluminescence traces (left panel) and the amount of phase shift after the light pulse (right panel) are shown. A WT sibling (WTp) from the cross was used as WT for this experiment. Spot cultures were exposed to a 5-minute pulse of violet (5 µmol m^{-2} s^{-1}), blue (38 µmol m^{-2} s^{-1}), yellow (20 µmol m^{-2} s^{-1}), and red (15 µmol $m^{-2}s^{-1}$) light at approximately the 34th hour after the onset of DD conditions. The amount of phase shift was calculated with respect to the dark control. Mean ± SD of 6-8 biological replicates are shown. *P*-values are based on Student's *t*-tests: * $P<0.05$, ** $P< 0.001$, and *** $P<0.0001$.

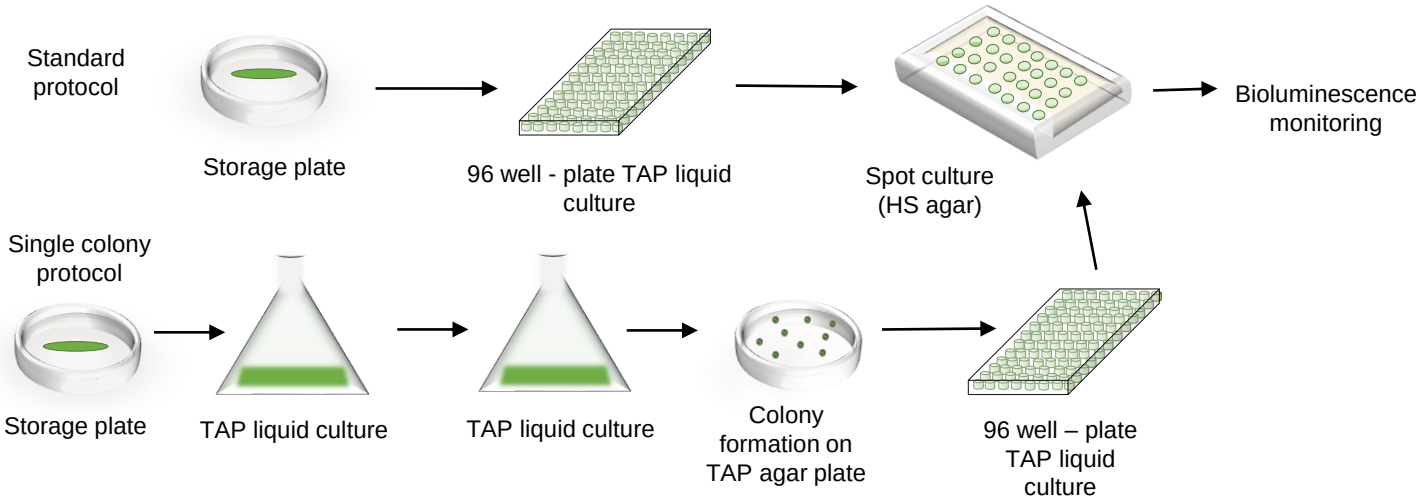

Fig 21. Standard protocol versus single colony protocol. Standard protocol: Cells were picked from a single patch on a storage plate and transferred to TAP medium in a 96 well plate. Cultures from the 96 well plate were then spotted on to HS agar plates (Materials and Methods: Culture conditions - Spot cultures for bioluminescence monitoring). **Single colony protocol**: An unsynchronized TAP culture was prepared from a single patch of cells on a storage plate (Materials and Methods: Culture conditions). Cells from this culture were spread onto TAP agar plates and allowed to form colonies. Colonies were picked at random from the plate and used in the preparation of a spot culture. In both protocols, cells were maintained in LL conditions at all stages of preparation until exposure to the appropriate light regime for synchronization.

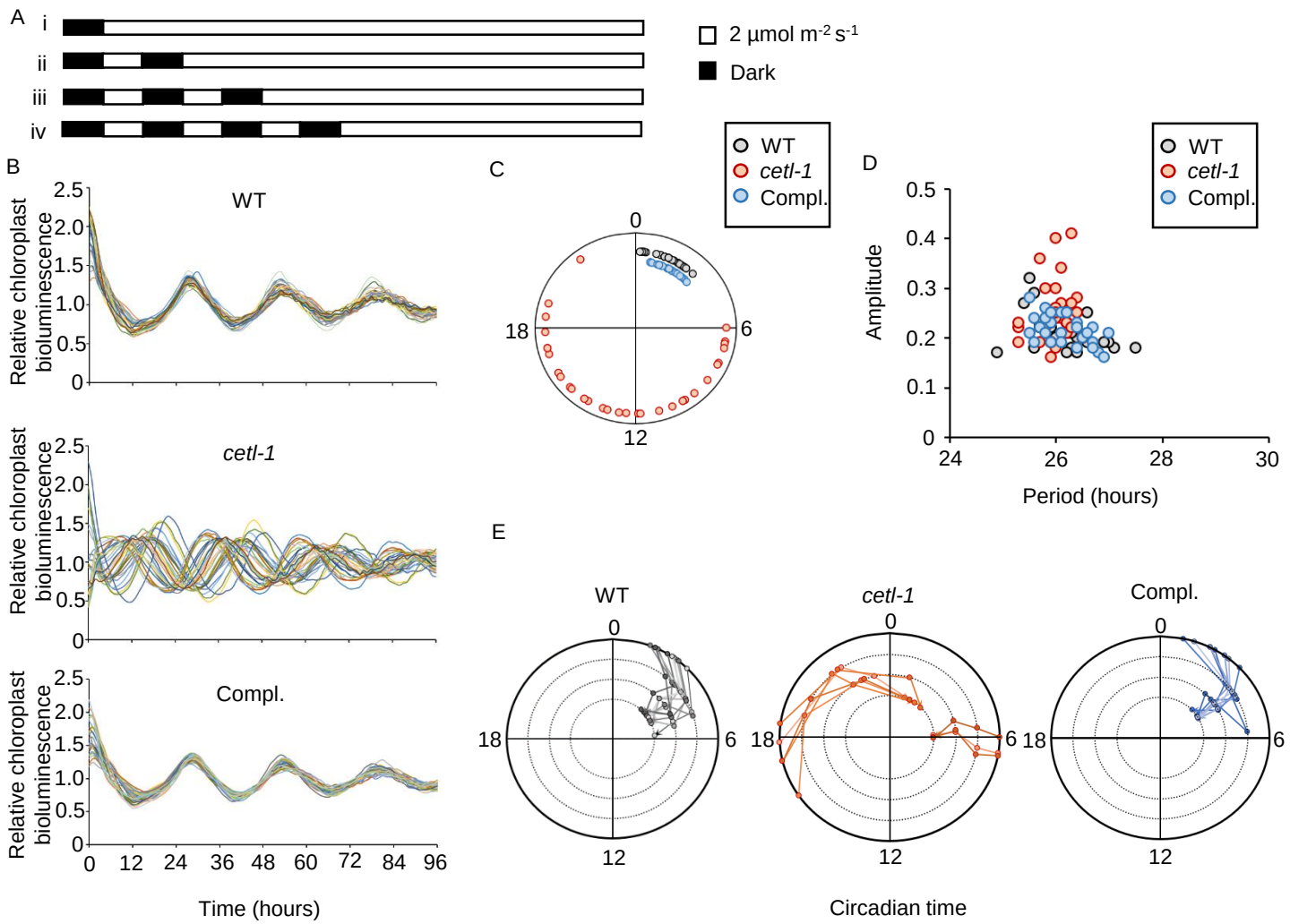

Fig 22. Phase distribution in LL in single colony protocol in *cetl-1*. The CBR (mt$^+$) (wild type [WT]), mutant progeny (*cetl-1*), and complement progeny (Compl.) from the cross mentioned in **Fig 16** were used to observe the chloroplast bioluminescence rhythm. Spot cultures were prepared using the single colony protocol depicted in **Fig 21**. **A.** Light regimes (**i**-**iv**) used for the experiment. Colonies were exposed to progressive LD (12 hours:12 hours) cycle before release into LL conditions (**ii-iv**). **B.** Chloroplast bioluminescence rhythms of the WT, *cetl-1*, and Compl. as observed after light schedule **i**. Cultures were maintained in 12 hours of darkness before release into LL conditions. Data of 28 biological replicates each, of WT and Compl., and 32 biological replicates of *cetl-1* from a single trial are shown. **C.** Phase diagram showing the circadian phases of *cetl-1*, WT and Compl. rhythms shown in B. **D.** Plot of period and amplitude of the bioluminescence rhythms shown in B. **E.** Peak phases of the quadruplicate spots of biological replicates after each of the four light schedules. The results after light schedules **i**-**iv** are plotted from the outermost ring to the innermost ring, respectively. Quadruplicate spots from the same independent culture are connected by a line. Data are shown only for cases where the rhythms were detected for all four spots in an independent culture, and correspond to results of a single trial.

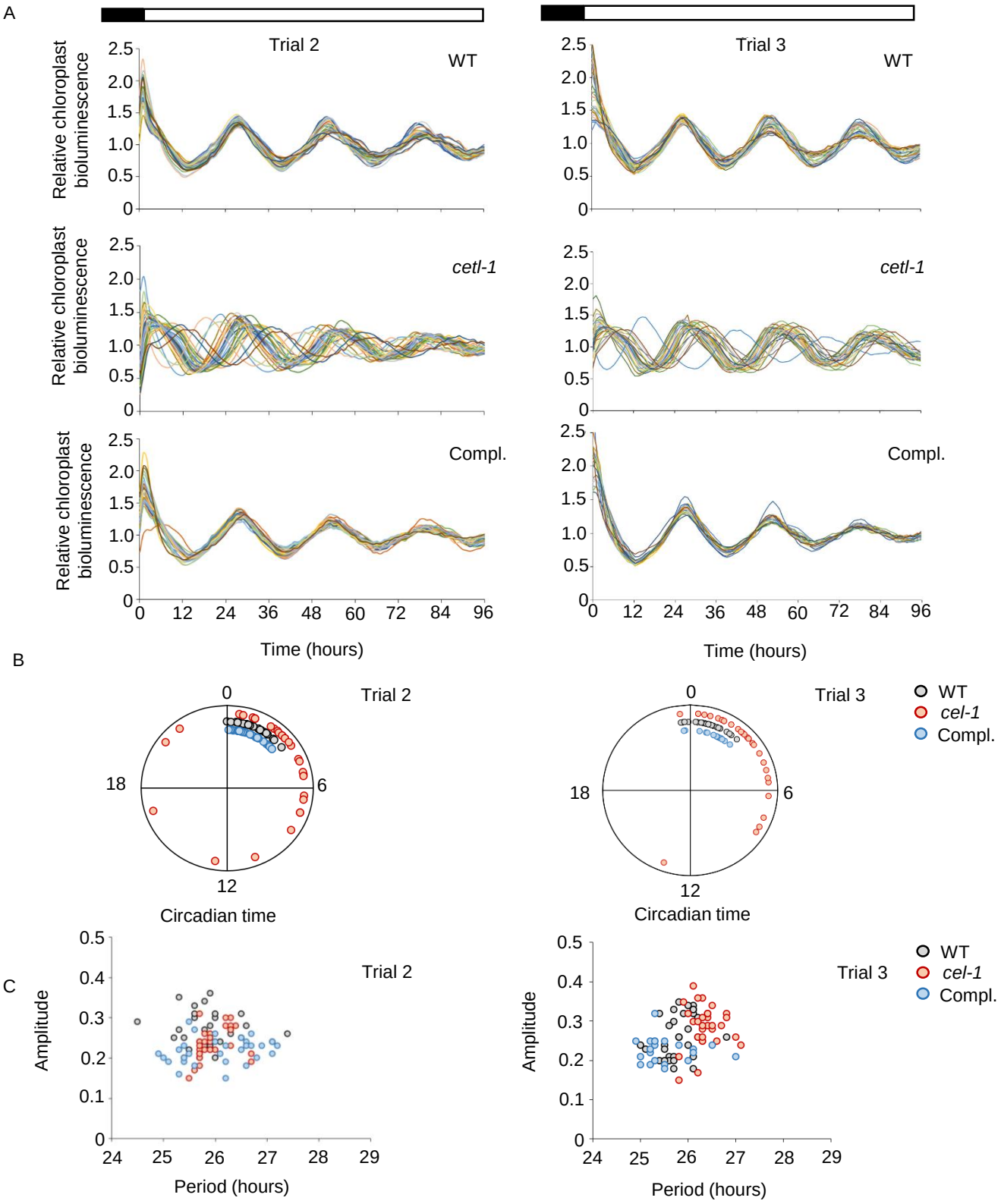

Fig 23. Phase distribution in the single colony protocol in *cetl-1*. Results from the subsequent trials are shown. Spot cultures were prepared in the same manner as in **Fig 22**. Cultures were maintained in a 12-hour dark period before release into LL conditions. **A.** Chloroplast bioluminescence rhythm after release into LL conditions. Trial 2-Data for 30 biological replicates each for WT and Compl. and 31 biological replicates of *cetl-1*, are shown. Trial 3-Data for 32 biological replicates of WT, 21 biological replicates of Compl., and 30 biological replicates of *cetl-1* are shown**. B.** Circadian phases of the rhythms shown in A. **C.** Plots of amplitude and period of the rhythms show in A**.** The circadian time (CT) at the beginning of LL was set to 0.

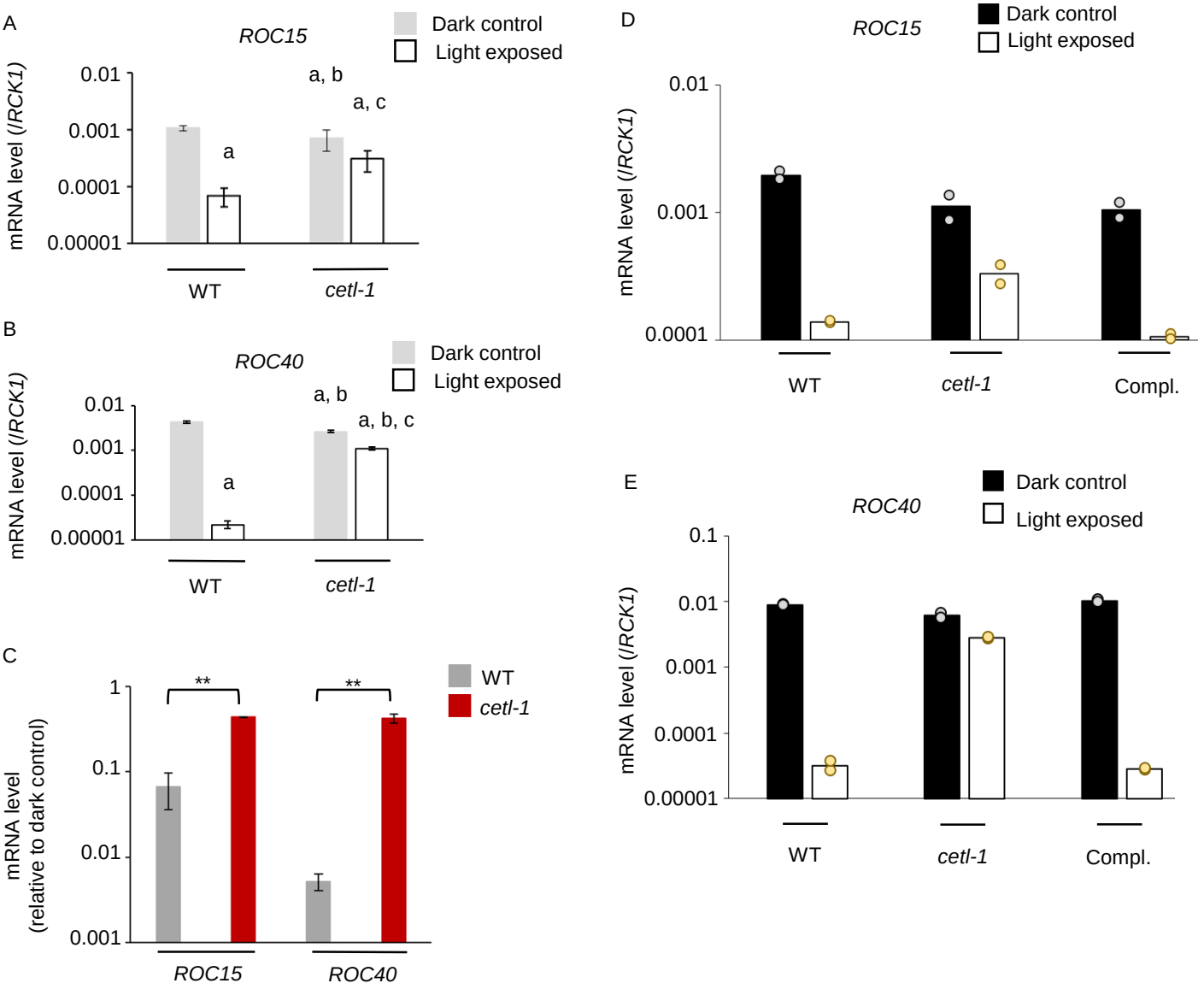

Fig 24. Light response of clock gene mRNAs in the *cetl-1* mutant. LD-entrained high-salt cultures were exposed to 30 µmol m^{-2} s^{-1} of white light at late night (ZT22, 2 hours before dawn). Cells were harvested from the light-exposed culture and the corresponding dark control after 1 hour. **A** and **B.** The mRNA levels of *ROC15* (A) and *ROC40* (B) in the wild type (WT; ROC15-LUC strain) and *cetl-1*. The mRNA levels have been calculated relative to the mRNA levels of *RCK1*. A two-way ANOVA indicated a significant interaction between genotype and light conditions for *ROC15* (genotype: $F_{1,8}$ = 0.46, *P*= 0.52, light conditions: $F_{1,8}$ = 54.61, *P*<0.0001, interaction: $F_{1,8}$ = 10.24, *P*< 0.05) and for *ROC40* (genotype: $F_{1,8}$ = 12.46, *P* = 0.0077, light conditions: $F_{1,8}$ = 1199.57, *P*<0.0001, interaction: $F_{1,8}$ = 272.17, *P*< 0.0001). Tukey's post hoc test was performed on the samples which were subdivided into four groups: WT dark control, WT light exposed, *cetl-1* dark control, and *cetl-1* light exposed. **a** (*P<0.05*) for comparisons with WT dark control, **b** (*P<0.05*) for comparisons with WT light exposed sample, **c** (*P<0.05*) for comparisons with *cetl-1* dark control. **C.** Extent of downregulation in WT and *cetl-1*. The mRNA abundance (i.e., mRNA levels relative to *RCK1* mRNA levels) of the light-exposed samples are shown relative to that of their respective dark control for easy comparison. *P*-values are based on Student's *t*- tests. ** *P*< 0.01. Mean ± SD of three biological replicates is shown (A-C). Note that these strains possess two copies of *ROC15*: an endogenous copy and *ROC15-LUC* transgene. The *ROC15* mRNA levels detected in this experiment are therefore a sum of the mRNA levels of the endogenous copy and the mRNA levels of the *ROC15-LUC* transgene. **D** and **E.** Light response of clock gene mRNAs in the complement. *ROC15* (**D**) and *ROC40* (**E**) mRNA levels were also analyzed in the complements (Compl.). The mean is represented by the bars and the value of each biological replicate is indicated by the dots. These strains possess two copies of *ROC15*: an endogenous copy and the *ROC15-LUC* transgene. The *ROC15* mRNA levels detected in this experiment are therefore a sum of the levels of mRNA from the endogenous copy and the *ROC15-LUC* transgene.

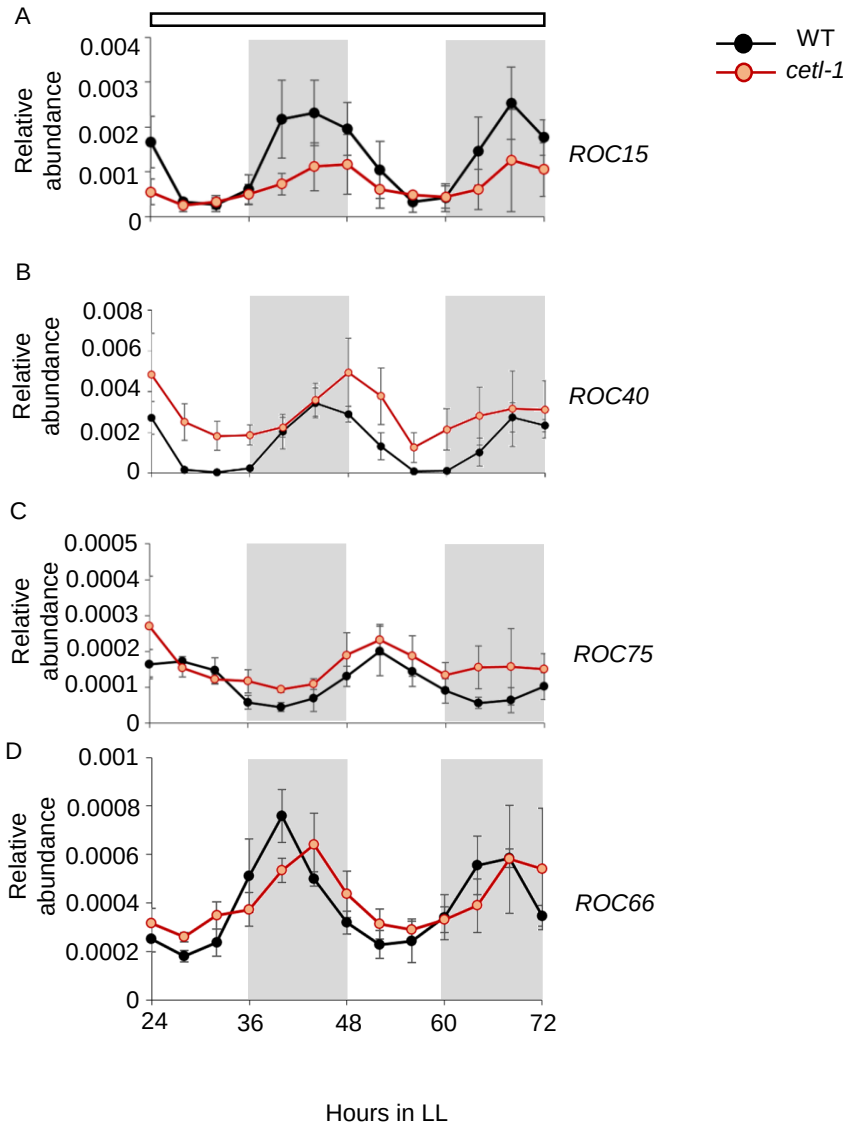

Fig 25. mRNA rhythm of clock genes in the mutant. Free-running high-salt cultures of the wild type (WT; ROC15-LUC strain) and *cetl-1* were harvested every four hours (between 24-72 hours) after release into LL conditions. Mean ± SD of 3 biological replicates are shown at most time points. The levels of *ROC15* mRNA in *cetl-1* mutant at the 56th hour correspond to the mean of two biological replicates. The bar above the graph indicates light conditions (i.e., LL conditions). The alternating white and grey background indicates subjective day and subjective night, respectively, that is expected from the light conditions prior to LL conditions. These strains possess an endogenous copy of *ROC15* and a *ROC15-LUC* transgene; therefore, the *ROC15* mRNA levels detected in this experiment are a sum of the levels of mRNA from the endogenous copy and the *ROC15-LUC* transgene.

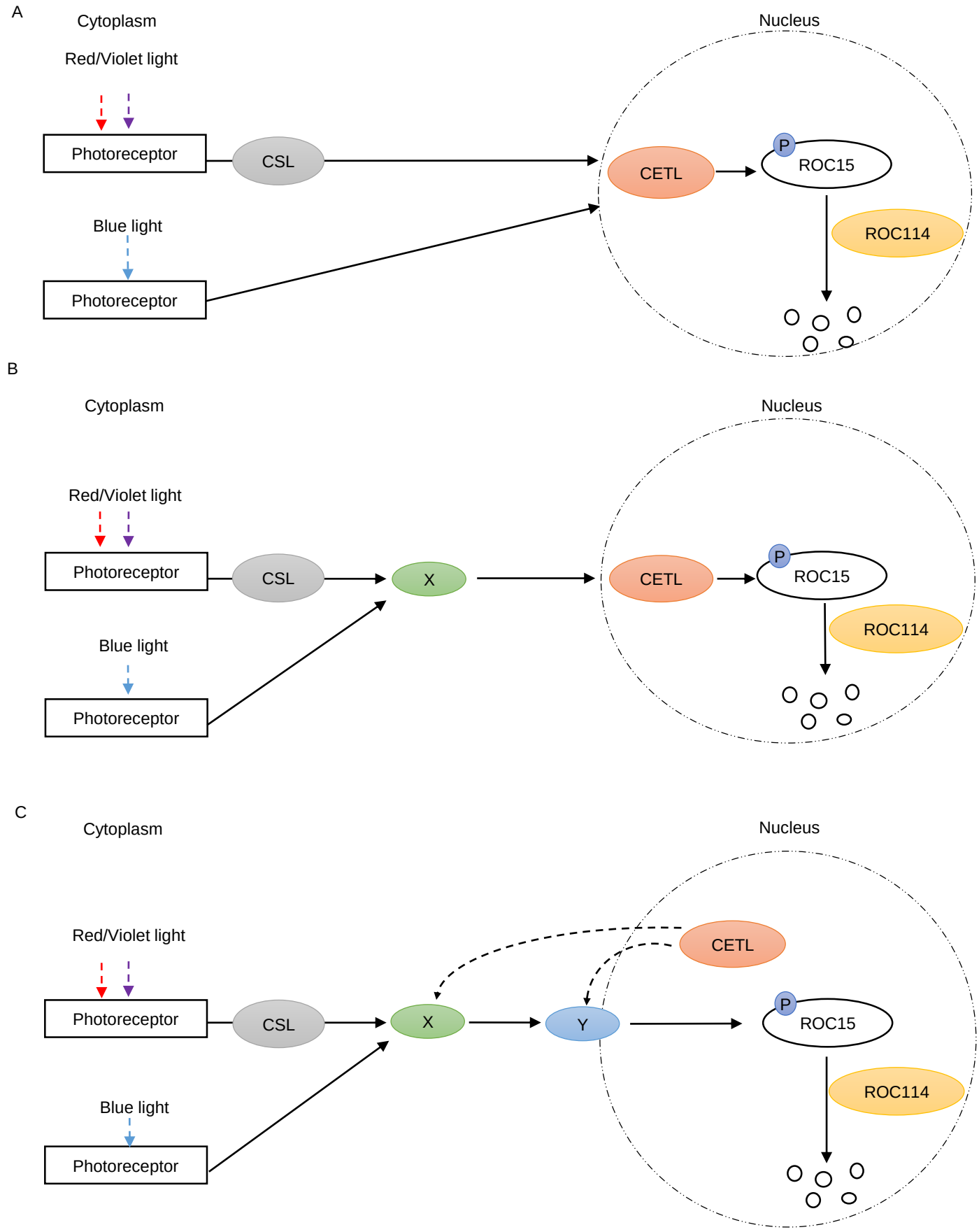

Fig 26. Diagrammatic representation of the light signaling pathway for ROC15 degradation. The current working models for the light-induced ROC15 degradation are shown.

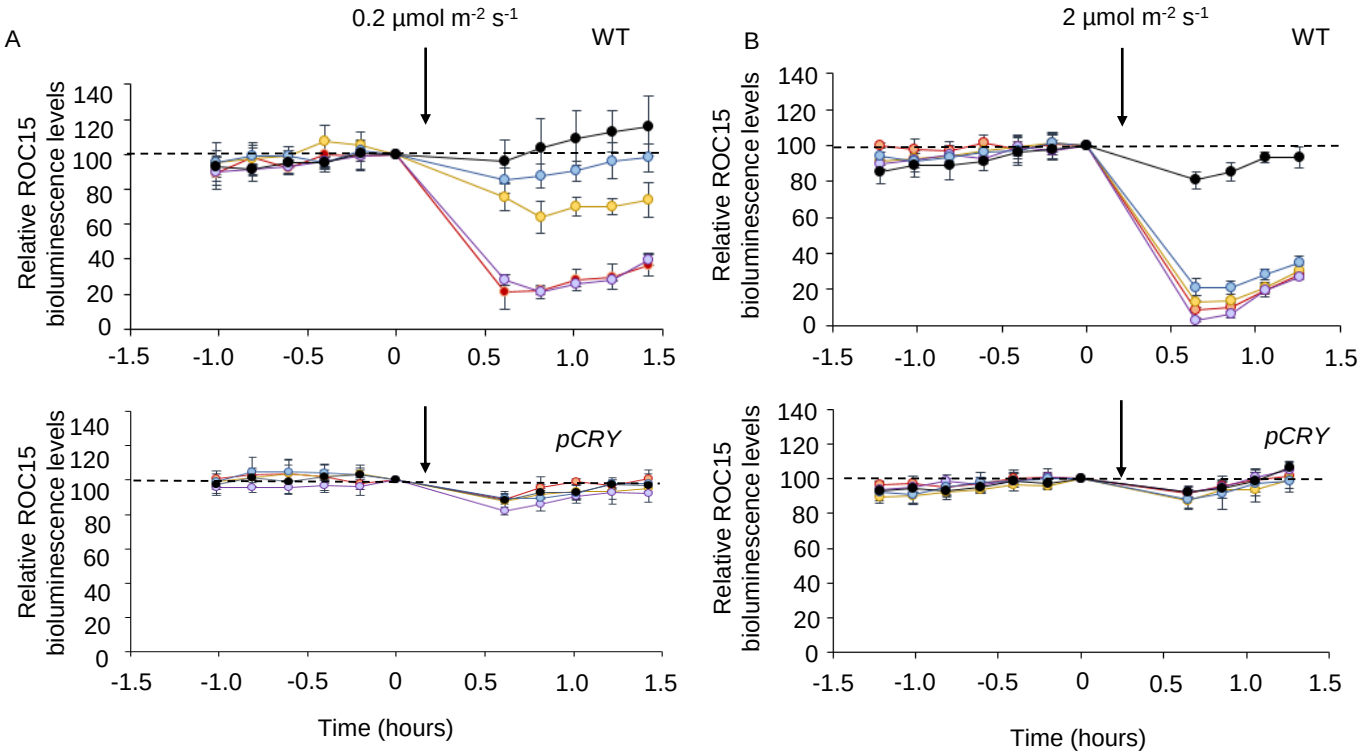

Fig 27. Light induced degradation of ROC15 in the *pCRY* mutant. Spot cultures of the mutant were transferred to 96 well black plates with Akalumine as the substrate for Luciferase. Plates were maintained in 3-6 hours of darkness to allow for ROC15 build-up before being exposed to 5-min pulses of blue, red, violet, and yellow lights at two intensities. Bioluminescence was monitored as described in Materials and Methods. **A** and **B.** Representative traces of ROC15 bioluminescence in response to light pulses with an intensity of 0.2 µmol m^{-2} s^{-1} and 2 µmol m^{-2} s^{-1} respectively. Top and bottom panel show the ROC15 bioluminescence traces of the WT and *pCRY* mutant respectively. Bioluminescence values were calculated relative to the value just before the light pulse. The response to each wavelength is depicted in the respective colour. The dark control is indicated in black. The mean ± standard deviation of four independent cultures is shown. The approximate time of the light pulse is indicated by the arrow.

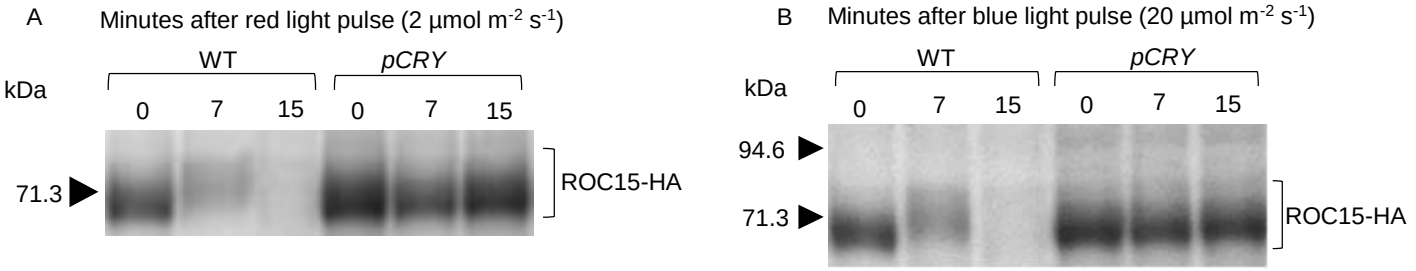

Fig 28. Light induced phosphorylation of ROC15 in the *pCRY* mutant. A genetic cross was performed between the *pCRY* mutant expressing ROC15-LUC fusion protein and a strain expressing ROC15-HA (WT, **Niwa et al. 2013**). The required progeny possessing the *pCRY* mutation and expressing ROC15-HA was selected by genomic PCRs and antibiotic resistance screening. **A** and **B.** Phosphorylation of ROC15 in response to red and blue light respectively. Unsynchronized TAP cultures of the mutant and WT were maintained in darkness for at least 6 hours to allow for ROC15 build-up before being exposed to 30-40 s pulse of red and blue light (2 µmol m^{-2} s^{-1} and 20 µmol m^{-2} s^{-1} respectively). Western blot was performed on whole cell protein extracts from cultures sampled at 0 minutes (before light pulse), and, 7 minutes and 15 minutes after light pulse.